MCEER
MULTIDISCIPLINARY CENTER FOR EARTHQUAKE ENGINEERING RESEARCH
A National Center of Excellence in Advanced Technology Applications
ISSN 1520-295X

Capacity Design of Bridge Piers and the Analysis of Overstrength

by

John B. Mander, Anindya Dutta and Pankish Goel
State University of New York at Buffalo
Department of Civil, Structural and Environmental Engineering
Buffalo, New York 14260

Technical Report MCEER-98-0003

June 1, 1998

This research was conducted at the State University of New York at Buffalo and was supported by the Federal Highway Administration under contract number DTFH61-92-C-00112.

NOTICE

This report was prepared by the State University of New York at Buffalo as a result of research sponsored by the Multidisciplinary Center for Earthquake Engineering Research (MCEER) through a contract from the Federal Highway Administration. Neither MCEER, associates of MCEER, its sponsors, the State University of New York at Buffalo, nor any person acting on their behalf:

a. makes any warranty, express or implied, with respect to the use of any information, apparatus, method, or process disclosed in this report or that such use may not infringe upon privately owned rights; or

b. assumes any liabilities of whatsoever kind with respect to the use of, or the damage resulting from the use of, any information, apparatus, method, or process disclosed in his report.

Any opinions, findings, and conclusions or recommendations expressed in this publication are those of the author(s) and do not necessarily reflect the views of MCEER or the Federal Highway Administration.

MULTIDISCIPLINARY CENTER FOR EARTHQUAKE ENGINEERING RESEARCH
A National Center of Excellence in Advanced Technology Applications

Capacity Design of Bridge Piers and the Analysis of Overstrength

by

J.B. Mander[1], A. Dutta[2] and P. Goel[2]

Publication Date: June 1, 1998
Submittal Date: April 18, 1998

Technical Report MCEER-98-0003

Task Number 112-D-5.2(a)

FHWA Contract Number DTFH61-92-C-00112

1 Associate Professor, Department of Civil, Structural and Environmental Engineering, State University of New York at Buffalo
2 Research Assistant, Department of Civil, Structural and Environmental Engineering, State University of New York at Buffalo

MULTIDISCIPLINARY CENTER FOR EARTHQUAKE ENGINEERING RESEARCH
State University of New York at Buffalo
Red Jacket Quadrangle, Buffalo, NY 14261

Preface

The Multidisciplinary Center for Earthquake Engineering Research (MCEER) is a national center of excellence in advanced technology applications that is dedicated to the reduction of earthquake losses nationwide. Headquartered at the State University of New York at Buffalo, the Center was originally established by the National Science Foundation in 1986, as the National Center for Earthquake Engineering Research (NCEER).

Comprising a consortium of researchers from numerous disciplines and institutions throughout the United States, the Center's mission is to reduce earthquake losses through research and the application of advanced technologies that improve engineering, pre-earthquake planning and post-earthquake recovery strategies. Toward this end, the Center coordinates a nationwide program of multidisciplinary team research, education and outreach activities.

MCEER's research is conducted under the sponsorship of two major federal agencies, the National Science Foundation (NSF) and the Federal Highway Administration (FHWA), and the State of New York. Significant support is also derived from the Federal Emergency Management Agency (FEMA), other state governments, academic institutions, foreign governments and private industry.

The Center's FHWA-sponsored Highway Project develops retrofit and evaluation methodologies for existing bridges and other highway structures (including tunnels, retaining structures, slopes, culverts, and pavements), and improved seismic design criteria and procedures for bridges and other highway structures. Specifically, tasks are being conducted to:

- assess the vulnerability of highway systems, structures and components;
- develop concepts for retrofitting vulnerable highway structures and components;
- develop improved design and analysis methodologies for bridges, tunnels, and retaining structures, which include consideration of soil-structure interaction mechanisms and their influence on structural response;
- review and recommend improved seismic design and performance criteria for new highway structures.

Highway Project research focuses on two distinct areas: the development of improved design criteria and philosophies for new or future highway construction, and the development of improved analysis and retrofitting methodologies for existing highway systems and structures. The research discussed in this report is a result of work conducted under the new highway structures project, and was performed within Task 112-D-5.2(a), "Capacity Detailing of Members to Ensure Elastic Behavior" of that project as shown in the flowchart on the following page.

The overall objective of this task was to develop seismic design and capacity detailing recommendations for portions of highway bridge substructures that do not particpate as primary energy dissipation elements. This report describes the development of deterministic procedures to obtain

overstrength factors for bridge columns on the basis of moment-curvature analysis. The authors propose a simplified design methodology based on plastic analysis of overstrength moment capactiy, and demonstrate the methodology through its application to a design example.

SEISMIC VULNERABILITY OF NEW HIGHWAY CONSTRUCTION
FHWA Contract DTFH61-92-C-00112

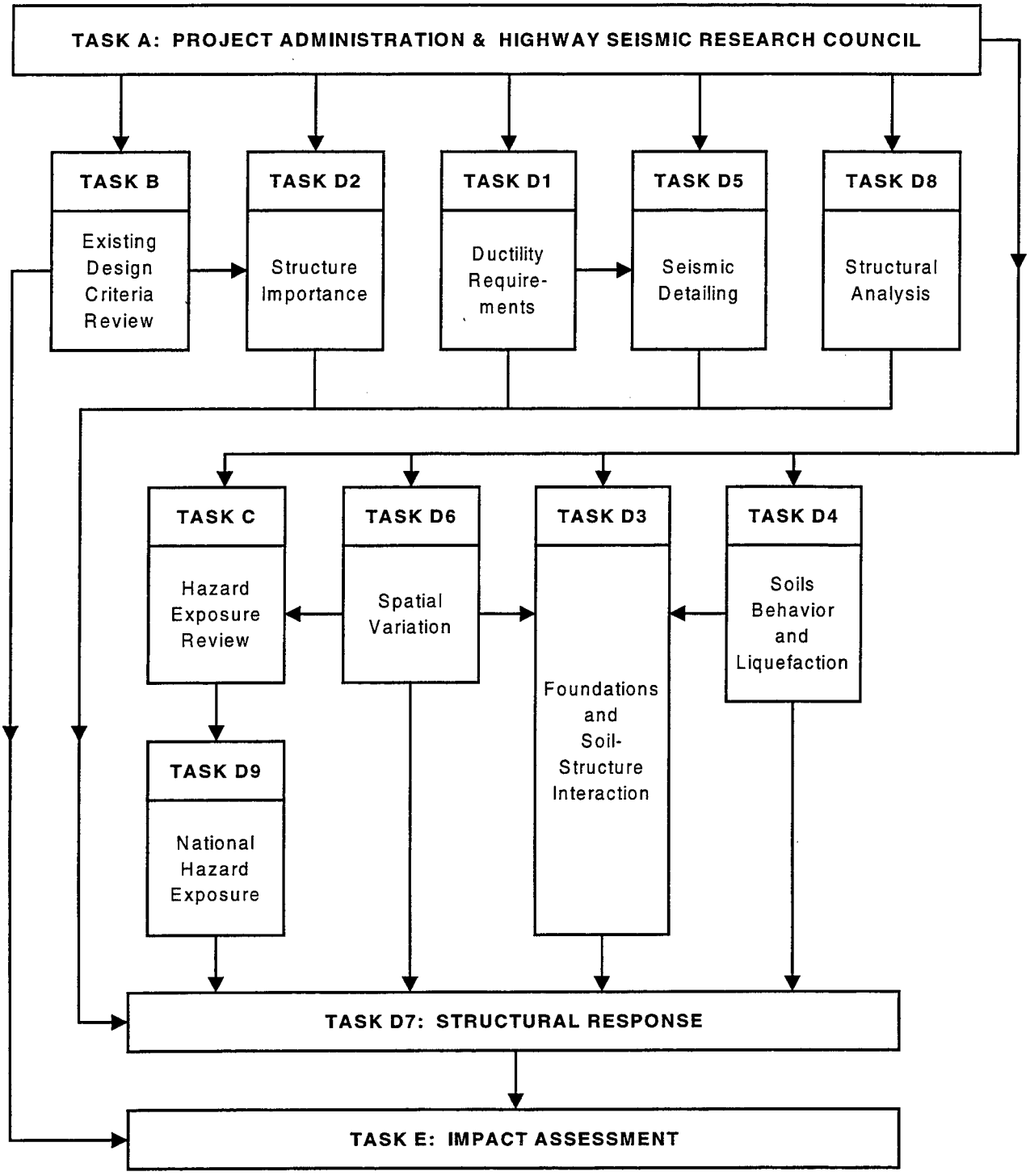

ABSTRACT

The capacity design philosophy has now become the design norm for the seismic design of most structural systems. For bridge systems, this means it is necessary to assess the overstrength capacity of columns prior to proceeding with the design of the foundation and superstructure. This research is devoted to developing deterministic procedures to obtain overstrength factors for column elements. For this purpose, a moment-curvature approach is explored. A parametric study is then conducted to investigate the factors that effect overstrength. A simplified design methodology is proposed based on plastic analysis of overstrength moment capacity. A design example showing the step by step procedure is also presented.

ACKNOWLEDGEMENTS

This research was carried out at the Department of Civil, Structural and Environmental Engineering at the State University of New York at Buffalo.

Financial support is gratefully acknowledged from the National Center for Earthquake Engineering Research through contract with the Federal Highway Administration on Seismic Vulnerability of New Highway Construction (FHWA Contract DTFH61-92-00112).

TABLE OF CONTENTS

TABLE OF CONTENTS (Cont'd)

TABLE OF CONTENTS (Cont'd)

LIST OF ILLUSTRATIONS

LIST OF ILLUSTRATIONS (CONT'D.)

LIST OF TABLES

LIST OF SYMBOLS

A_{bh} = area of cross section of a single transverse reinforcement

A_{cc} = area of core concrete measured to the centerline of transverse reinforcement

A_g = gross area of the concrete section

A_{si} = area of steel at the i-th location

A_{st} = total area of longitudinal reinforcement

A_{sx} = total area of cross section of transverse reinforcement in the X direction

A_{sy} = total area of cross section of transverse reinforcement in the Y direction

C_c = concrete compression force

D = overall depth of the section

D' = depth of the section measured from centers of extreme tension and compression steel

D'' = depth of the section measured from the centers of transverse reinforcement

E_c = modulus of elasticity of concrete

E_s = Young's Modulus of reinforcement

E_{sh} = strain hardening modulus

F_{si} = force in the i-th reinforcement layer

K = confinement ratio of concrete

L = column length

L_c = length of the column minus plastic hinge length

M_{bo} = maximum overstrength moment in an overstrength moment interaction curve

M_c = moment generated by the cover concrete

M_{cc} = moment general by the core concrete

M_{cn} = nominal moment capacity of the compression stress block

M_d = moment at the center of the deck

M_n = provided nominal moment capacity of the plastic hinge zone

M_{nb} = maximum nominal moment in a nominal moment interaction curve

M_{np}^x = nominal moment capacity along the X direction for the capacity protected element

M_{np}^{y} = nominal moment capacity along the Y direction for the capacity protected element

M_{nw}^{x} = nominal moment capacity along the X direction for the capacity weakened element

M_{nw}^{y} = nominal moment capacity along the Y direction for the capacity weakened element

M_{nx} = nominal moment capacity along the X direction

M_{ny} = nominal moment capacity along the Y direction

M_{oc} = maximum overstrength concrete moment

M_{os} = maximum overstrength steel moment

M_{po} = overstrength moment capacity at the center of the hinge

M_s = moment generated by the longitudinal reinforcement

M_{sn} = nominal moment capacity of the reinforcing steel layers

M_u = ultimate moment capacity of the section for a given curvature

M_x = moment demand along the X direction

M_y = moment demand along the Y direction

P_{bo} = axial load corresponding to M_{bo} in overstrength moment interaction curve

P_e = applied axial load on a section

P_{nb} = axial load corresponding to M_{nb} nominal moment interaction curve

P_{nt} = nominal tensile axial load capacity

P_{to} = overstrength tensile axial load capacity

P_u = ultimate load capacity of a section

S_n = nominal strength of a section

S_0 = overstrength of a section

Z_p = plastic section modulus of steel

a = lower limit of Gauss integration

b = upper limit of Gauss integration

b' = lateral dimension of a rectangular section measured from centerline of outermost steel

b'', b_c = breadth of the confined core concrete

b_0 = breadth of the cover concrete

c = neutral axis depth

d = depth of the deck

d' = distance from the concrete compression fiber to the c.g. of nearest compression steel

f_c = differential concrete stress

f'_c = unconfined compression strength of concrete

f_{cc} = stress in the confined core concrete

f'_{cc} = peak value of confined concrete stress

f_{co} = stress in the cover concrete

f_l = confining stress exerted by the transverse reinforcement in circular and square sections

f_{l_x} = confining stress exerted by the transverse reinforcement in the X direction

f_{l_y} = confining stress exerted by the transverse reinforcement in the Y direction

f_s = stress in the steel reinforcement

f_{si} = i-th steel stress

f_{su} = ultimate stress of the longitudinal reinforcement

f_y = yield strength of the longitudinal reinforcement

k_e = confinement effectiveness coefficient

m = mean value for a normal distribution

$n = E_c \varepsilon'_{cc} / f'_{cc}$

p = power associated with steel constitutive relation

s = center to center spacing of transverse reinforcement

s' = clear spacing of transverse reinforcement

w_i = width of the i-th parabola between two adjacent longitudinal bars in a rectangular column

w_k = weight factor associated i-th the k-th Gauss point

y_k = location of the k-th Gauss point

$x_{\alpha\beta}^{max}$ = normalized strain at $\alpha\beta^{max}$

y = distance measured from geometric centroid with the convention positive downward

y_i = distance of the i-th reinforcement layer from the geometric centroid

$z = 6.8 f'_c K^{-6}$

Φ = standard cumulative distribution function

α, β = stress block factors

α, β_1 = stress block parameters defined by AASHTO/ACI

$\alpha\beta^{max}$ = maximum value of $\alpha\beta$

α_{cc}, β_{cc} = confined concrete stress block factors

α_{co}, β_{co} = unconfined concrete stress block factors

α_{cc}, β_{cc}^{max} = maximum product of confined concrete stress block parameters

β_v = lognormal standard deviation for a lognormal distribution = $\sigma_{\ln Y}$

χ = a parameter = 0.5 for spirals and = 1.0 for circular hoops

$\varepsilon_{cc}^{\prime}$ = strain of peak confined concrete stress

ε_s = strain in the steel reinforcement

ε_{sh} = strain hardening strain reinforcement

ε_{si} = strain at the i-th reinforcement location

ε_{su} = strain at ultimate stress

ε_0 = strain at the geometric centroid of the section

$\varepsilon_{\alpha\beta}^{max}$ = value of strain where $\alpha\beta$ is maximum

ϕ = section curvature

κ_c = factor that locates the position of the plastic centroid of core cover concrete

κ_0 = factor that locates the position of the plastic centroid of core cover concrete

λ_{mo} = moment overstrength factor

λ_{mo}^{x} = moment overstrength in the X direction

λ_{mo}^{y} = moment overstrength in the Y direction

θ = median value associated with a lognormal distribution

ρ_{cc} = longitudinal steel ratio with respect to the core concrete

ρ_s = volumetric ratio of transverse reinforcement

ρ_t = longitudinal steel ratio

ρ_x = volumetric ratio of transverse reinforcement in the X direction

ρ_y = volumetric ratio of transverse reinforcement in the Y direction

σ = standard deviation associated with a normal distribution

SECTION 1
INTRODUCTION

1.1 BACKGROUND

In the seismic design of bridge structures, there is now a common awareness that excessive strength is neither essential nor desirable for good performance in strong earthquakes. The emphasis in seismic design has shifted from resistance of large seismic forces to the control of deformations. Hence inelastic structural response (specially for large earthquakes in a multi-level design space) has become the expected norm when designing a structure to resist earthquake forces.

It is also well accepted that certain modes of inelastic behavior are more desirable than others. This is because undesirable behavioral modes may lead to failure, while others provide a controlled ductile response; an essential attribute of maintaining strength while the structure is subjected to reversals of inelastic deformations under seismic response. Therefore, undesirable inelastic deformation modes can be deliberately avoided by amplifying their strength in comparison with those of the desirable inelastic modes. Thus, for concrete structures, the required shear strength must exceed the required flexural strength to ensure that inelastic shear deformations, associated with large deterioration of stiffness and strength, do not occur.

It has also become a norm that seismic design should encourage structural forms that possess ductility. This relates to the careful choice of plastic hinge locations where plastic flexural deformations may occur. These plastic hinges are designed for high ductility while potentially brittle sections of the structure are designed for a higher strength capacity than those of the plastic hinge sections. These concepts form the basis of the capacity design philosophy currently followed in many seismic design codes.

To summarize, capacity design requires: (i) selection of a suitable structural configuration for inelastic response, (ii) selection of suitable and appropriately designed plastic hinge locations

for inelastic deformations to be concentrated, and (iii) creation of suitable strength differentials so that inelastic deformations do not occur at undesirable locations or by undesirable structural modes.

1.2 Plastic Hinge Zones

In plastic hinge regions that support significant axial load, the ultimate compression strain of unconfined concrete is inadequate to allow the structure to achieve the desired level of ductility. Closely spaced transverse reinforcement in conjunction with longitudinal reinforcement acts to restrain the lateral expansion of concrete, enabling higher compression stresses and more importantly, much higher compression strains to be sustained by the compression zone before failure occurs. Therefore, by providing a nominal strength in plastic hinge zones greater than that required from the earthquake forces and by designing the column for a high ductility by confining the plastic hinge section, both the objectives of required strength and high ductility, required for capacity design, can be fulfilled in concrete columns.

1.3 Overstrength Factors in Confined Concrete Columns

In capacity design the prevention of undesirable inelastic deformation modes is usually achieved by ensuring that the section strength exceeds the demands originating from the overstrength of plastic hinges. Overstrength of a plastic hinge section takes into account all possible factors that may contribute to strength exceeding the nominal strength provided. Hence, determination of overstrength factors is very important in capacity design to maintain the correct hierarchy of capacities and hence, of failure modes and locations for the structure.

This can be illustrated by the example shown in figure 1-1 which represents a concrete bridge with a plastic hinge zone designed at the base of the column. The required strength of the bridge deck has to be assessed assuming the deck itself as a brittle section with no capacity for inelastic deformations. If M_n is the real provided nominal moment capacity of the plastic hinge zone and M_{po} is the overstrength moment capacity at the center of the hinge length due to confinement of concrete and strain-hardening of the longitudinal steel, then the moment

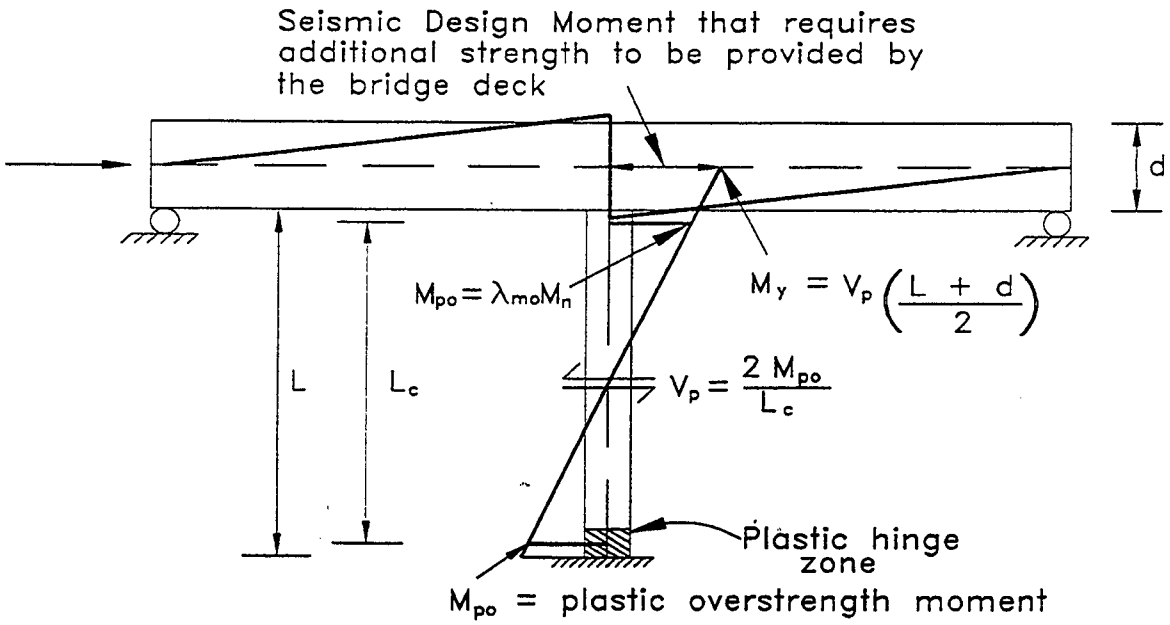

(a) Longitudinal Response

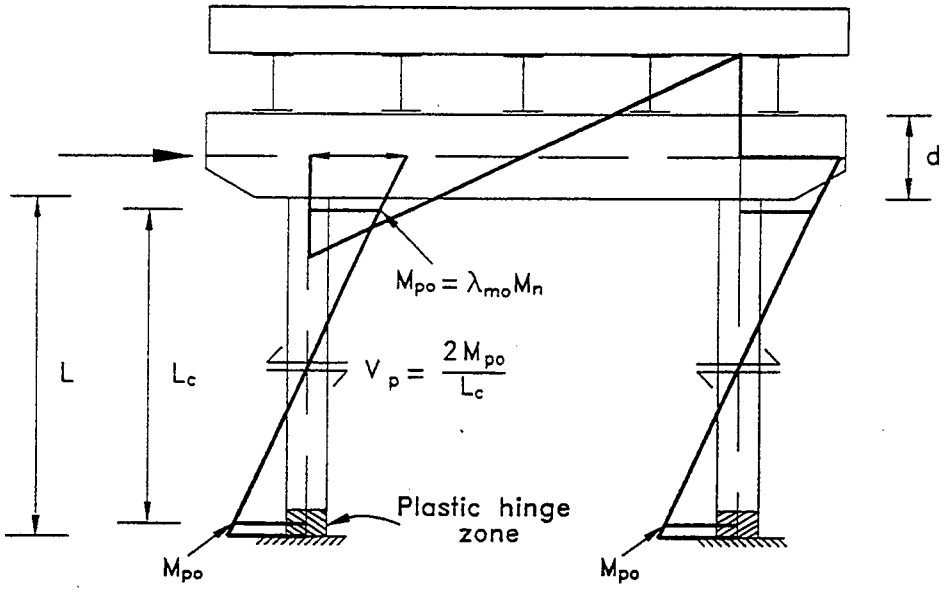

(b) Transverse Response

Figure 1-1 Capacity Design of Bridges using Overstrength Concepts.

overstrength factor (λ_{mo}) is defined as:

$$\lambda_{mo} = \frac{M_{po}}{M_n} \tag{1-1}$$

The minimum (dependable) design moment at the center of the bridge deck is found by extrapolating the overstrength moment (M_{po}) to the center of the bridge deck. This connection moment is then distributed to the two bridge beams in ratio of their relative stiffness. For the example shown in figure 1-1, the moment at the center of the deck for an integral construction is given by

$$M_d = \lambda_{mo} M_n \left(\frac{L+d}{L_c} \right) \tag{1-2}$$

where L is the column length, d is the depth of the deck, and L_c is the column length minus the plastic hinge zone length. This moment is then distributed into the deck based on the relative stiffness of each span and resisted either by providing additional prestress, supplementary mild steel reinforcement, or both.

1.4 Previous Research

Most of the previous research has been limited to the development of constitutive relationships for confined concrete and very limited research has been conducted on the overstrength factor determination of confined concrete.

Kent and Park (1971), and Mander et al. (1988a) proposed analytical models for confined concrete which are most frequently used in analysis nowadays. Ang et al. (1985) proposed an empirical equation for determination of moment overstrength factors in concrete columns based on the results from the experiments conducted on confined concrete columns. The results from the experiments and the proposed equations are shown in figure 1-2. However, the research lacked an in-depth study on the effects of various material and sectional parameters which significantly affect overstrength factors. Andriono et al. (1986) used the statistical results of the stress-strain properties of the steel reinforcement to determine the moment overstrength factors

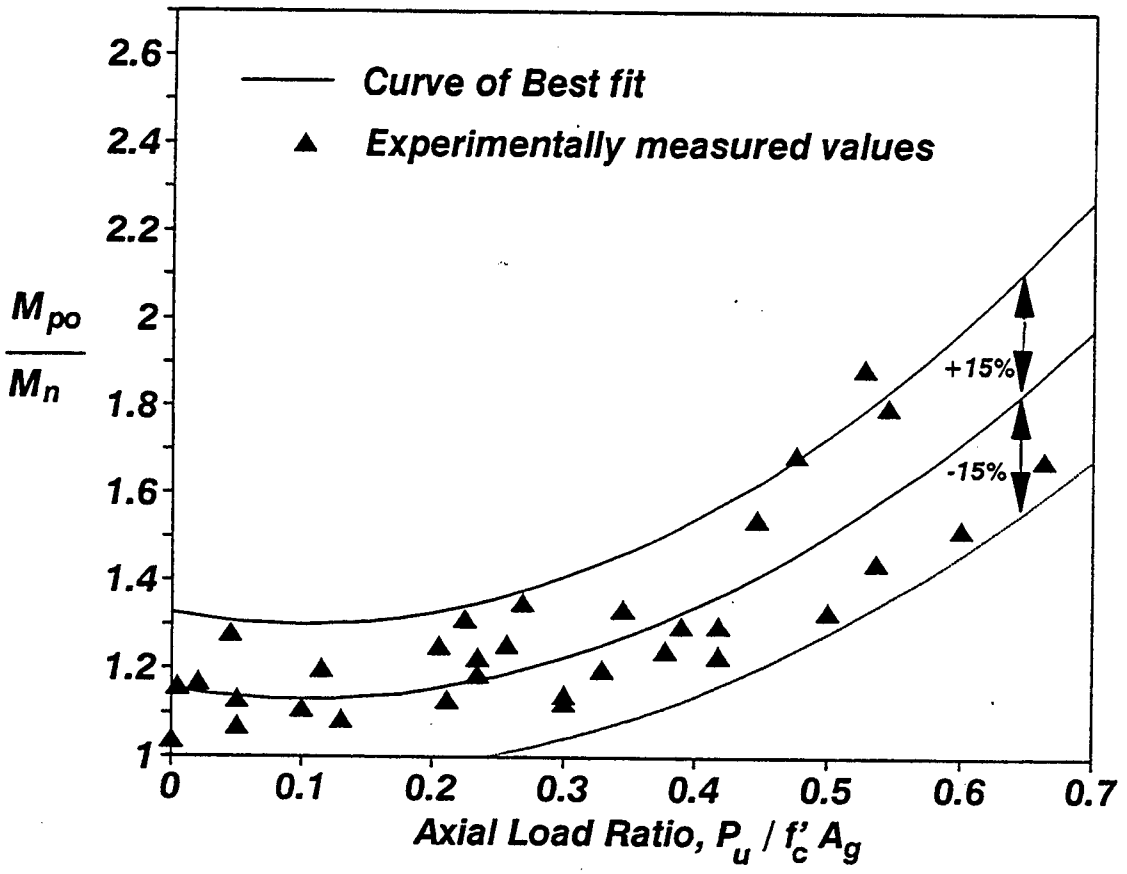

Figure 1-2 Moment Overstrength Factors for Confined Concrete Columns at different Axial Load Levels by Ang et al (1985).

of reinforced concrete beam sections. This study was limited to beam sections and hence axial loads which have significant effect on overstrength factors were not considered.

1.5 OUTLINE OF THIS STUDY

In this study, an attempt has been made to develop deterministic analytical procedures for moment-curvature analysis and hence to determine the overstrength factors for concrete columns. The effects of various material and sectional properties on the overstrength factors has also been studied. This study is reported in two parts. The first part deals with development of the procedure to conduct moment-curvature analysis using a Gauss Quadrature integration scheme. The latter part deals with presentation of results obtained from the parametric study conducted on overstrength factors. The proposed theory is validated with experimental results. An axial load-moment interaction curve approach is proposed for determining overstrength factors to be used as part of the capacity design process. This uses a plastic analysis approach where special stress block factors are used to determine the plastic strength contribution of the concrete. Explicit stress block parameters that take confinement into consideration are developed from a proposed stress strain relationship of concrete. Design recommendations are then made based on the analytical studies conducted herein.

SECTION 2
MOMENT-CURVATURE ANALYSIS: A TOOL FOR DETERMINING OVERSTRENGTH FACTORS

2.1 INTRODUCTION

This section presents a moment-curvature analysis procedure for columns with confined concrete. By determining the maximum obtainable moment capacity (M_{po}), the overstrength capacity can be defined as

$$\lambda_{mo} = \frac{M_{po}}{M_n} \tag{2-1}$$

where M_n = provided nominal moment capacity that is defined in accordance with the usual AASHTO/ACI design approach—that is elasto-plastic steel behavior together with the Whitney stress block. The theoretical basis of the moment-curvature analysis procedure is presented in the following subsections.

2.2 MOMENT-CURVATURE ANALYSIS OF A CONFINED CONCRETE COLUMN

For a given cross sectional strain profile, the moment capacity (M) of a section (figure 2-1) can be determined by using two equilibrium equations in conjunction with strain compatibility. For a given concrete strain in the geometric centroid of the section ε_0 and section curvature ϕ, the strain at any location can be found from

$$\varepsilon_{si} = \varepsilon_0 + \phi y \tag{2-2}$$

where y denotes the location of the point from the geometric centroid of the section with the convention positive downward. Steel strains ε_{s1}, ε_{s2}, ε_{s3} ... can be determined using the same equation and the stresses f_{s1}, f_{s2}, f_{s3} ... corresponding to these strains can be evaluated from stress-

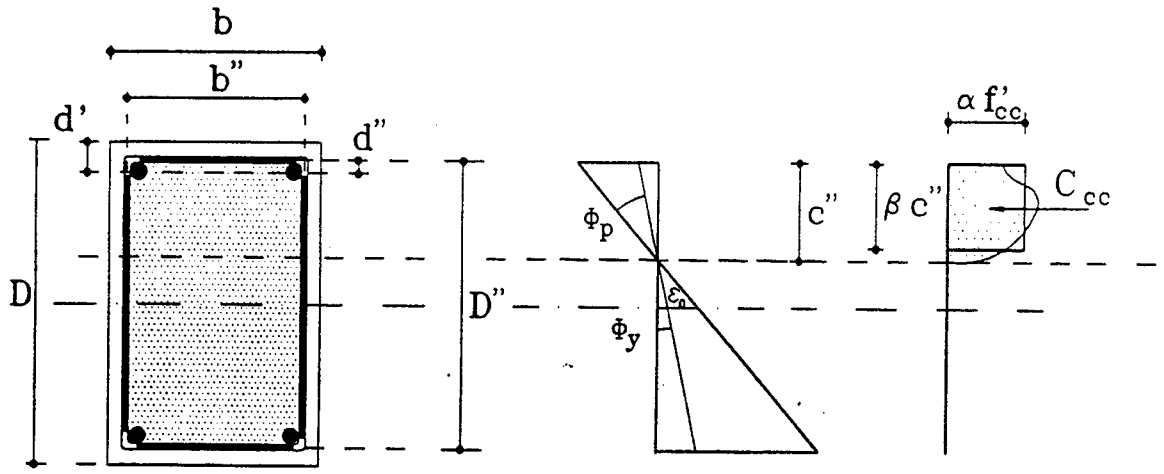

(a) Rectangular Section

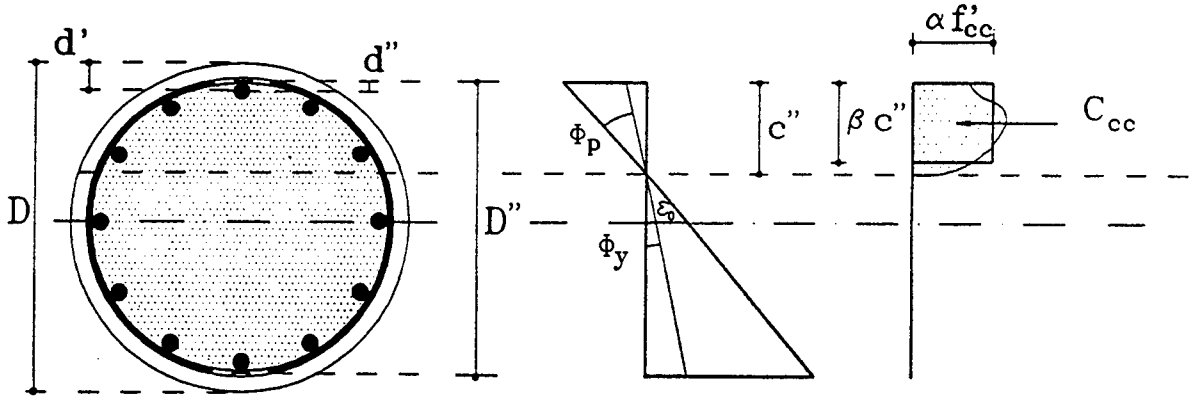

(b) Circular Section

Figure 2-1 Sectional Parameters for Rectangular and Circular Sections.

strain curves of steel. Steel forces may then be determined from the steel stresses and steel areas. For the bar i, the force equation is

$$F_{si} = f_{si} A_{si} \tag{2-3}$$

Force equilibrium requires

$$C_c + \sum_{i=1}^{n} A_{si} f_{si} = P_u \tag{2-4}$$

where C_c is the sum of concrete forces from confined core concrete and unconfined cover concrete obtained by integrating the respective concrete stresses over the cross sectional area in compression as

$$\iint f_c \, dx \, dy \tag{2-5}$$

Normalizing

$$\frac{C_c}{f'_c A_g} = \frac{P_u}{f'_c A_g} - \sum_{i=1}^{n} \frac{A_{si} f_{si}}{f'_c A_g} \tag{2-6}$$

The moment-curvature relationship for a given axial load level is determined by incrementing the curvature ϕ. For each value of ϕ, the centroidal strain ε_0 is found by adjusting it until the force equilibrium of equation (2-4) is satisfied. The internal forces and centroidal strain so determined are then used to calculate the moment M

$$M = \iint f_c \, y \, dx \, dy + \sum_{i=1}^{n} A_{si} f_{si} y_i \tag{2-7}$$

In order to evaluate the integral in equation (2-5) and (2-7) and to maintain generality without sacrificing accuracy, a numerical integration strategy that employs Gauss Quadrature is investigated.

2.2.1 Gauss Quadrature Technique

Gauss Quadrature is a very powerful method of numerical integration which employs unequally spaced intervals. The numerical integration of $\int_a^b f(x)\,dx$ is given by

$$\bar{I} = \Omega\,[\,w_1 f(x_1) + w_2 f(x_2) + \cdots\cdots + w_n f(x_n)\,] \tag{2-8}$$

where x_k are the n equally spaced points determined by the type and degree of orthogonal polynomial used, and the w_k are the weight factors associated with each integration point. The quantity Ω is a constant determined by the limits of the integral and expressed as

$$\Omega = (b - a) \tag{2-9}$$

Thus by using Gauss Quadrature, it is possible to break down any difficult integral into a summation of discrete products with an associated weight factor. Although this form of numerical integration is widely applied to finite element analysis, the use of this technique in moment-curvature analysis is new and appealing due to its simplicity. The weight factors to be used for integration are dependent on the degree of polynomial used and can be obtained from any textbook on mathematical functions (e.g. Chapra and Canale, 1985). The weight factors and integration points for 4, 5 and 6 Gauss points with limits from 0 to 1 are shown in table 2-1.

Table 2-1 Integration Points and Weights for Gauss Quadrature

Order	Integration Points	Weight Factors	Truncation Error
4	0.069432 0.330009 0.669991 0.930568	0.173928 0.326072 0.326072 0.173928	$\frac{1}{3.473 \times 10^6} f^{(8)}(\xi)$
5	0.046910 0.230765 0.500000 0.769235 0.953089	0.118463 0.239312 0.284450 0.239312 0.118463	$\frac{1}{1.238 \times 10^9} f^{(10)}(\xi)$
6	0.033765 0.169395 0.380690 0.619310 0.830605 0.966235	0.085617 0.180381 0.233957 0.233957 0.180381 0.085617	$\frac{1}{1.426 \times 10^{15}} f^{(8)}(\xi)$

Although it is obvious that the level of numerical accuracy improves with the higher number of Gauss points, it was observed through a number of test runs that an optimum level of accuracy is achieved by the use of fourth and sixth order polynomials for rectangular and circular sections respectively. The use of a higher order polynomial for circular sections was necessitated by the added non-linearity involved due to the shape of the section. A typical example of a comparison of an "exact" analysis and the Gauss Quadrature method is shown in figure 2-2. Here the results of a rigorous fiber element analysis of a circular section are compared with a six point Gaussian integration scheme using the parameters listed in table 2-1.

2.2.2 Moment Curvature Analysis using Gauss Quadrature Technique

For a confined concrete column, the moment capacity of eccentric compressive concrete stress block consists of the following:

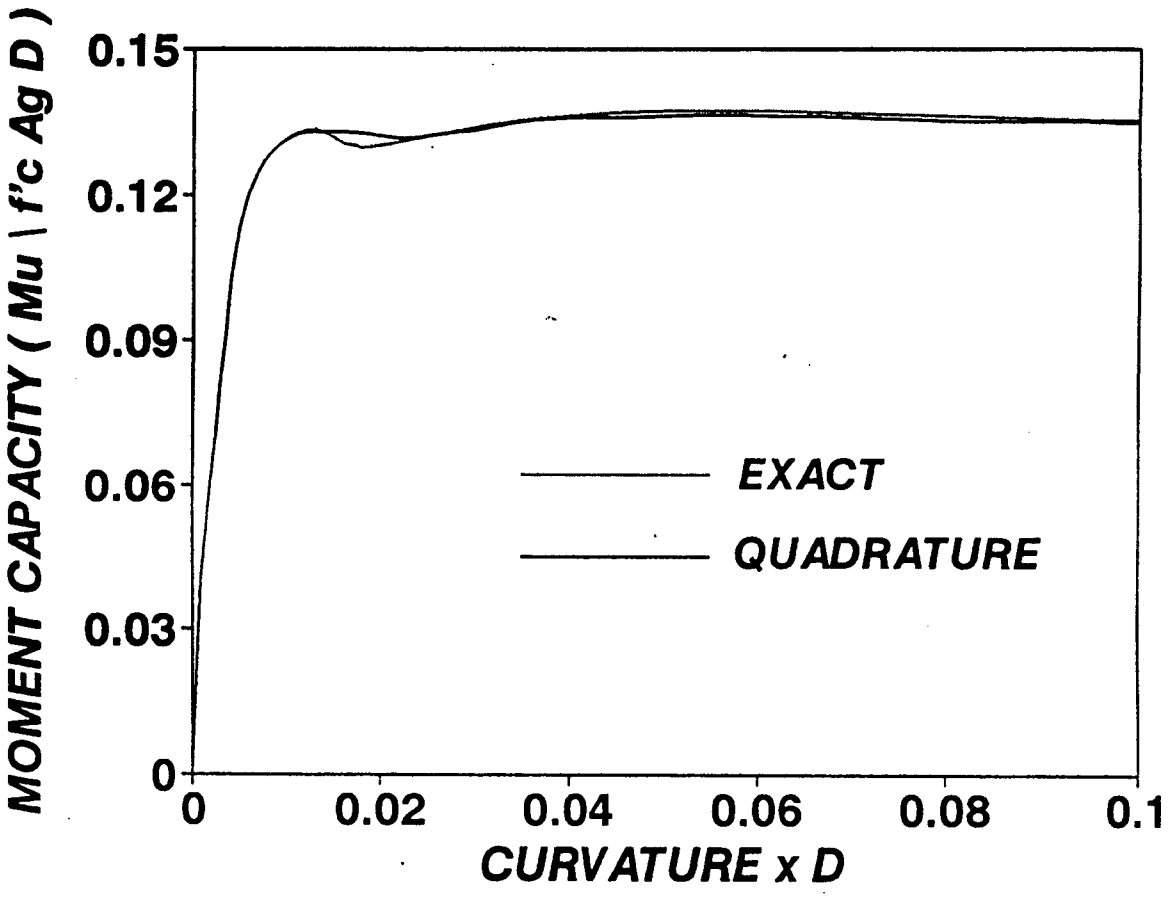

Figure 2-2 Comparison of the Exact and Gauss Quadrature Method for Moment Curvature Analysis.

$$M_u = M_s + M_c + M_{cc} \tag{2-10}$$

where M_u = the ultimate moment capacity of the section for a given curvature ϕ that also has an associated centroidal strain ε_0 and neutral axis depth c (figure 2-1), M_s = moment generated by the longitudinal reinforcement, and M_c, M_{cc} = moment generated by the cover and core concrete respectively.

Following the numerical integration scheme, the axial load contribution from the concrete (both cover and core) can be calculated as

$$C_c = c \sum_{k=1}^{6} w_k \left(b_o f_{co} + b_c f_{cc} \right)_k \tag{2-11}$$

where w_k = weight factor, b_o, b_c = breadth of the cover and confined core concrete, f_{co}, f_{cc} = cover and core concrete stress at the k-th Gauss point and c = depth of the neutral axis. The moment capacity of the reinforcing steel can be calculated taking moment of all the steel forces about the middle of the section. Hence,

$$M_s = \sum_i A_{si} f_{si} y_i \tag{2-12}$$

in which i = index to refer to the ith layer of steel, A_{si} = = area of steel in the ith layer, f_{si} = the steel stress corresponding to calculated steel strain, and y_i = the distance from the mid-depth reference axis to the center of the ith longitudinal reinforcement. Using the same integration scheme, the concrete contribution to the moment can be calculated as

$$M_c + M_{cc} = c \sum_{k=1}^{6} w_k y_k \left(b_o f_{co} + b_c f_{cc} \right)_k \tag{2-13}$$

where the symbols are as explained previously. The term y_k in equation (2-13) refers to the distance of the k-th Gauss point from the middle of the section.

If the centroidal strain ε_0 and curvature ϕ are known, the axial force (P_u) and the moment (M_u) can be easily calculated. But normally the inverse problem in which ε_0 and ϕ are

to be determined from known values of P_u and M_u, or a mixed problem, is encountered. In this case, some degree of iteration is required to find a solution. The Newton-Rhapson algorithm can be utilized for the purpose. Considering the first terms only in the Taylor's series expansion

$$\begin{Bmatrix} \varepsilon_{0_{i+1}} \\ \phi_{i+1} \end{Bmatrix} = \begin{Bmatrix} \varepsilon_{0_i} \\ \phi_i \end{Bmatrix} + \begin{Bmatrix} \Delta\varepsilon_{0_i} \\ \Delta\phi_i \end{Bmatrix} \tag{2-14}$$

where the incremental strain $\Delta\varepsilon_{0_i}$ and curvature $\Delta\phi_i$ are determined from

$$\begin{Bmatrix} \Delta P_{u_i} \\ \Delta M_{u_i} \end{Bmatrix} = \begin{bmatrix} \frac{\partial P_u}{\partial \varepsilon_0} & \frac{\partial P_u}{\partial \phi} \\ \frac{\partial M_u}{\partial \varepsilon_0} & \frac{\partial M_u}{\partial \phi} \end{bmatrix} \begin{Bmatrix} \Delta\varepsilon_{0_i} \\ \Delta\phi_i \end{Bmatrix} \tag{2-15}$$

Using the first row of equation (2-15), $\Delta\varepsilon_{0_i}$ can be solved as

$$\Delta\varepsilon_{0_i} = \frac{\Delta P_{u_i} - \frac{\partial P_u}{\partial \phi}\Delta\phi_i}{\frac{\partial P_u}{\partial \varepsilon_0}} \tag{2-16}$$

where the partial differentials are evaluated using a numerical differentiation technique.

2.2.3 Stress-Strain Relations for Concrete and Steel

Appropriate stress strain models for confined and unconfined concrete need to be used for the evaluation of the concrete component of the moment. Although significant research has been performed on formulating appropriate stress-strain models (eg. Popovics (1973), Kent and Park (1971)), most of them are unable to accurately control the descending branch of concrete for both confined and unconfined cases. However, Tsai's (1988) equation, capable of describing the behavior of both confined and unconfined concrete fairly satisfactorily, was chosen for describing the stress-strain behavior of concrete. The parameters to be used in the equation are based on the recommendations made by Chang and Mander (1994). These were calibrated against actual experiments to improve the quality of analytical predictions. The stress-strain

model (refer to figure 2-3) together with the parameters necessary for determining the confined concrete behavior are described in Appendix A.

Reinforcing Steel Stress-Strain Relations: Reinforcing steel forms an important component of structural concrete. Hence, accurate modeling of its behavior is important. For nominal strength calculations, an elasto-perfectly-plastic stress-strain model is customarily assumed. However, for a rigorous moment-curvature analysis capturing the effects of the strain-hardening branch is important since large moment capacity of the section may be obtained at very large strains.

In this study, the stress-strain behavior of reinforcing steel considering the strain hardening branch can be accurately represented by the single relationship suggested by Chang and Mander (1994), which is given by

$$f_s = \frac{E_s \varepsilon_s}{\left\{1 + \left|\frac{E_s \varepsilon_s}{f_y}\right|^{20}\right\}^{0.05}} + \left(\frac{1 + sign(\varepsilon_s - \varepsilon_{sh})}{2}\right)(f_{su} - f_y)\left[1 - \left|\frac{\varepsilon_{su} - \varepsilon_s}{\varepsilon_{su} - \varepsilon_{sh}}\right|^p\right] \qquad (2\text{-}17)$$

in which, ε_{sh} = strain hardening strain, f_{su} = ultimate stress, E_{sh} = strain hardening modulus, ε_{su} = ultimate strain of reinforcement and the power p is given by

$$p = E_{sh}\frac{\varepsilon_{su} - \varepsilon_{sh}}{f_{su} - f_y} \qquad (2\text{-}18)$$

Based on the Chang and Mander model (1994), the stress-strain curves for typical grades of steel reinforcement are plotted in figure 2-3.

2.3 Nominal Moment Capacity

The nominal moment capacity of a section (M_n) is derived from the code specified nominal material strength properties. Thus, the nominal moment capacity of a concrete section is the capacity of the section calculated with the following assumptions:

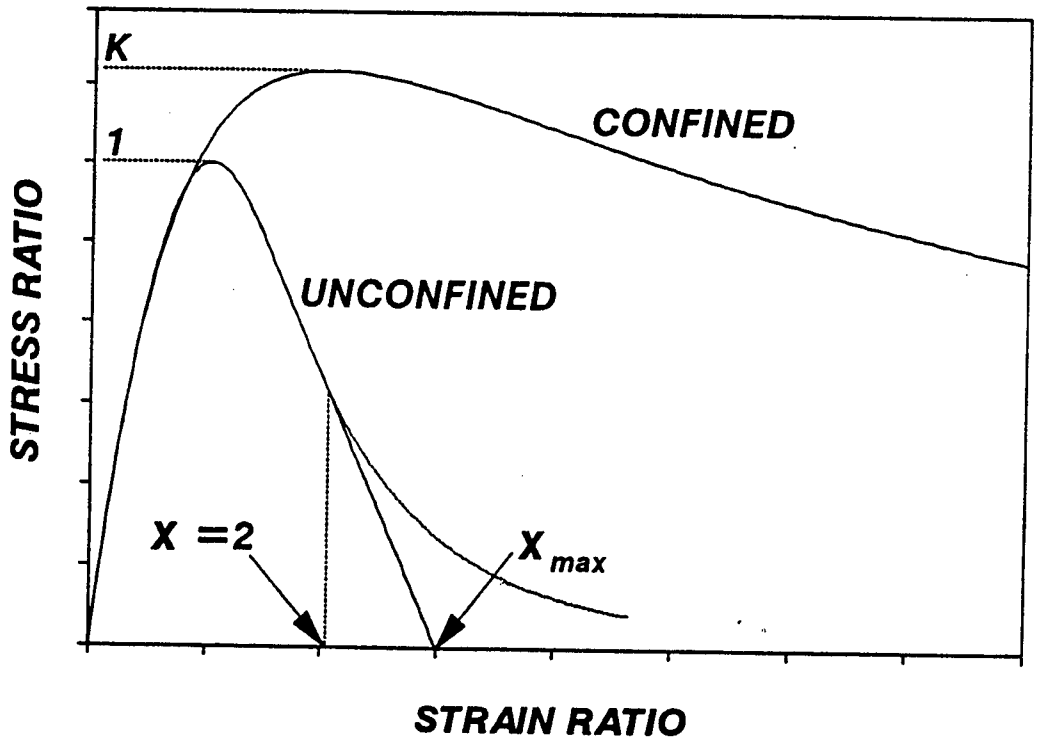

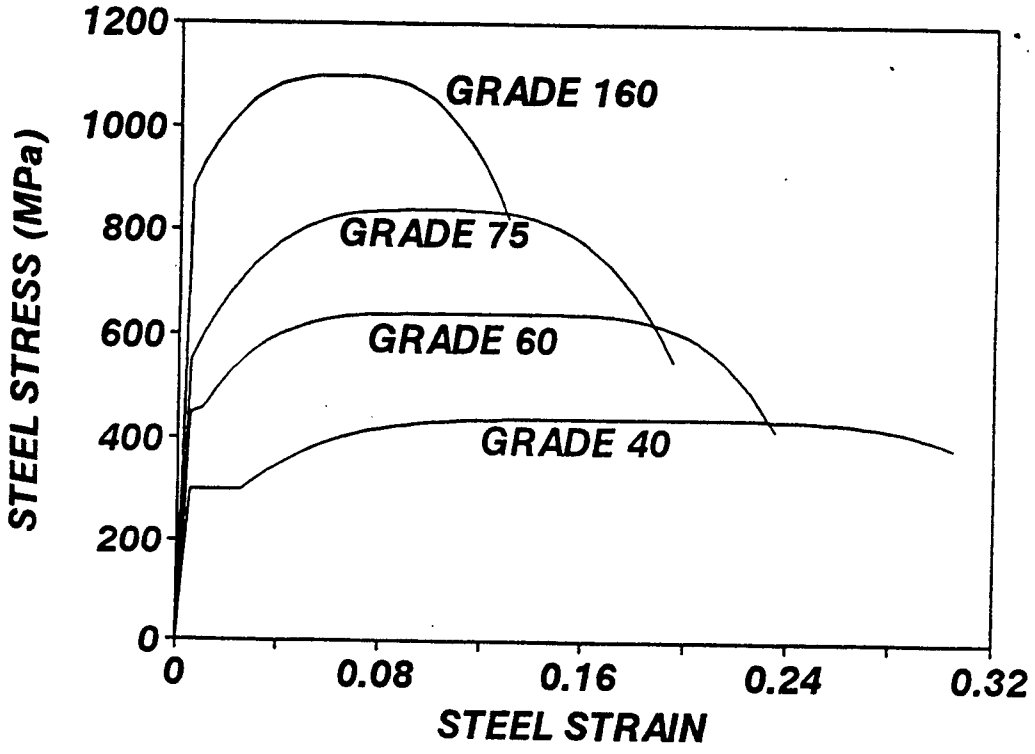

Figure 2-3 Constitutive Relations for Unconfined and Confined Concrete and Reinforcing Steel.

1) The whole section consists of unconfined concrete with a strength of f_c'.

2) Ultimate compression strain of 0.003 exists at the extreme compression fiber. Hence, the concrete stress can be represented by a Whitney type stress block of magnitude $\alpha_1 f_c'$ and depth $\beta_1 c$, c being the neutral axis depth. The values of the stress block parameters are discussed in detail in section 4.

3) Elasto-perfectly plastic stress-strain curve for steel is assumed. Thus

$$f_s = E_s \varepsilon_s \tag{2-19}$$

in which E_s = Young's Modulus, ε_s = strain at any stress f_s, f_y = yield stress. Using Chang and Mander's model, the bilinear curve can be represented by a single equation

$$f_s = \frac{E_s \varepsilon_s}{\left\{1 + \left|\frac{E_s \varepsilon_s}{f_y}\right|^{25}\right\}^{0.04}} \tag{2-20}$$

The nominal moment capacity of a section consists of the following:

i) Moment due to compression stress block (M_{cn}).

ii) Moment due to reinforcing steel layers (M_{sn}).

i) Moment Due to Compression Stress Block

This is calculated by considering stress block parameters defined by AASHTO/ACI codes (discussed in detail in section 4) and using the unconfined concrete strength. Hence, nominal moment of the concrete stress block with respect to mid-axis of the section is

$$\frac{M_{cn}}{f_c' A_g D} = 0.5 \alpha \beta_1 \left(\frac{c}{D}\right)\left[1 - \beta_1 \left(\frac{c}{D}\right)\right] \tag{2-21}$$

where α, β_1 = stress-block parameters of unconfined concrete as defined by AASHTO/ACI codes, D = overall depth, c = is the neutral axis depth from the top fiber of the compression zone and is calculated as

$$\left(\frac{c}{D}\right) = \frac{C_c}{\alpha\, \beta_1 f_c' A_g} \qquad (2\text{-}22)$$

ii) Moment Due to Reinforcing Steel Layers

Moment carried by the reinforcing steel is same as calculated as in equation 2-10 by calculating f_{si} using the AASHTO/ACI code bilinear model for steel.

The section dimensions, strain compatibility and force equilibrium for nominal moment capacity of a section are shown in figure 2-1 for both rectangular and circular columns.

2.4 EXAMPLES

The moment overstrength theory presented so far is best illustrated with a numerical example. Two illustrative analyses are performed. The results are plotted in figure 2-4. The first example (figure 2-4(a)) shows the effect of confinement on the moment overstrength. In this case, a constant axial load is maintained so that $P_u = 0.1 f_c' A_g$, while the confinement ratio (refer to Appendix A) is varied from $K = 1.0$ to $K = 2.0$. From the analysis it is evident that the column section with a higher level of confinement provides a higher value of the overstrength capacity.

The second example (figure 2-4(b)) shows the effect of axial load on overstrength capacity. For this purpose a column section is chosen with a confinement ratio of 1.5 in the core. The axial load is varied from 0.0 to 0.5. The column with a higher axial load gives a higher value of the maximum moment. The overstrength factor however, is larger at higher and lower axial loads respectively. The column section chosen is $915\,mm$ in diameter with a clear cover $51\,mm$ up to the hoop reinforcement which consists of $13\,mm$ diameter spirals. Concrete in the column is assumed to have an unconfined compression strength of $30\,MPa$ and $29\,mm$ diameter longitudinal steel of yield strength $450\,MPa$.

2.5 CONCLUSIONS

In this section, a complete procedure to determine the ultimate moment capacity of concrete columns was presented. Expressions were derived for the moment capacity of confined and unconfined concrete columns using the Gauss Quadrature numerical integration scheme. It was that the procedure of moment-curvature analysis can be easily automated and lends itself for application in spreadsheet-type programming. This is very useful, specially for highly irregular cross sections where the usual fiber element method may prove time consuming. This procedure was used to conduct moment curvature analysis of a number of concrete sections to determine their overstrength capacity and hence conduct a parametric study on the overstrength factors. The results of the parametric study are presented in the next section.

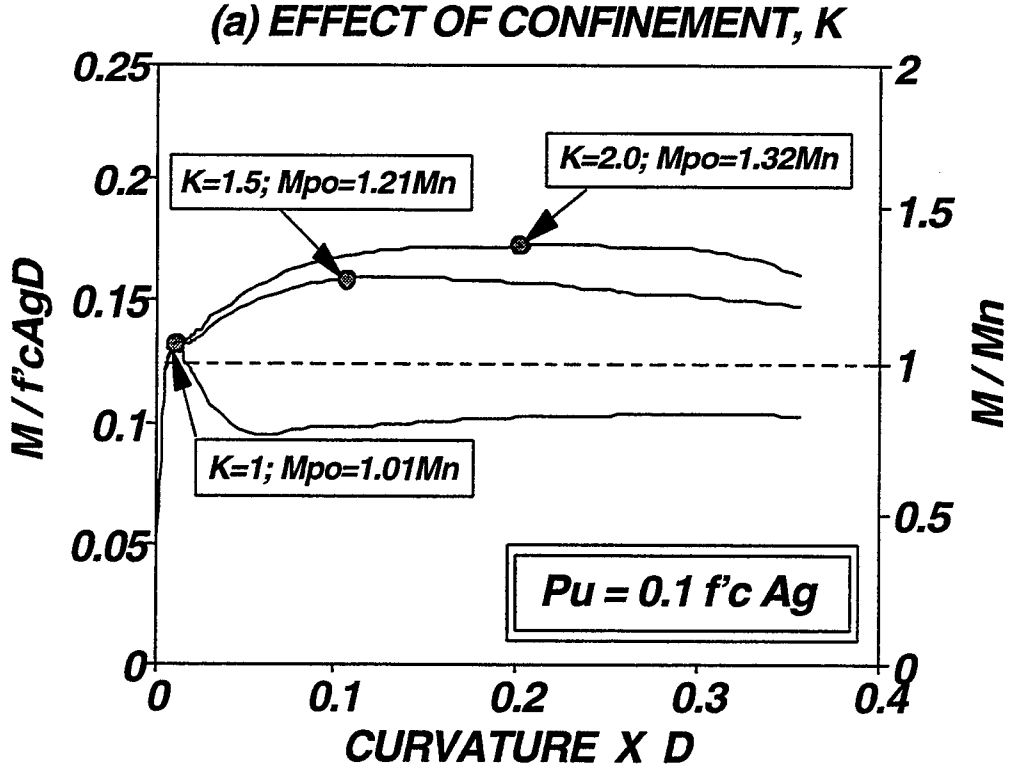

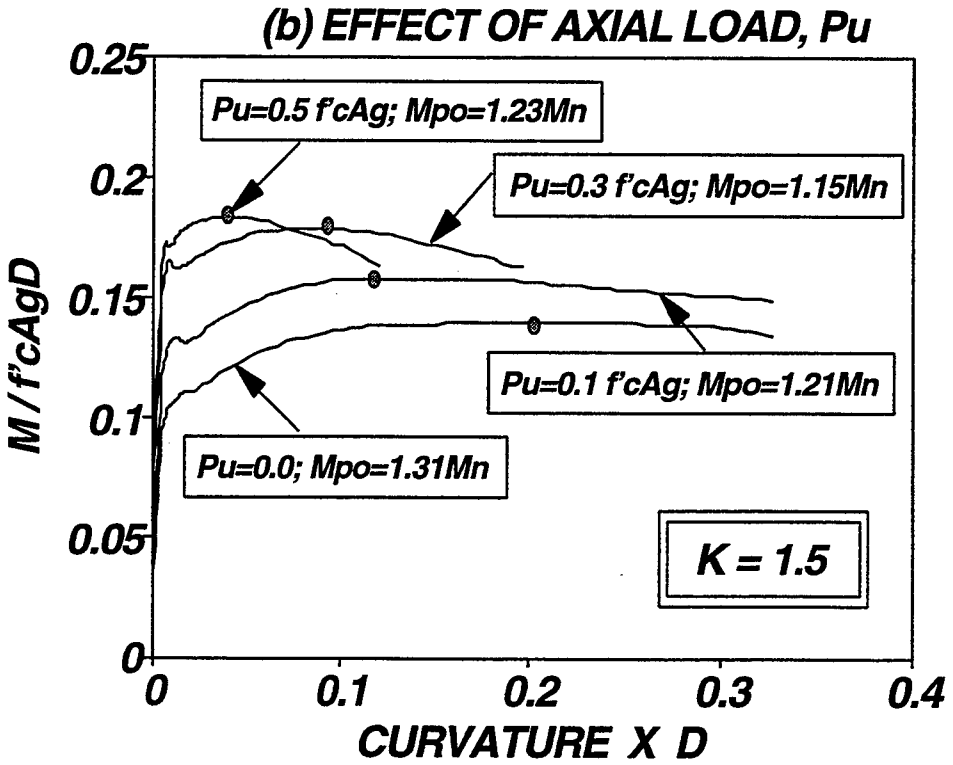

Figure 2-4 Moment-Curvature Analysis of Circular Column (f'_c=30 MPa, f_y=450 Mpa) showing (a) effect of confinement and (b) effect of axial load on overstrength.

SECTION 3
MOMENT OVERSTRENGTH ANALYSIS FOR COLUMN SECTIONS

3.1 INTRODUCTION

In the seismic design of structures using the capacity design philosophy, the designer chooses a hierarchy of plastic failure mechanisms. Flexural inelastic modes of deformation which provide ductility are preferred and all undesirable inelastic deformation modes which potentially could lead to brittle failure are prevented by deliberately amplifying their strengths in comparison to desirable modes. Flexural modes, being ductile, are the preferred inelastic modes of deformation. Moreover, brittle regions are protected by ensuring that their strength exceeds the demands originating from the maximum flexural strength of plastic zones. Hence, determination of overstrength moment of flexural plastic zones beyond their ideal strength is of paramount importance in capacity design. This section demonstrates the methodology of overstrength factor determination using the moment-curvature analysis for concrete columns presented in the previous section. Results of a parametric study are presented for different concrete sections showing the effects of different constituent material properties and geometric factors on overstrength. The results are discussed and compared with experimental observations.

3.2 OVERSTRENGTH FACTORS USING MOMENT CURVATURE ANALYSIS

Overstrength of a section (S_o) is the strength above the nominal strength taking into account all possible factors that may contribute to strength exceeding the nominal value. For a confined concrete column, the following factors contribute to overstrength:

i) Compression strength enhancement of the concrete due to its confinement.

ii) Additional strength enhancement of steel due to strain-hardening at large deformations.

iii) Steel strengths greater than the specified yield strength.

The overstrength of a section is related to the nominal strength (S_n) of the same section by

$$S_o = \lambda_o S_n \tag{3-1}$$

where λ_o = the overstrength factor due to strength enhancement of the constituent materials. This is an important property that must be accounted for in the capacity design when large ductility demands are imposed on the structure since brittle elements must possess strengths exceeding the maximum feasible strength (overstrength) of ductile plastic hinge zones.

To quantify the hierarchy of strength in ductile structures, it is convenient to express the overstrength of a member in flexure ($S_o \equiv M_{po}$) at a specified section in terms of the nominal flexural strength ($S_n \equiv M_n$) at the same section. The ratio so formed,

$$\lambda_{mo} = \frac{M_{po}}{M_n} \tag{3-2}$$

is defined as the moment overstrength factor. The moment overstrength factor (λ_{mo}) of a plastic hinge zone can be obtained by determining the maximum moment capacity of a confined concrete section. The maximum moment is found by conducting a moment-curvature analysis of the section. Hence using the proposed analytical procedure, parametric studies were conducted to assess overstrength factors for unconfined and confined columns. The results are presented below.

3.3 Unconfined Concrete Columns

The effects of the following parameters on moment overstrength of plastic hinge zones of unconfined concrete columns was studied and the results are plotted in figure 3-1 and 3-2 for circular and rectangular sections, respectively.

(i) Percentage of Steel: Analytical studies were conducted for following percentages of steel: 0.5, 1.0, 1.5, 2.0. It can be observed from the figures 3-1 and 3-2 that the effect of percentage of steel on moment overstrength is not very significant in the medium axial load levels for both circular and rectangular sections. However, for both column shapes, overstrength increases with decreasing percentage of steel at high axial load levels. Similar results are also noticed at low axial load levels both for circular and rectangular sections. Note that the effect of percentage of steel on rectangular sections is more pronounced than circular sections especially at low axial load levels.

(ii) Strength of Steel: The following strengths of steel were considered, f_y = 300, 450, 550, 870 *MPa*. It may be observed that increasing the yield strength of steel increases moment overstrength at high levels of axial load for both circular and rectangular sections. The same trend is also observed even at low levels of axial load for both circular and rectangular sections.

(iii) Concrete Strength: Parametric studies were conducted for concrete compressive strengths of f_c'=30, 45, 60 *MPa*. From figures 3-1 and 3-2, it may be observed that the effect of concrete strength is minimal on moment overstrength at high levels of axial load. For rectangular sections this effect is more significant when $P_u < 0.2 f_c' A_g$ when the overstrength tends to be affected by the variation in concrete strengths.

It can be concluded from the above observations that moment overstrength in unconfined concrete columns is most pronounced at low ($P_u < 0.15 f_c' A_g$) and high ($P_u > 0.55 f_c' A_g$) levels of axial loads. The latter case rarely exists for bridge columns, whereas for building columns it is the general norm. In summary, the contribution to overstrength in unconfined concrete columns is due to large strains in the flexural reinforcement at low axial load levels. The effect of strain-hardening in the flexural reinforcement leads to moment overstrength at high ductility factors. Based on this analysis, it is recommended that a value of λ_{mo} = 1.2 be adopted as a conservative estimate of overstrength in unconfined concrete columns.

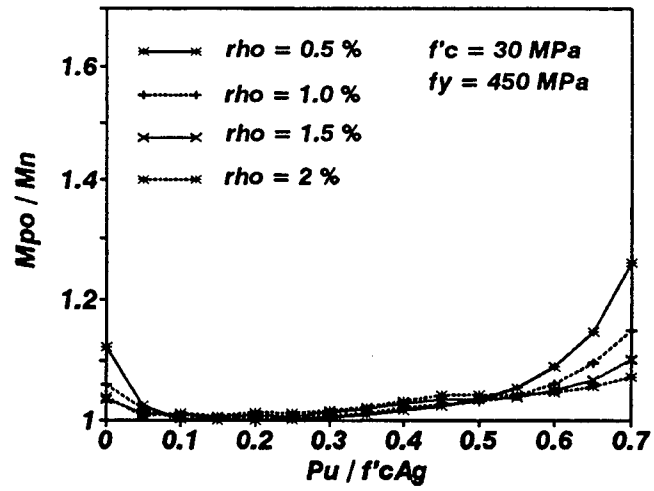

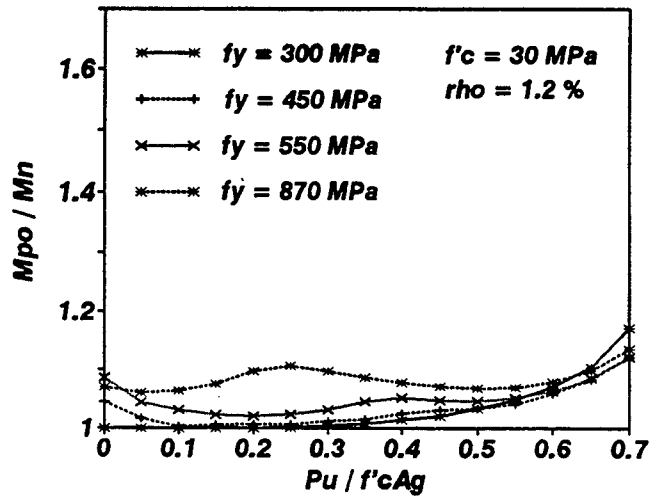

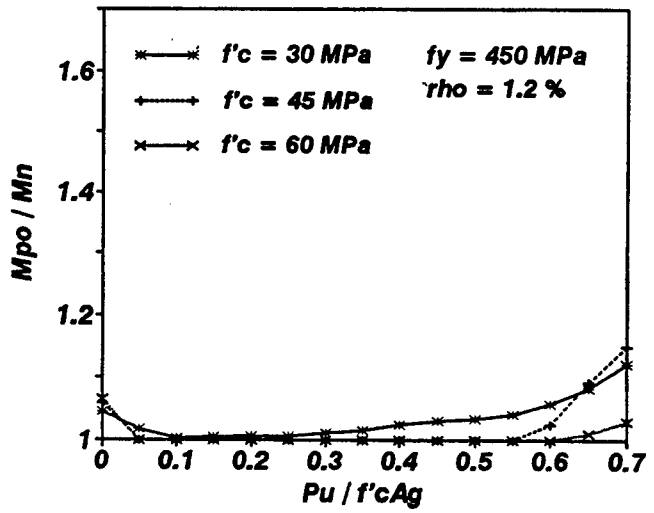

Figure 3-1 Effect of Various Parameters on Moment Overstrength of Unconfined Circular Columns.

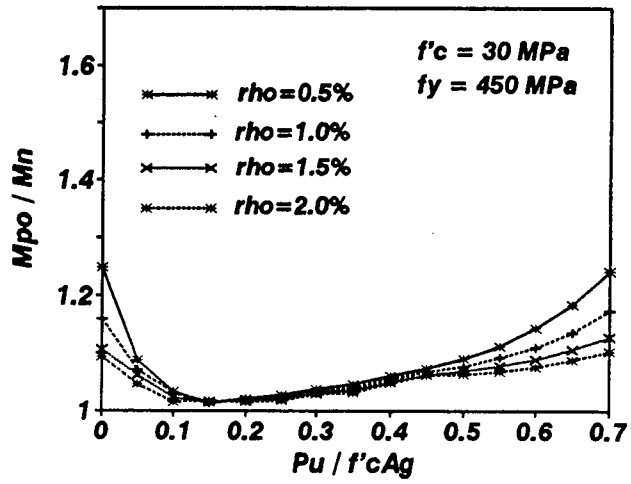

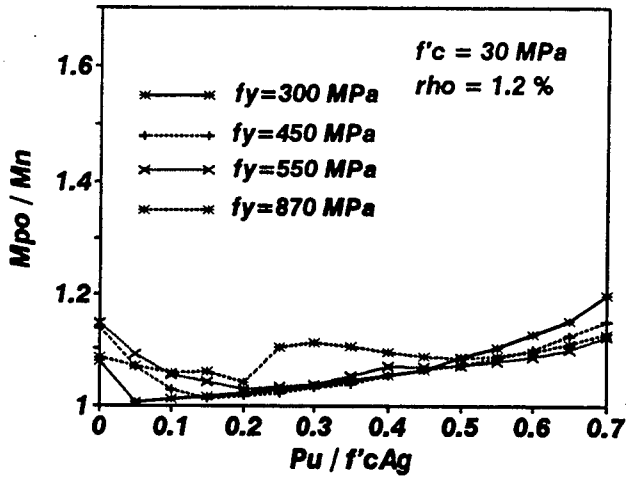

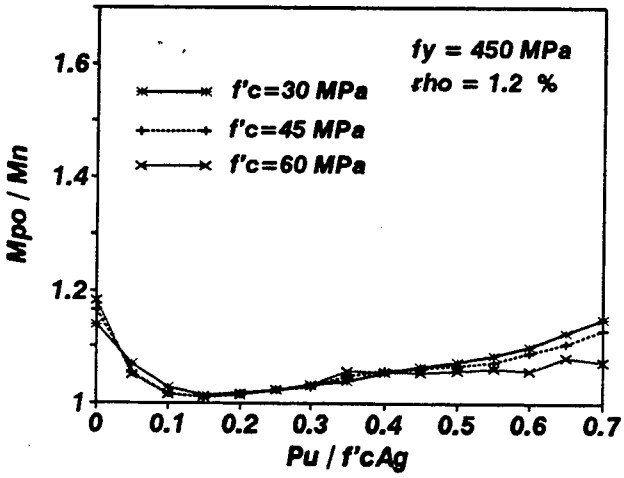

Figure 3-2 **Effect of Various Parameters on Moment Overstrength of Unconfined Rectangular Columns.**

3.4 Confined Concrete Columns

As compared to unconfined columns, significant moment overstrength may be observed at both high and low levels of axial loads for confined concrete columns. At high axial load levels, overstrength is due to the increased influence of the confined compression strength of concrete. At low levels of axial loads, larger moment overstrength arises because large compression strains can be sustained in the steel leading to strain hardening of the steel. This subsection presents the results of the parametric study on confined concrete columns under combined axial load and flexure. Studies were conducted to determine the effect of following parameters on the moment overstrength factor for the standard confinement ratios, $K(=f'_{cc}/f'_c)$ = 1.0, 1.2, 1.5, 2.0:

3.4.1 Effect of Longitudinal Steel Volume

Analytical studies were conducted for following volumes of steel: 0.5, 1.0, 1.5, 2.0 and the results are plotted in figures 3-3 and 3-4 for circular and rectangular sections. It may be observed from these figures that at low levels of axial loads, moment overstrength increases with increasing steel volume. At low levels of axial loads, maximum moment takes place at very high strains and is mainly due to the strain-hardening effects of steel. Hence, as the proportion of the steel contribution to total moment increases with increasing steel volumes, the moment overstrength factor also increases.

For higher levels of axial load, moment overstrength is not governed by the steel but rather by the confined concrete contribution. This is due to the fact that at higher values of axial load, much of the flexural steel remains in the elastic zone. In figures 3-5 and 3-6, the same data is presented in order of increasing confinement ratio corresponding to a particular longitudinal steel volume. The graphs clearly show the importance of the confined concrete strength in the computation of overstrength as the value of K influences the overstrength over the entire axial load range.

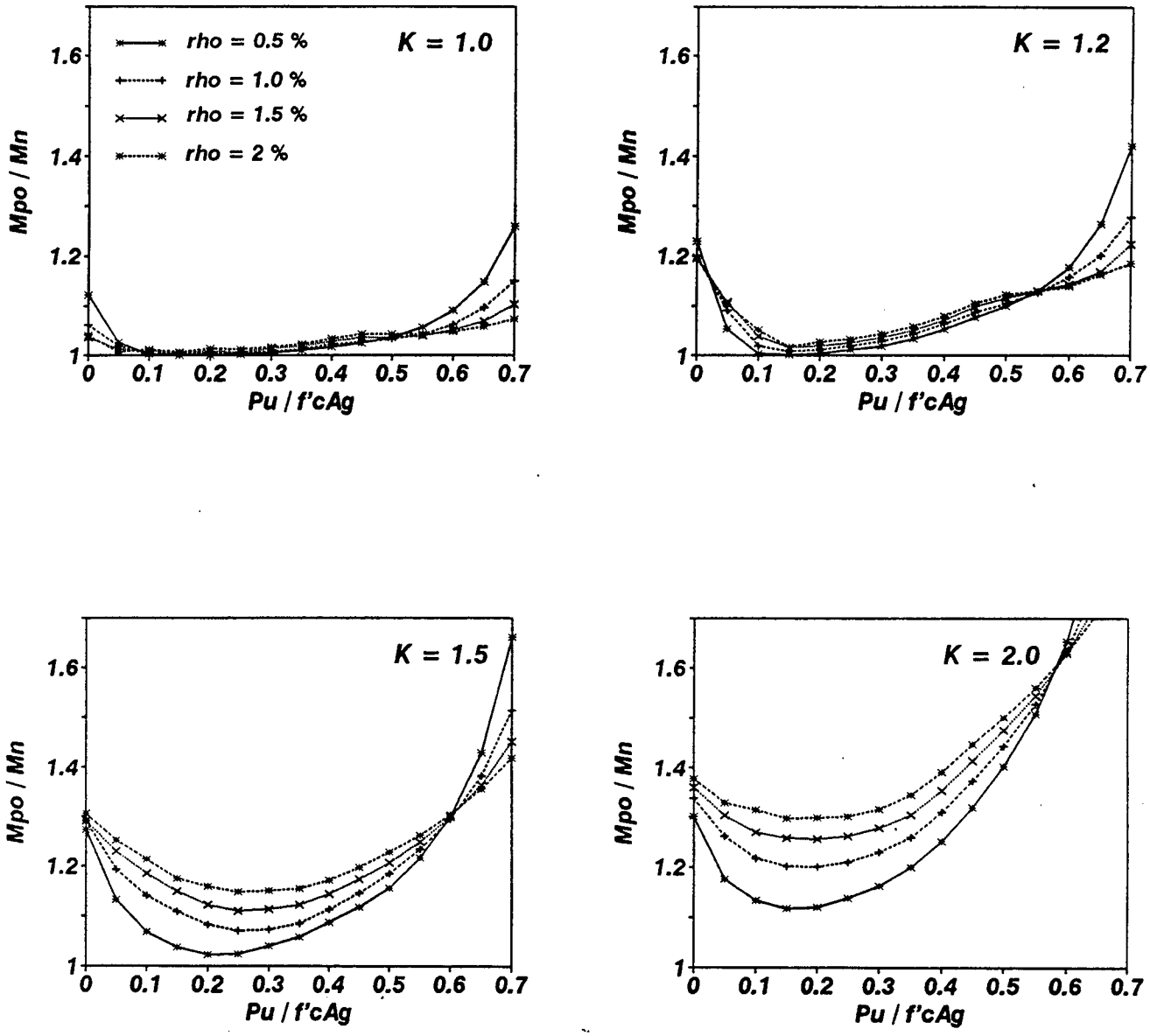

Figure 3-3 Effect of Longitudinal Steel Volume on Moment Overstrength for Circular Sections.

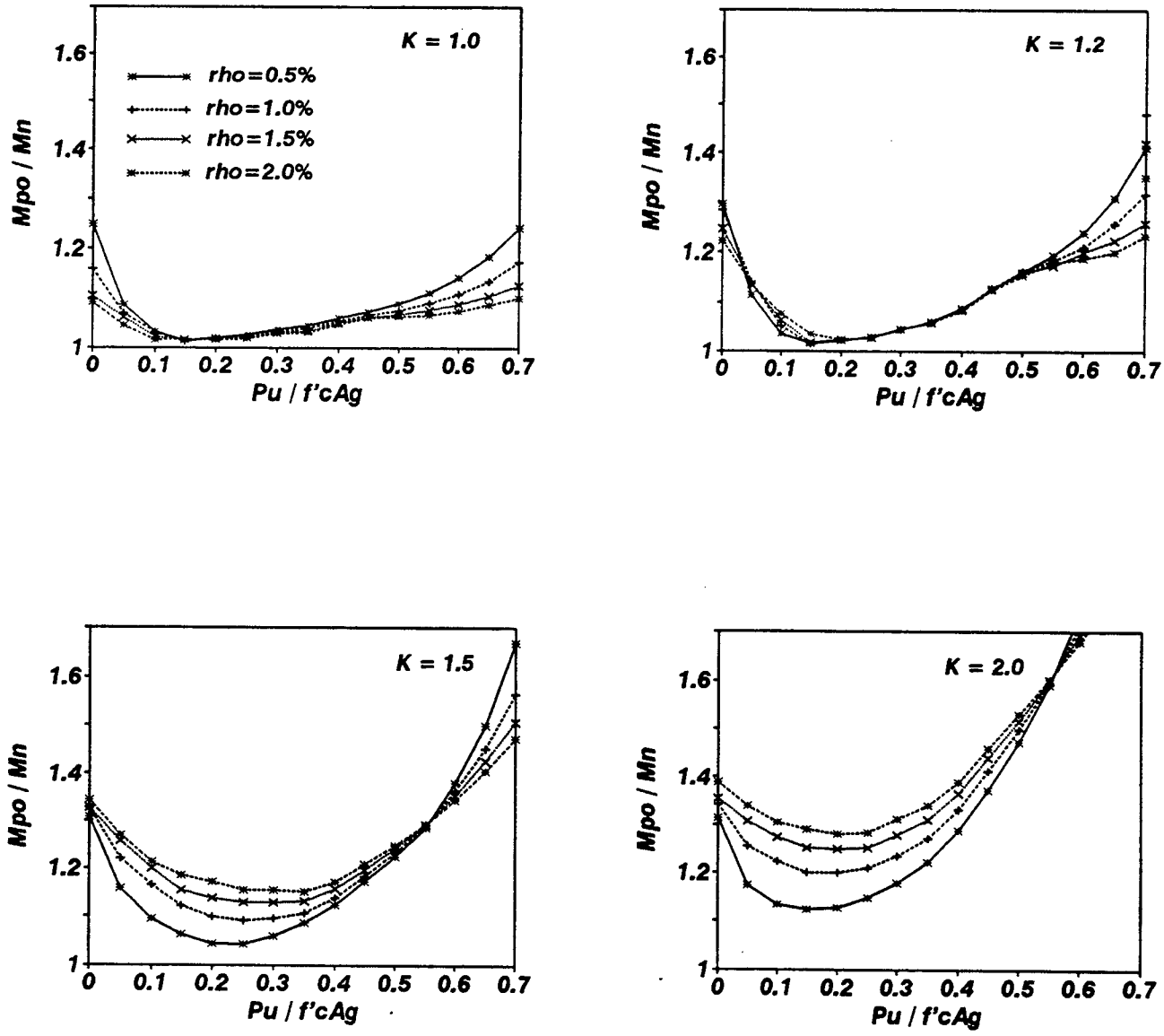

Figure 3-4 Effect of Longitudinal Steel Volume on Moment Overstrength for Rectangular Sections.

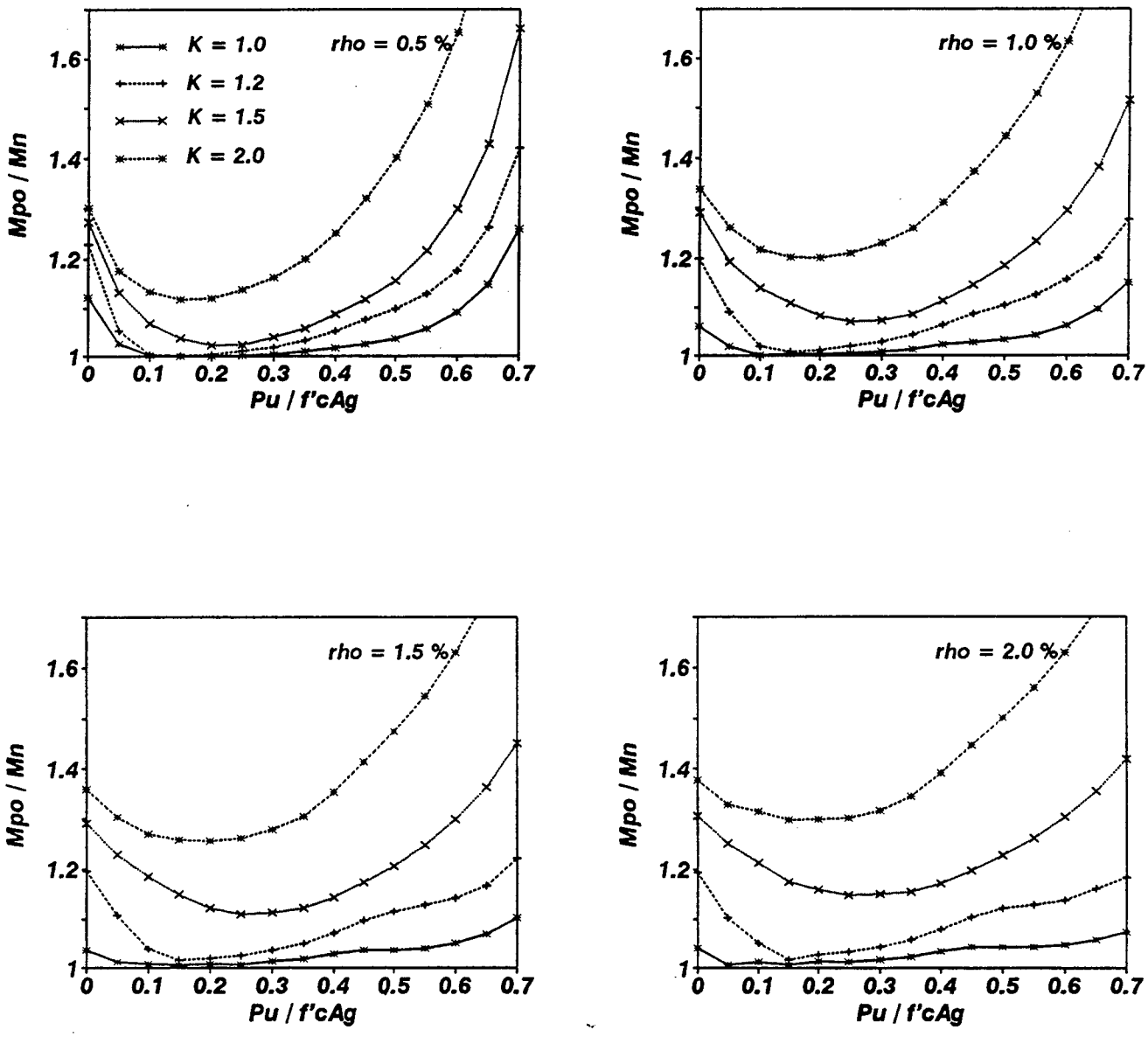

Figure 3-5 Influence of Longitudinal Steel Volume on Moment Overstrength for Circular Sections.

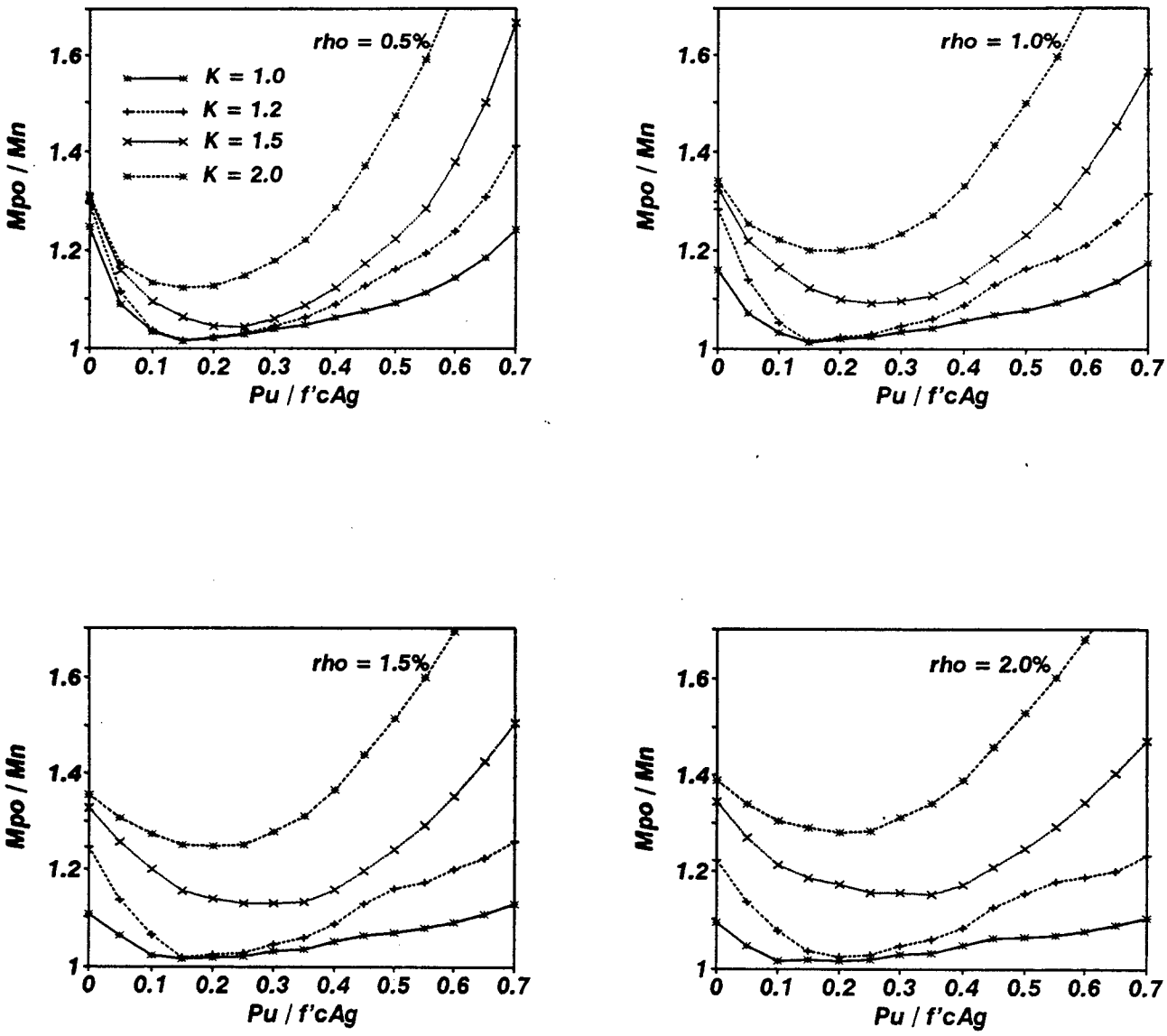

Figure 3-6 Influence of Longitudinal Steel Volume on Moment Overstrength for Rectangular Sections.

3.4.2 Effect of Longitudinal Steel Strength

The following steel strengths were considered, f_y = 300, 450, 550, 870 *MPa* and the results are shown in figures 3-7 and 3-8. It may be observed from these figures that at lower levels of axial loads, moment overstrength increases with increasing longitudinal steel strength. Steel moment from strain hardening depends upon ε_{su} , ε_{sh} and the ratio of f_{su}/f_y. As the steel strength increases, ε_{sh} and ε_{su} occur at much lower strain (figure 2-4) and high steel moments at lower strains are obtained where concrete moment is still high and therefore larger moment overstrength factors are obtained. Steel with $f_y = 870\,MPa$ differs from the normal behavior of lower strengths at low levels of axial load because ε_{sh} and ε_{su} occur at very low strains and hence at low axial loads, maximum moment occurs at strain, $\varepsilon_s > \varepsilon_{su}$ and hence lower moment overstrengths are observed. It is also observed that at high axial load levels, moment overstrength increases in the same way with higher steel strengths although the difference between various varieties of steel is less significant. This is because the moment overstrength factor (λ_{mo}) can be expressed as a combination of the concrete and steel capacities as explained below:

$$\lambda_{mo} = \frac{M_{po}}{M_n} = \frac{(M_c + M_{cc} + M_s)_o}{(\overline{M_c + M_{cc}} + M_s)_n} \qquad (3\text{-}3)$$

where M_{po} = the ultimate moment, M_n = the nominal moment, M_c, M_{cc} = the unconfined and confined concrete contribution to respective moments, M_s = the steel contribution to the respective moments. At high levels of axial load, due to the force equilibrium requirements, with increase in steel strength, C_c increases and hence moment of concrete, $(M_c + M_{cc})_o$ and $(\overline{M_c + M_{cc}})_n$ increases but increase in $(M_c + M_{cc})_o$ is much more than $(\overline{M_c + M_{cc}})_n$ and hence, with steel strength, moment overstrength increases as seen in equation 3-3. The effect of confinement for a particular steel strength is illustrated by figures 3-9 and 3-10 where the results are plotted in order of increasing confinement. As expected, the overstrength increases with confinement over the entire axial load range for both circular and rectangular sections.

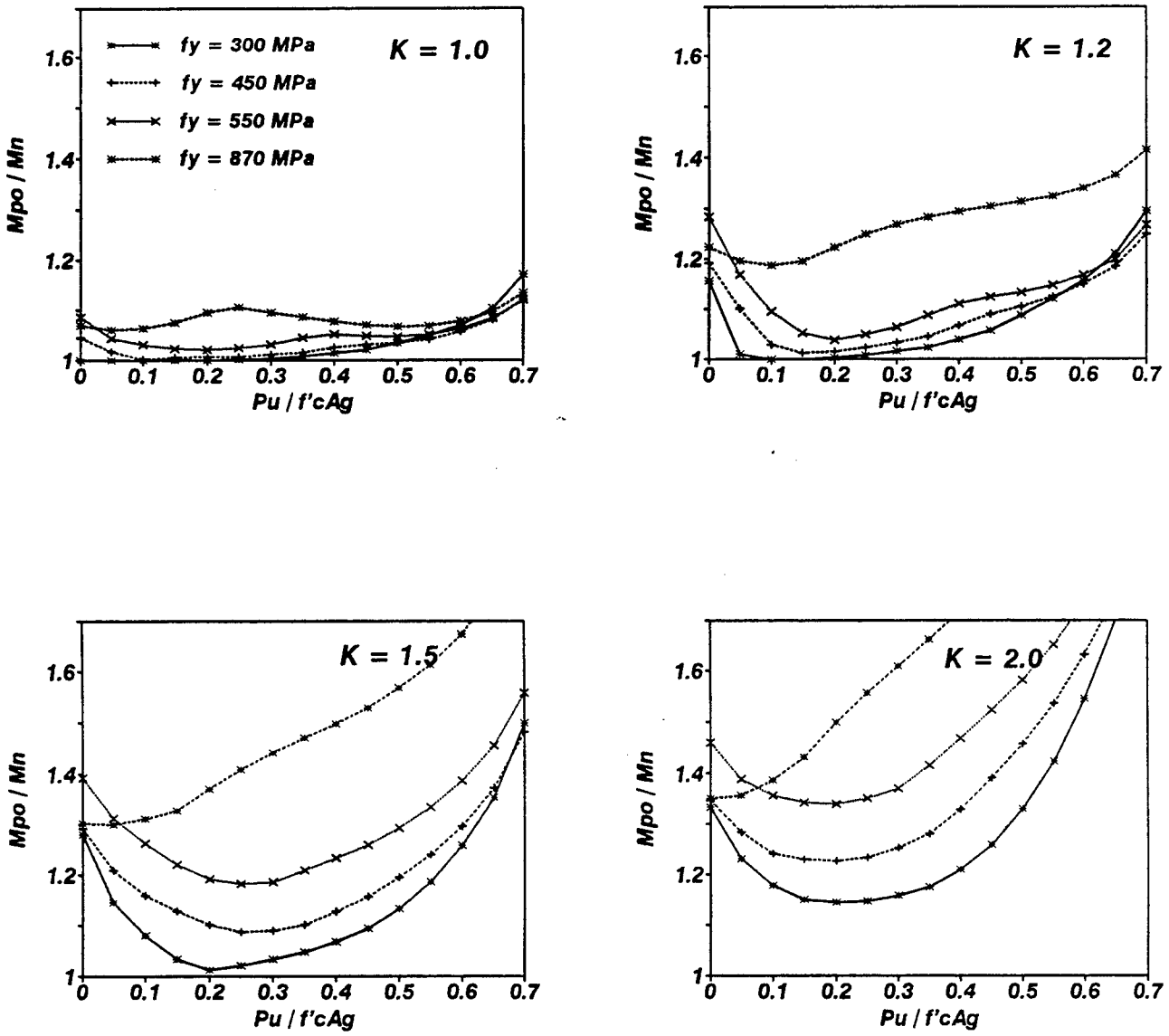

Figure 3-7 Effect of Longitudinal Steel Strength on Moment Overstrength for Circular Sections.

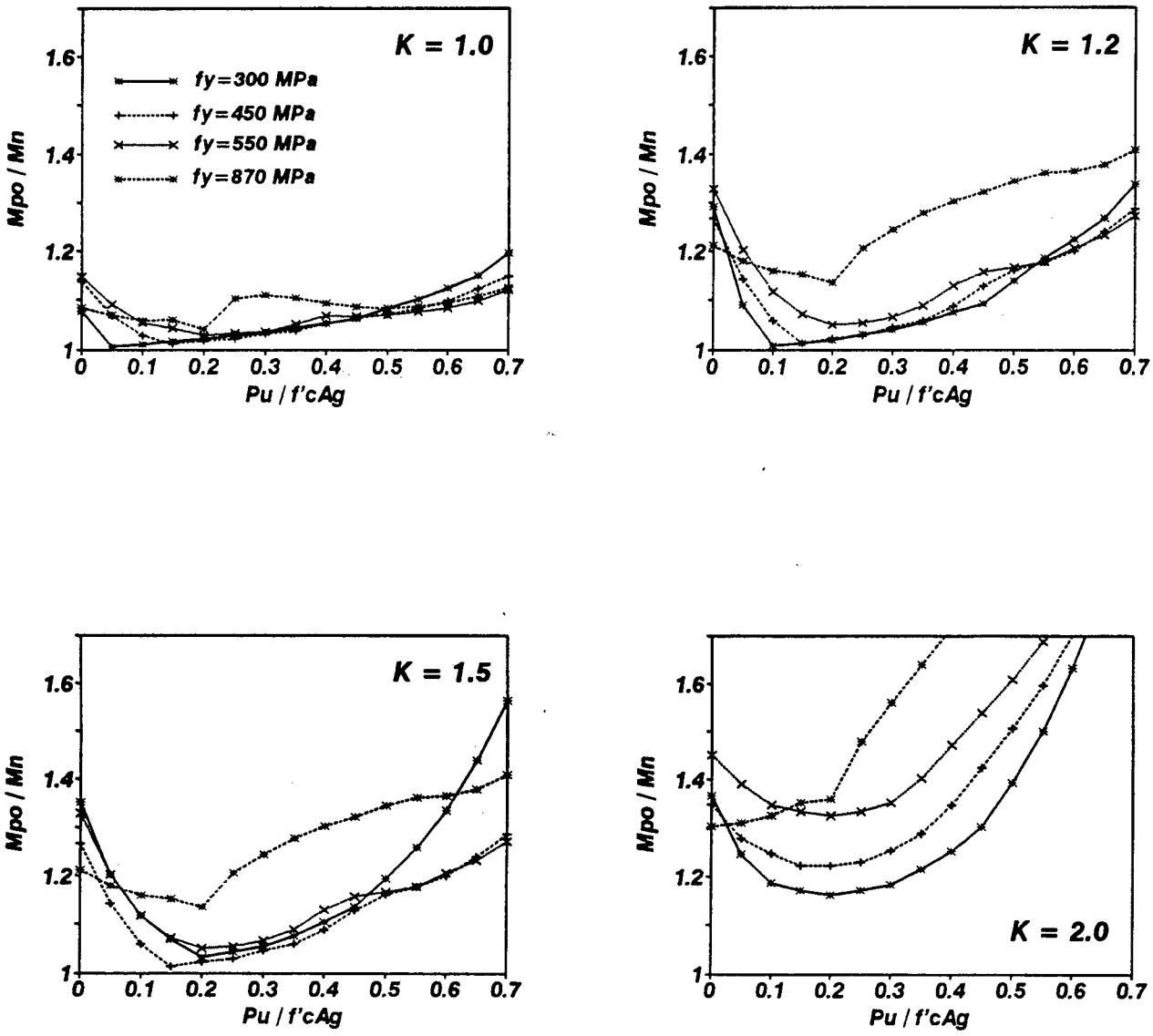

Figure 3-8 Effect of Longitudinal Steel Strength on Moment Overstrength for Rectangular Sections.

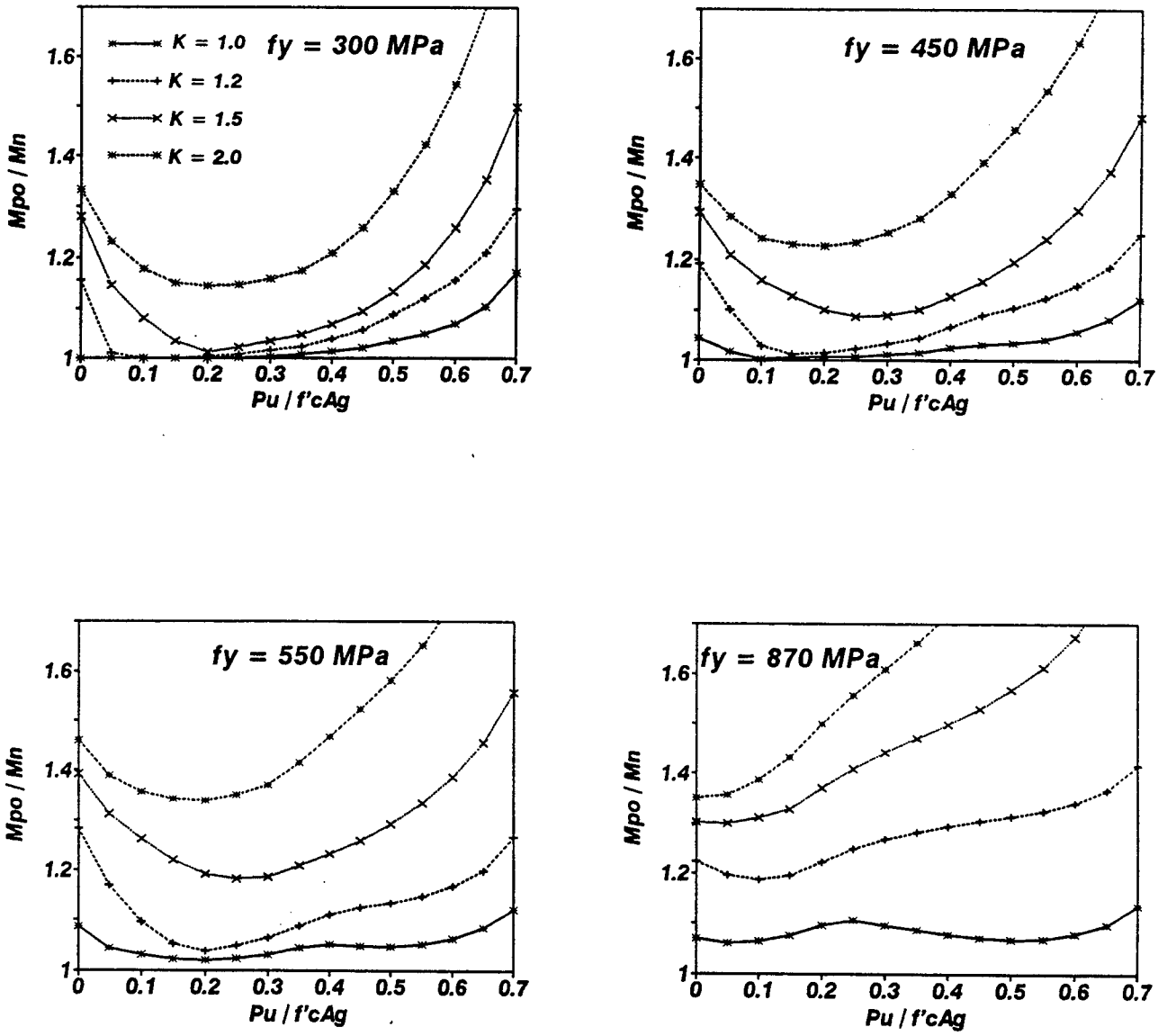

Figure 3-9 Influence of Longitudinal Steel Strength on Moment Overstrength for Circular Sections.

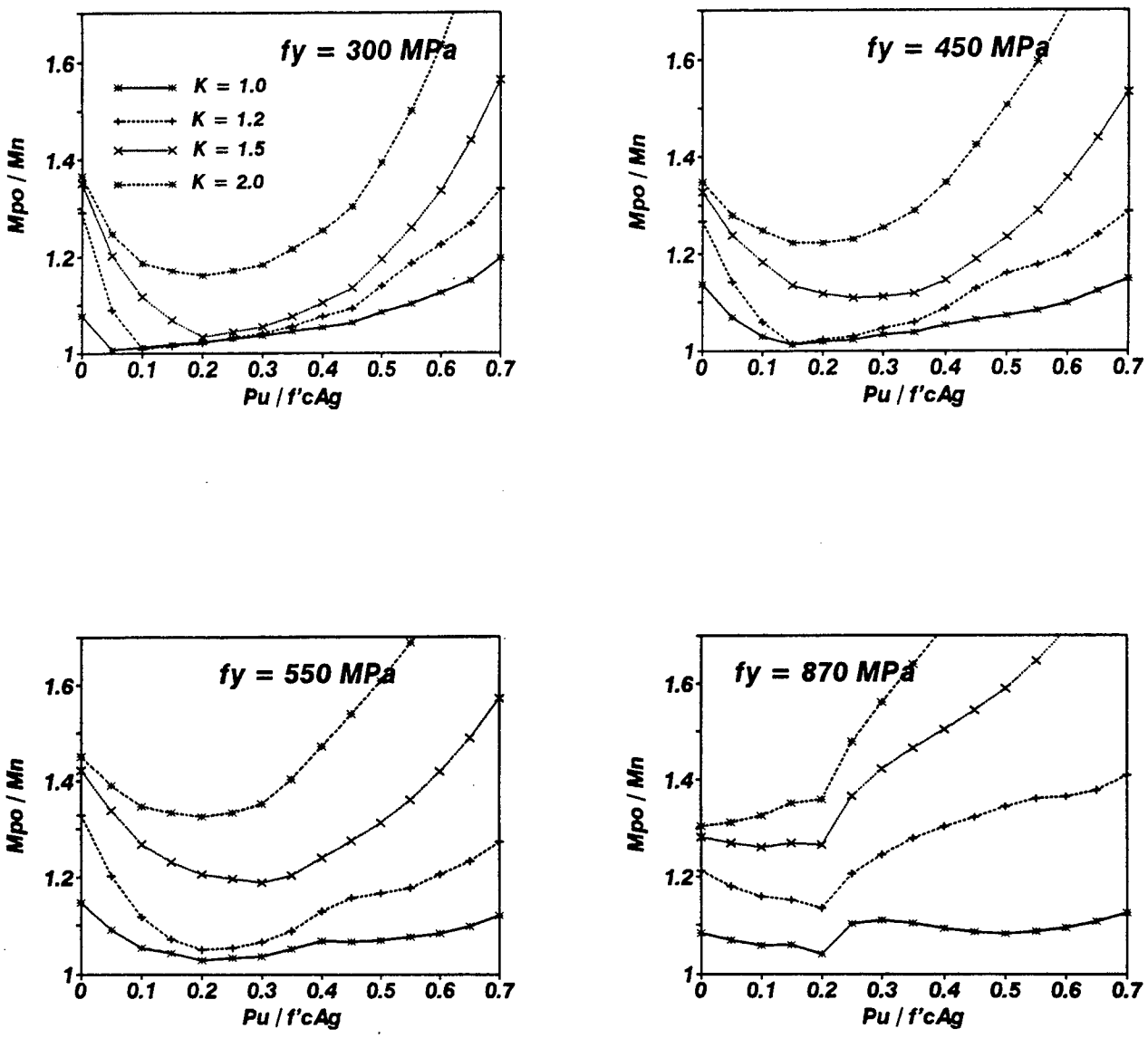

Figure 3-10 Influence of Longitudinal Steel Strength on Moment Overstrength for Rectangular Sections.

3.4.3 Effect of Concrete Strength

The studies were conducted for the following concrete maximum compressive strength, $f_c' = 30, 45, 60\,MPa$ and results plotted in figures 3-11 and 3-12, respectively. It is well known that as the compressive strength of concrete increases, concrete toughness (and hence ductility) decreases. Therefore, moment increase with increasing curvature takes place more slowly. However, at low levels of axial load, the maximum moment occurs at high strains where the concrete has little influence on the moment capacity, as demonstrated by similar overstrength factors obtained for all ranges of f_c' when $P_u < 0.05 f_c' A_g$. At high levels of axial load, moment capacity is dominated by the concrete component when the concrete with a higher strength has a more significant effect than a lesser strength variety. This is particularly observable at higher confinement where the overstrength tends to increase with higher concrete strengths beyond $P_u / f_c' A_g > 0.65$. The effect of confinement corresponding to any particular concrete strength is portrayed by the graphs in figures 3-13 and 3-14, where the overstrength increases with increasing concrete strength irrespective of sectional shape.

3.4.4 Effect of Longitudinal Steel Placement

The distance between the extreme compression fiber and the center of the transverse reinforcement has significant effect on moment overstrength as it determines the strain and hence the stress in the longitudinal reinforcement and the percentage of confined concrete in the section. This effect was studied by considering the following values of the distance between the extreme compression fiber and the center of the transverse reinforcement normalized with respect to the total depth of the section, $(0.0, 0.1, 0.2)$. The results obtained are plotted in figures 3-15 and 3-16.

Moment overstrength decreases with increasing distance between the extreme compression fiber and the compression reinforcement and it is observed that axial load level does not have any effect on the behavior of overstrength factors. This occurs because with increase

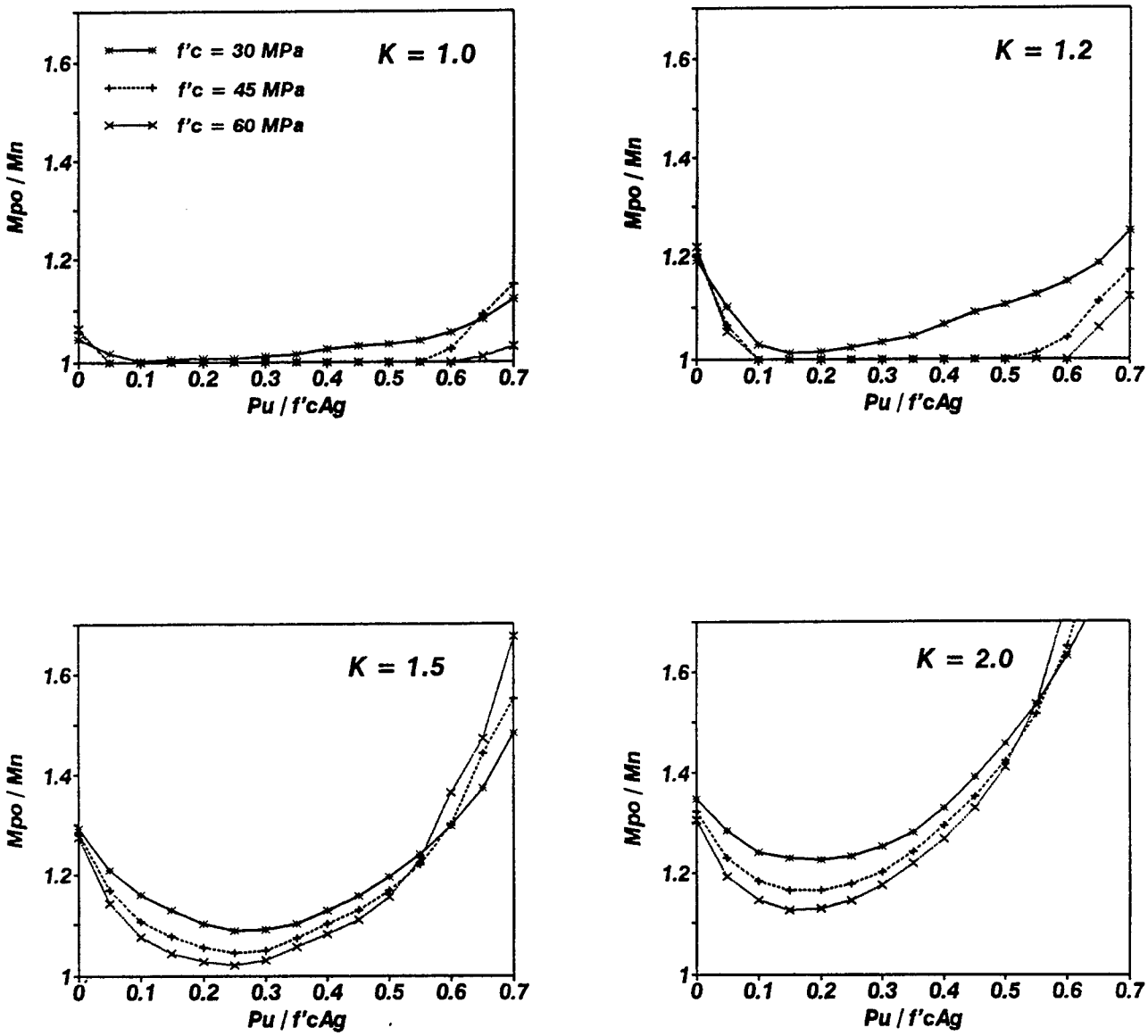

Figure 3-11 Effect of Concrete Strength on Moment Overstrength for Circular Sections.

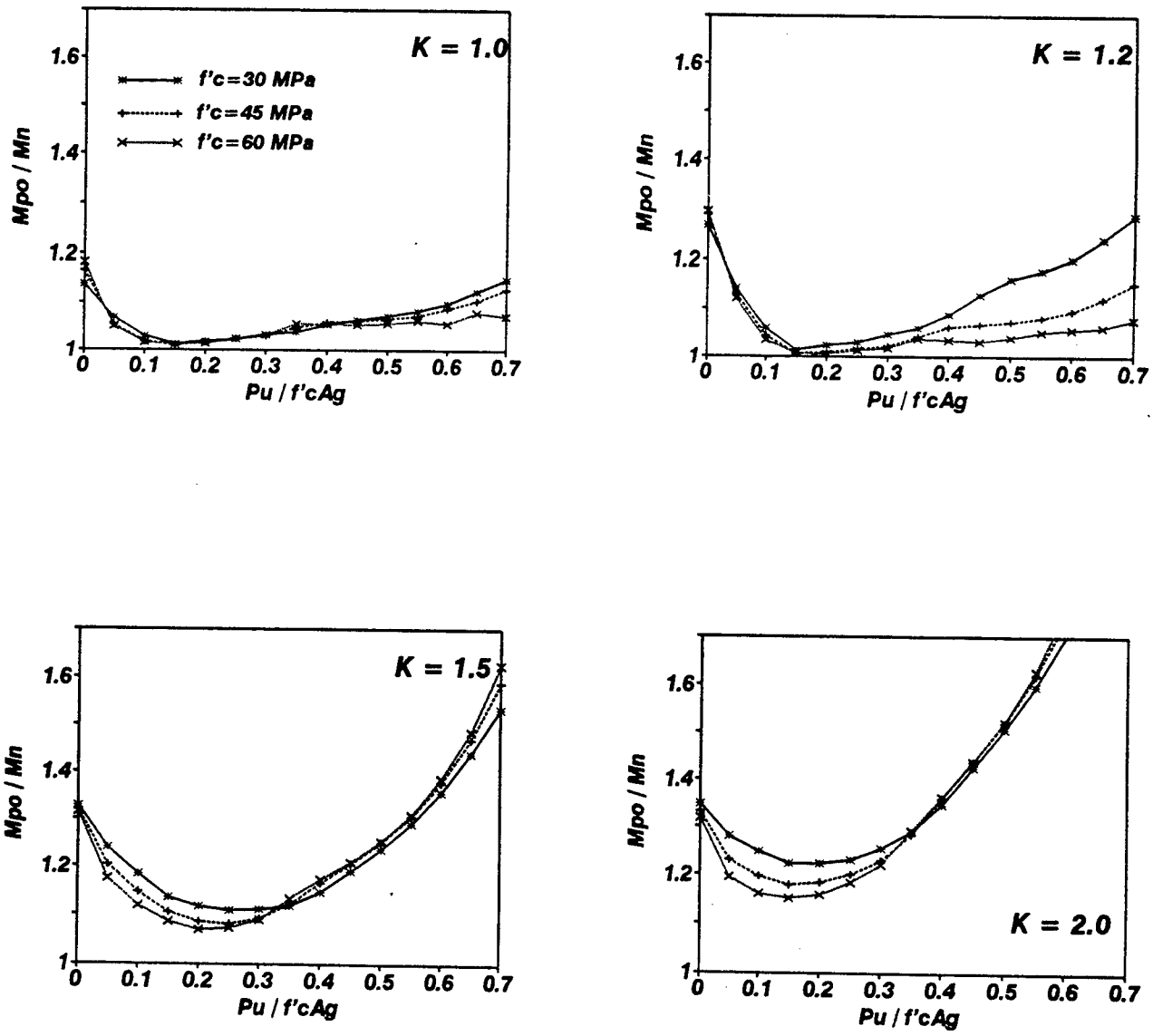

Figure 3-12 Effect of Concrete Strength on Moment Overstrength for Rectangular Sections.

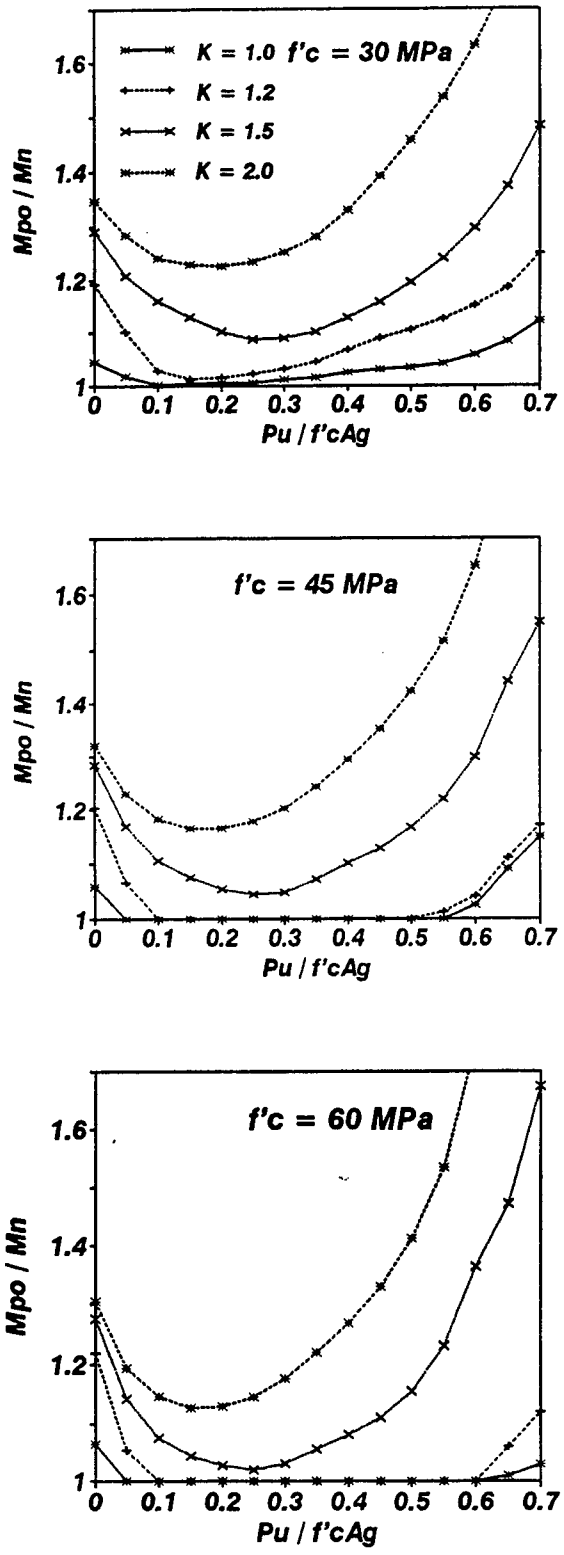

Figure 3-13 Influence of Concrete Strength on Moment Overstrength for Circular Sections.

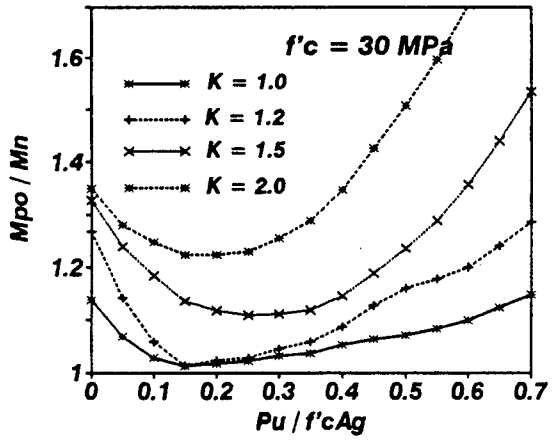

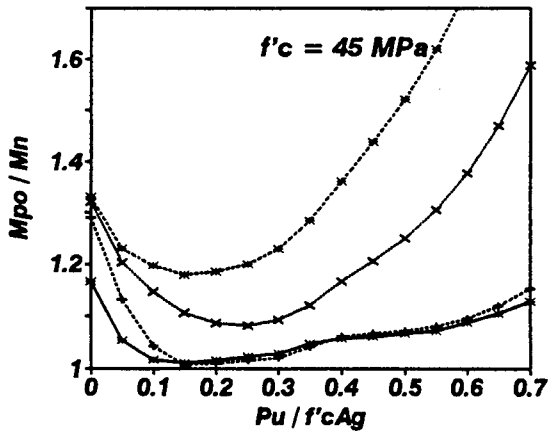

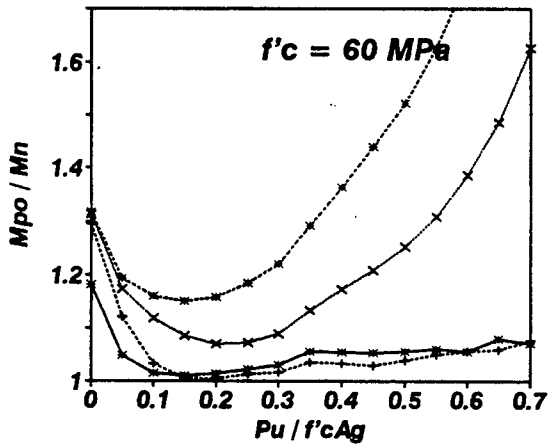

Figure 3-14 Influence of Concrete Strength on Moment Overstrength for Rectangular Sections.

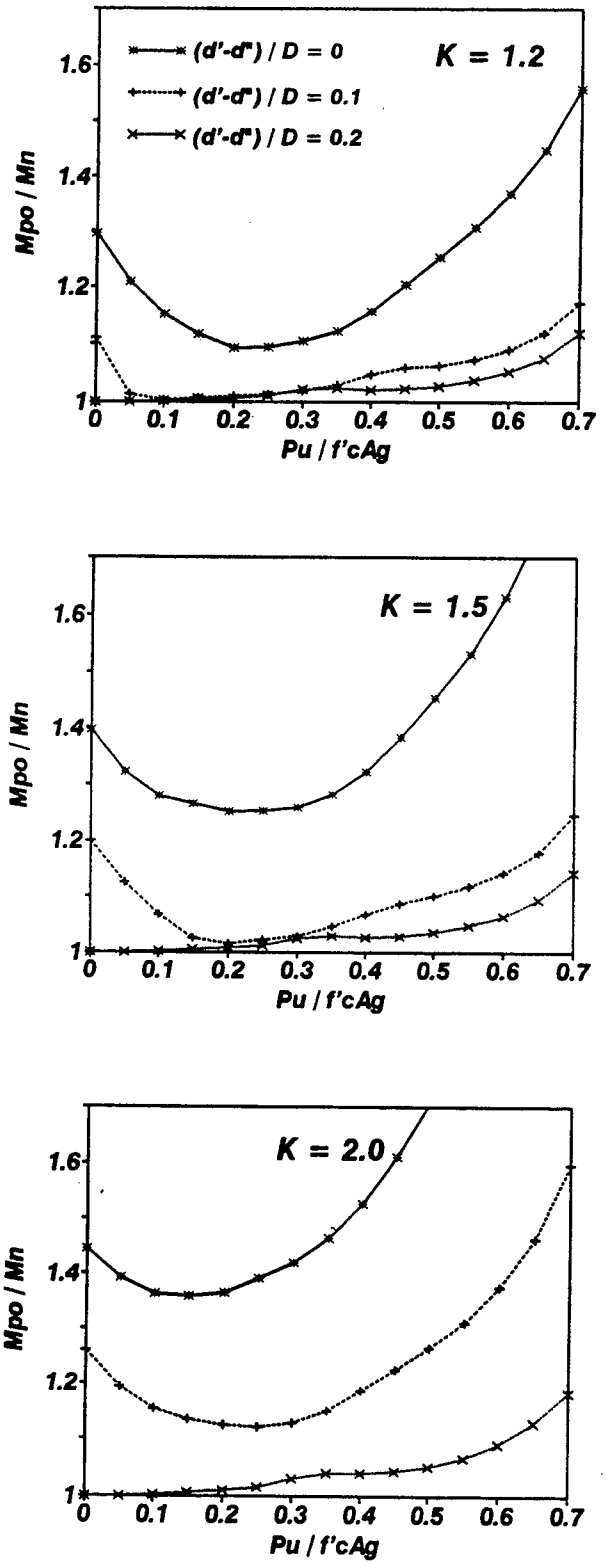

Figure 3-15 Effect of Longitudinal Steel Placement on Moment Overstrength for Circular Sections.

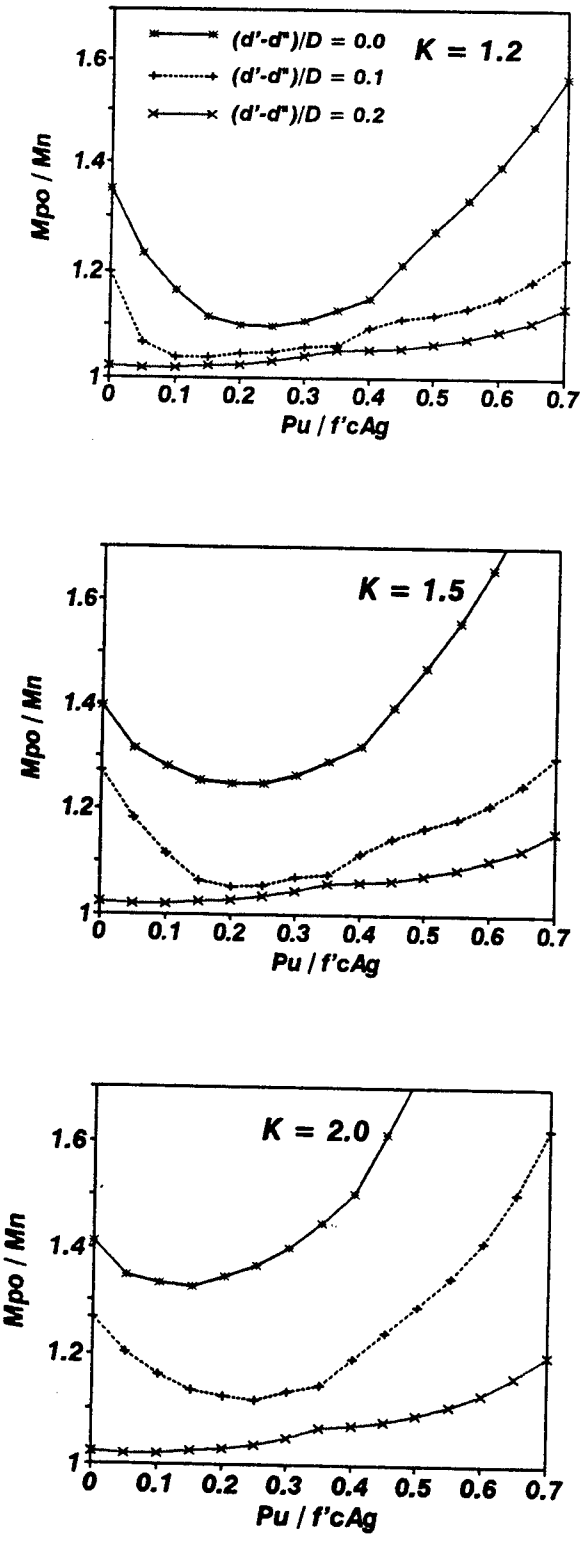

Figure 3-16 Effect of Longitudinal Steel Placement on Moment Overstrength for Rectangular Sections.

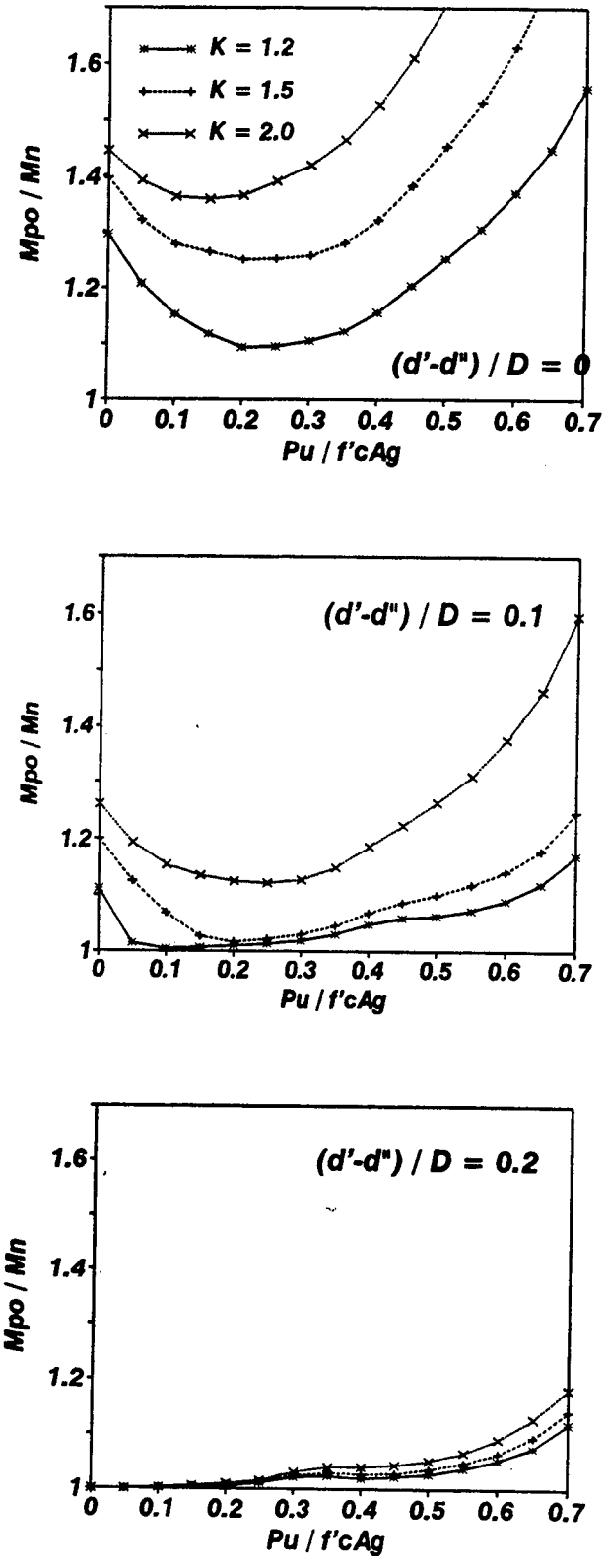

Figure 3-17 Influence of Longitudinal Steel Placement on Moment Overstrength for Circular Sections.

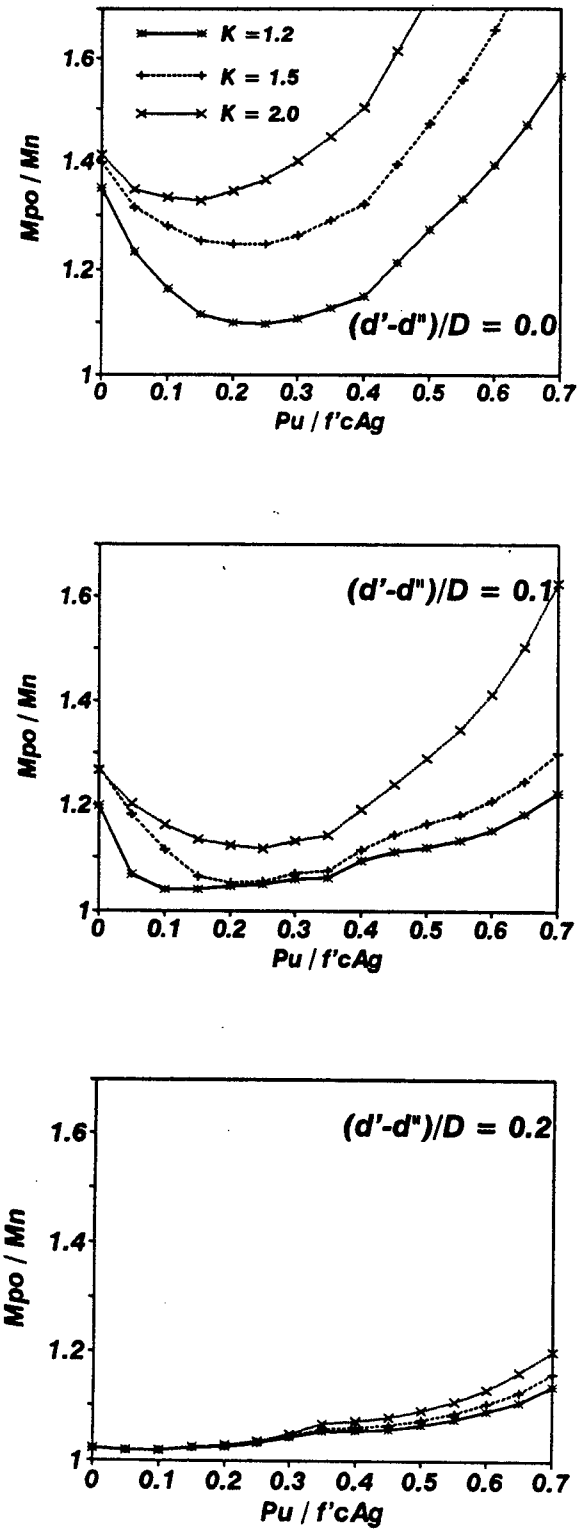

Figure 3-18 Influence of Longitudinal Steel Placement on Moment Overstrength for Rectangular Sections.

in the distance the percentage of confined concrete decreases; $(d'-d'')/D$ is a parameter which shows the percentage of confined concrete in a section. Higher values of $(d'-d'')/D$ means larger amount of unconfined concrete in the section. Hence, smaller the value of $(d'-d'')/D$, the larger the moment overstrength. This is typically the case for large bridge columns where the thickness of the cover with respect to the overall column size is small. The effect of confinement corresponding to any particular value of $(d'-d'')/D$ is shown in figures 3-17 and 3-18 for circular and rectangular sections, respectively. As before, overstrength is found to increase with increasing confinement irrespective of axial load and sectional shape.

3.5 Discussion of Results

The following conclusions can be drawn from the foregoing parametric study:

1. For unconfined concrete columns, the values of moment overstrength are significant at low and at very high levels. Since the axial load levels in bridge columns are small $(P_u < 0.15 f'_c A_g)$, it is recommended that λ_{mo} = 1.2 be adopted as a minimum value.

2. For confined concrete columns, the moment overstrength is significant at both low and high levels of axial load. Hence the consideration of moment overstrength is important for capacity design of both bridge and building columns designed with confined concrete plastic hinge zones. Moreover, the effects of various parameters on moment overstrength factors were found to be appreciable. Therefore, a simplified general method of analysis is needed to determine overstrength factors which considers both material and section properties. In the following section, an approach is proposed which uses a plastic method of analysis for determining overstrength.

3.6 VALIDATION WITH EXPERIMENTAL RESULTS

The analytical results of overstrength factors were confined within certain limits of the parameters studied and compared with experimental results of Ang et al. (1985) for the purpose of validating the presented moment overstrength analysis theory. Ang et al.(1985) conducted a number of experiments on confined concrete columns of various confinement ratios (K) and of various material and sectional properties. From the experimental results obtained, they established the maximum moment capacity observed for each specimen. Each experimental data point of maximum moment overstrength ratio was plotted on a graph with respect to axial load ratios ($P_u/f_c'A_g$) and the following empirical equation was developed representing the best fit curve for the moment overstrength factor:

$$\lambda_{mo} = \frac{M_{po}}{M_n} = 1.13 + 2.35\left(\frac{P_u}{f_c'A_g} - 0.1\right)^2 \qquad (3\text{-}4)$$

The experimental data was within ±15% of this equation.

Analytical studies conducted in the previous section led to the development of a number of graphs representing the variation of overstrength factors with various parameters. To make a comparison with the experimental results, the theoretical values were confined within the following values of various parameters to make an comparison with the experimental results mentioned above:

i) Concrete compressive strength: $f_c' = 30 - 45\ MPa$

ii) Longitudinal steel strength: $f_y = 276$ and $414\ MPa$

iii) Longitudinal steel volume: $\rho_t = 0.005 - 0.02$

The plots of maximum and minimum values of moment overstrength factors obtained within the above parameters represents the average values of analytically obtained strength enhancement

factors.

The analytical results obtained above were plotted against the experimental results and the best curve fit equation of Ang, Priestley and Paulay as shown in figure 3-19. The maximum value curve is observed to be in good agreement with the +15 percent experimental curve and encompasses most of the experimentally observed moment overstrength factors. Hence, the theory tends to be conservative, which is satisfactory from the design point of view. This curve can also serve as a design chart to determine the moment overstrength factor for the majority of the concrete columns designed with normal strength materials.

3.7 CLOSURE

The analytical method of performing moment curvature analysis, derived in the previous section, was used to carry out a complete overstrength analysis for circular and rectangular sections. A large number of parametric studies were conducted to better understand the individual and cumulative effects of various parameters on the influence of moment overstrength. The analytical curves so obtained were also compared with experimental results of Ang (1985). The theoretical results were conservative, which is desirable from a design point of view. Although the analysis reported herein was limited to circular and rectangular sections only, similar exercise can be performed on sections of any arbitrary shape. In view of the apparent complexity of the whole approach, the necessity to develop a relatively simple method is evident. Thus an interaction approach of evaluating overstrength factors is developed which is discussed in detail in the next section.

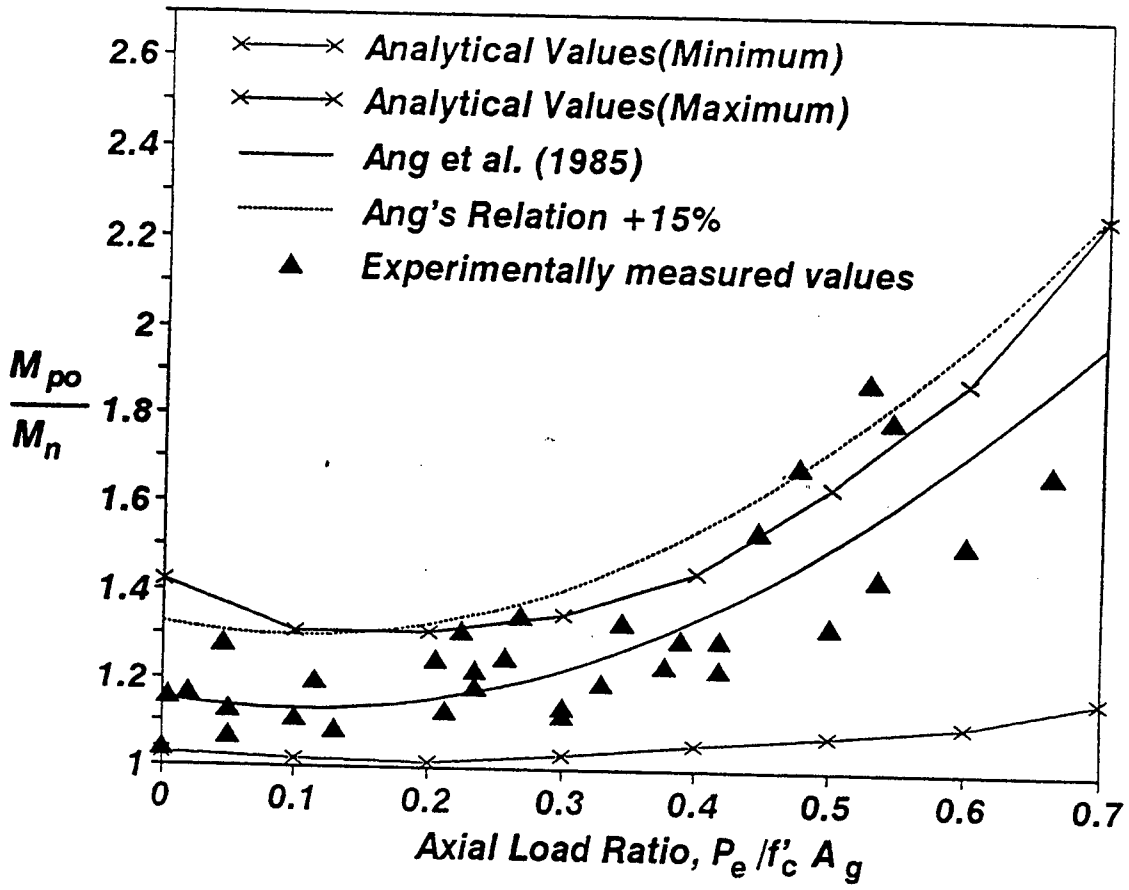

Figure 3-19 Comparison of Analytical Results with Experimental Results.

(f'_c = 30-45 MPa, Steel Grade 40-60, Steel Volume= 0.5% to 2%)

SECTION 4
SIMPLIFIED ANALYSIS USING A STRESS BLOCK INTERACTION DIAGRAM APPROACH

4.1 INTRODUCTION

In the previous section, an "exact" approach using moment-curvature analysis was used to compute the overstrength factors for any general section. Although the method is extremely accurate, it is necessary to develop a simple yet sufficiently accurate method for everyday design office applications. This prompted the development of the stress block interaction diagram approach for computing the overstrength factors. This method uses a plastic analysis method and as an obvious result ignores strain compatibility though maintaining force equilibrium-an essential attribute of any limit based analysis. However, before discussing the method in detail it is important to look back into the concept of stress block analysis. Although stress block analysis was used extensively by Mander et al. (1984), he used a numerical integration approach which is not particularly suitable for spreadsheet-type computer programming. Hence discreet closed form expressions for stress block parameters taking into account confinement is developed and integrated into the evaluation of approximate overstrength factors. This is discussed in the following subsection.

4.2 STRESS BLOCK ANALYSIS

From the general stress block theory, stress block parameters can be obtained by numerical integration of the various stress-strain relations of concrete. The stress blocks so obtained though functions of the concrete strength, level of confinement and maximum strain, are implicit and hence difficult to utilize in a computational moment-curvature analysis of concrete columns. Hence, to obtain explicit analytical expressions of stress blocks, stress-strain relations for concrete which can be easily integrated were formulated. Using a proposed stress-strain relation for concrete, explicit expressions for stress block parameters which are a function of the concrete strength, level of confinement and maximum strain were formulated (Appendix-

B). Using maximum values of these stress block parameters, maximum overstrength moment is evaluated which is discussed later in the section. The nominal moment capacity is also obtained using the same approach but using stress block parameters specified by ACI which is described in the next subsection.

4.2.1 AASHTO/ACI Stress Block Parameters for Unconfined Concrete

For deriving the flexural strength, only the magnitude and the position of the concrete compression force need to be known. The U.S. practice, as represented by AASHTO (1996) and ACI (1995) code, has been to replace the actual stress block by an equivalent rectangle. On the basis of extensive direct measurements as well as indirect evaluation of axially and eccentrically loaded specimens, AASHTO/ACI adopted the following values of equivalent rectangular stress block parameters:

$$\alpha = 0.85 \quad \textit{for all values of } f_c' \tag{4-1}$$

$$0.85 \geq \beta_1 = 0.85 - 0.08\,(f_c' - 30) \geq 0.65 \quad MPa \tag{4-2}$$

These are plotted in figure 4-1.

4.2.2 Proposed Maximum Stress Block Parameters

The proposed stress-strain equations (Appendix B) and the explicit stress block parameters are plotted in figure 4-2 for illustrative purposes. It can be observed from these figures that the magnitude of the stress block parameters depend on the level of confinement and strain. It is conceivable that the maximum concrete compressive moment occurs when $\alpha\beta$ is maximum. The value of strain ($\varepsilon_{\alpha\beta}^{max}$) where $\alpha\beta$ is maximum is given by

$$x_{\alpha\beta}^{max} = \frac{\varepsilon_{\alpha\beta}^{max}}{\varepsilon_{cc}'} = \sqrt{1 + \left(\frac{2}{(n+1)z\,\varepsilon_{cc}'}\right)} \tag{4-3}$$

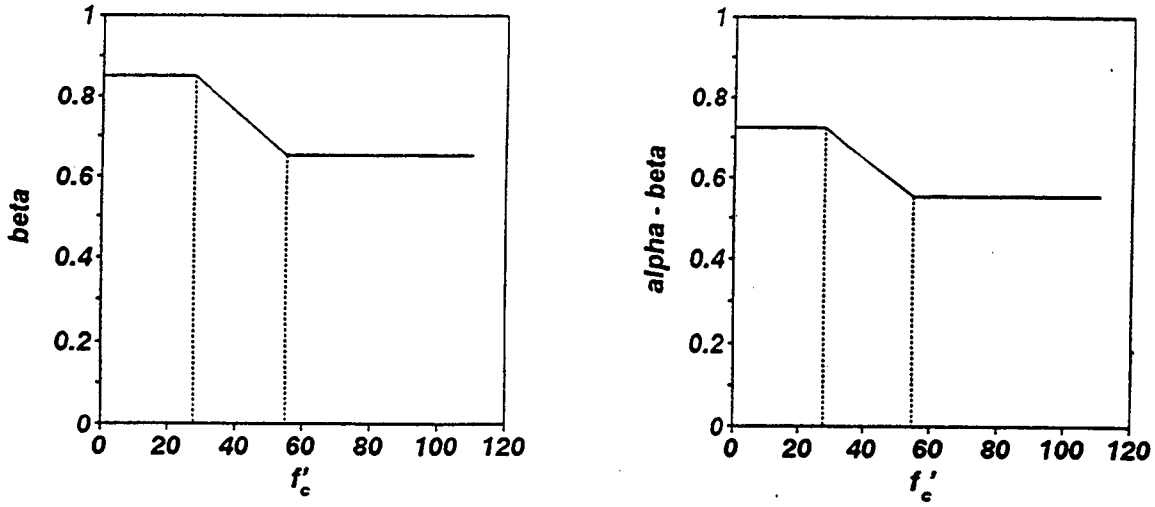

(a) ACI assumed Rectagular Stress Block Parameters for Concrete Compressive Stress Distribution.

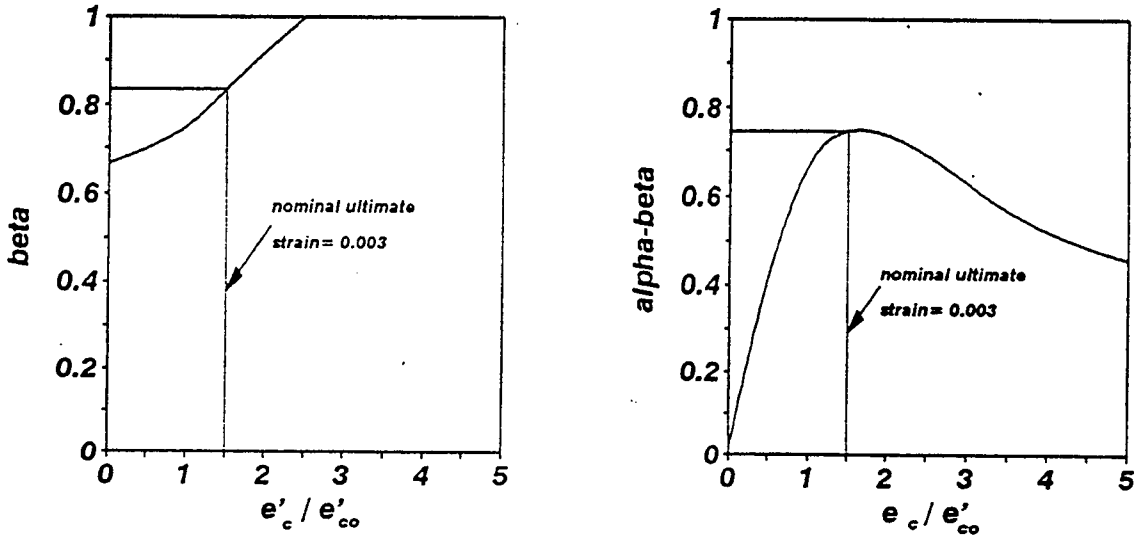

(b) Stress Block Parameters for Unconfined Concrete using Piecewise Equation.

Figure 4-1 Stress Block Parameters for Unconfined Concrete.

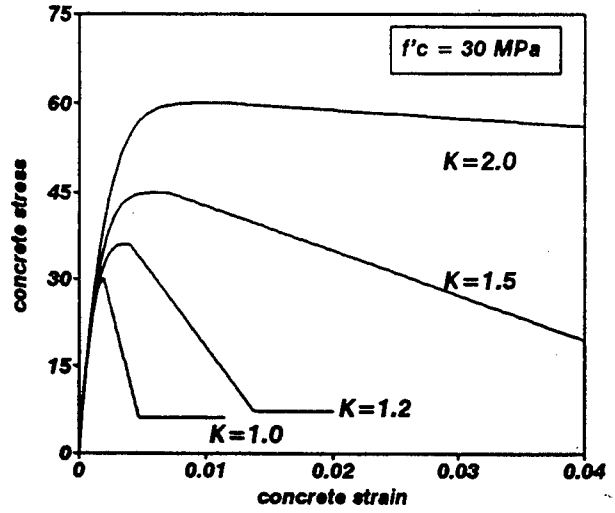

(a) Proposed Stress-Strain Curve

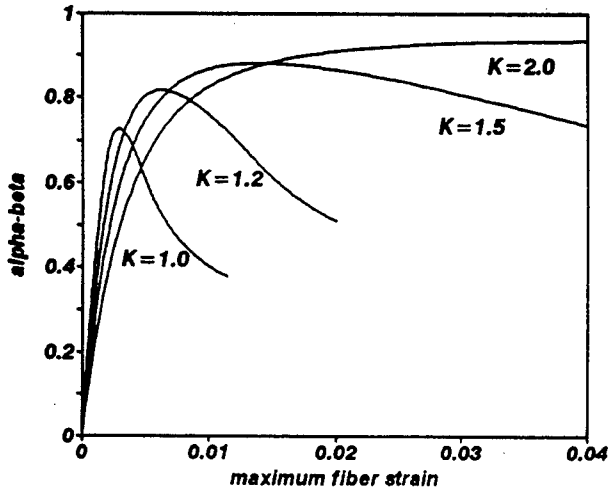

(b) alpha-beta parameter

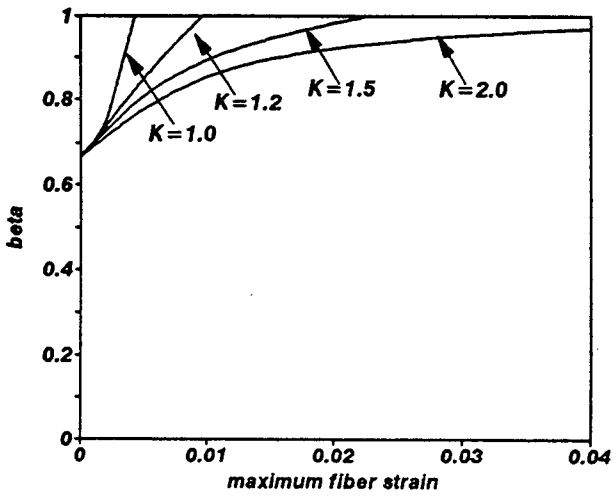

(c) beta parameter

Figure 4-2 Proposed Explicit Stress Block Parameters for Unconfined and Confined Concrete.

It can be observed that the maximum value of $\alpha\beta$ will occur in the descending branch of the stress-strain model of concrete. Hence, substituting the above equation of strain in equation B-6, the following expression for maximum $\alpha\beta$ was obtained

$$\alpha\beta^{max} = \frac{\frac{n}{(n+1)} + \left(x_{\alpha\beta}^{max} - 1\right)\left(1 - \frac{z\varepsilon'_{cc}}{2}\left(x_{\alpha\beta}^{max} - 1\right)\right)}{x_{\alpha\beta}^{max}} \tag{4-4}$$

The corresponding value of the stress block depth factor β can be obtained from equation B-11

$$\beta = 2 - \frac{\left[\left(x_{\alpha\beta}^{max2} - 1\right) - \frac{z\varepsilon'_{cc}}{3}\left(2x_{\alpha\beta}^{max3} - 3x_{\alpha\beta}^{max2} + 1\right) + \frac{n(n+3)}{(n+1)(n+2)}\right]}{x_{\alpha\beta}^{max2}\,\alpha\beta^{max}} \tag{4-5}$$

In the above equations $n = E_c\,\varepsilon'_{cc}/f'_{cc}$ and $z = 6.8 f'_c K^{-6}$. The peak values of the confined concrete stress and the corresponding strain ($f'_{cc}, \varepsilon'_{cc}$) are obtained by the procedure outlined in Appendix A for circular and rectangular sections respectively. The peak values of the stress block parameter $\alpha\beta^{max}$ can be divided by the parameter β in equation 4-5 to obtain discreet values of stress block parameters to be used for design. These parameters are plotted in figure 4-3 against the confinement ratio K along with their simple curve fit approximations given by

$$\alpha = 0.85 + 0.12(K-1)^{0.4} \tag{4-6}$$

and

$$\beta = 0.85 + 0.13(K-1)^{0.6} \tag{4-7}$$

4.3 Axial Load-Moment Interaction Approach to Overstrength

Axial load-moment interaction curves have been used by engineers for design of columns. The analytical procedure is iterative and hence requires the use of computers. Hence, a theory based on plastic design concepts was devised to draw axial load-moment interaction curves for both maximum overstrength moment capacity and nominal moment capacity. Nominal moment interaction curve is constructed for columns by the procedure outlined by AASHTO/ACI considering

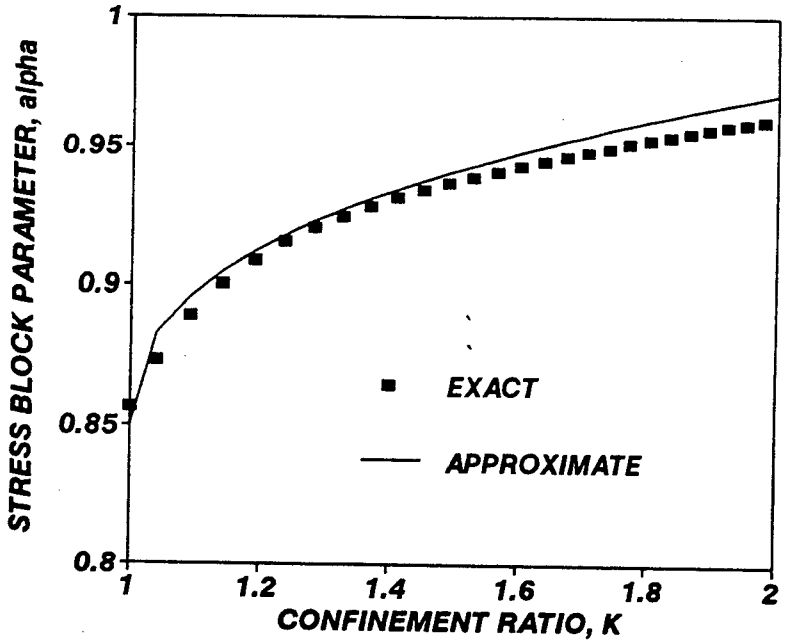

(a) Variation of Parameter alpha with Confinement, K.

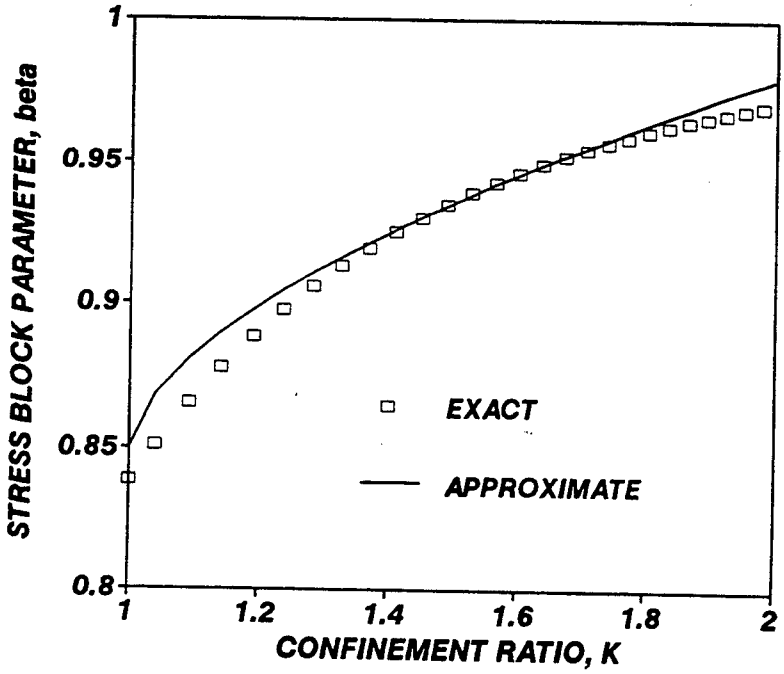

(b) Variation of Parameter beta with Confinement, K.

Figure 4-3 Showing Exact and Approximate values of the Stress Block Parameters.

maximum compression strain ε_{cm} = 0.003 and as was discussed in section 2.3. The maximum overstrength moment capacity interaction curve is drawn using maximum stress block parameters of confined sections given by equations 4-6 and 4-7. Hence overstrength factors at an axial load level can be determined by the ratio of maximum overstrength moment to nominal moment determined from the constructed interaction curves. The parabolic approximate interaction curve procedure of moment capacities represents a hand tool for the engineer to determine overstrength factors of columns at various axial loads. The procedure for this is presented below.

(i) Parabolic P-M Interaction Curve of Maximum Overstrength Capacity:

Maximum Moment Point: From the principles of plastic analysis, the maximum moment point (M_{bo}, P_{bo}) on the axial load-overstrength moment interaction curve should be obtained when the neutral axis depth from the extreme compression fiber of the section (c/D) is 0.5. Axial load capacity is the sum of the contributions from confined core concrete and unconfined cover concrete. Hence using this value of neutral axis depth and the familiar stress block notation, the axial load capacity is determined as

$$\frac{P_{bo}}{f'_c A_g} = \frac{C_c}{f'_c A_g} = 0.5\,\alpha_{cc}\beta_{cc}^{\max} K \frac{A_{cc}}{A_g} + 0.5\,\alpha_{co}\beta_{co}\left(1 - \frac{A_{cc}}{A_g}\right) \tag{4-8}$$

where the confined and unconfined concrete stress block parameters are determined at the strain corresponding to the maximum stress blocks of confined concrete calculated from equation 4-3 with A_{cc}/A_g denoting the ratio of the core concrete to the gross area. The maximum overstrength moment is determined as

$$M_{bo} = M_{oc} + M_{os} \tag{4-9}$$

where M_{oc} = moment contribution of concrete to the ultimate moment and is determined by taking the moment of the concrete cover and cover forces about the middle of the section. Assuming that the neutral axis depth parameter β_{co} for unconfined concrete is equal to 1.0 at the strain at which $\alpha_{cc}\beta_{cc}^{\max}$ occurs, for circular sections this can be written as

$$\frac{M_{oc}}{f_c' A_g D} = 0.25\left(1-\frac{A_{cc}}{A_g}\right)\alpha_{co}\beta_{co}(1-\kappa_o) + 0.25\,K\,\alpha_{cc}\beta_{cc}^{\max}\frac{A_{cc}}{A_g}(1-\kappa_c\,\beta_{cc})\left(\frac{D''}{D}\right) \qquad (4\text{-}10)$$

where κ_o is a factor that locates the position of the centroid of the cover concrete from the topmost fiber of the section. For circular sections κ_o can be taken to be 0.4. For rectangular sections this can be determined by using principles of strength of materials as illustrated in figure 4-4. Similarly κ_c locates the position of the centroid of $\beta_{cc}A_{cc}$ from the center of the transverse steel (figure 4-4) and can be taken as 0.6 and 0.5 for circular and rectangular sections respectively. The steel moment contribution M_{os} can be determined as

$$M_{os} = Z_p f_{su} \qquad (4\text{-}11)$$

in which Z_p = the plastic section modulus of steel. This is calculated assuming that the longitudinal steel is distributed uniformly over a depth $D'=D-2d'$ and width $b'=b-2d'$ and is given by

$$\begin{aligned} Z_p &= \left(1+\frac{2b'}{D'}\right)\frac{A_{st}}{4(b'+D')}(D')^2 && \textit{for rectangular columns} \\ &= 0.375\,A_{st}D' && \textit{for square columns} \\ &= 0.32\,A_{st}D' && \textit{for circular columns} \end{aligned} \qquad (4\text{-}12)$$

where the parameters are as described before. Hence the maximum point on the interaction curve can be determined.

The Tension Axial Load Capacity Point $(0,P_{to})$: The tension axial load capacity $(P_{to})$for ultimate moment capacity curve of the section can be determined as

$$\frac{P_{to}}{f_c' A_g} = -\frac{\rho_t f_{su}}{f_c'} \qquad (4\text{-}13)$$

where all the parameters are as described before.

The two points obtained on the maximum overstrength moment capacity curve can be used to approximate the overstrength interaction curve as a parabolic curve and overstrength

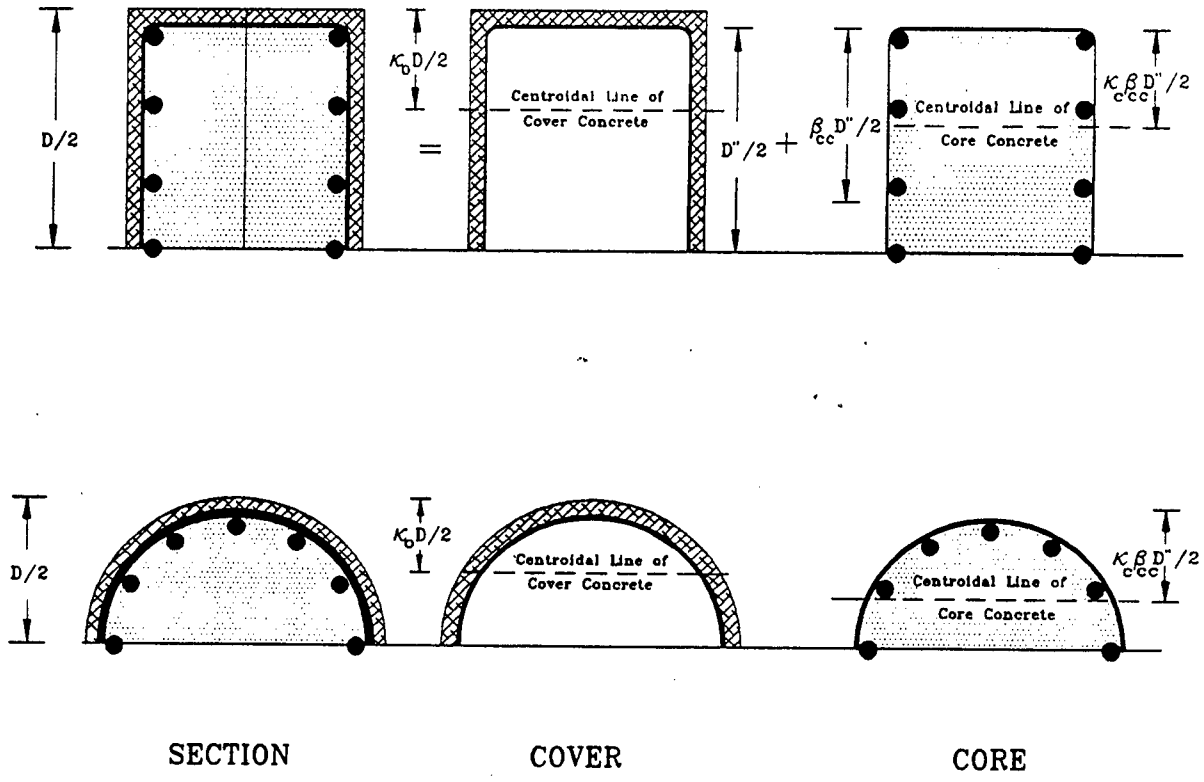

Figure 4-4 Control Parameters for the Evaluation of the Maximum Moment for the Approximate Method.

moments at any intermediate axial load (P_e) determined as

$$M_{po} = M_{bo}\left(1-\left(\frac{P_e-P_{bo}}{P_{to}-P_{bo}}\right)^2\right) \tag{4-14}$$

Hence the overstrength moment M_{po} can be determined. The control parameters of the approximate maximum overstrength moment curve is shown in figure 4-5.

(ii) Approximate Interaction Curve of Nominal Capacity Interaction Curve:

Nominal Maximum Moment Point:(M_{nb},P_{nb}) It was observed that the nominal maximum moment is obtained when the neutral axis depth of the section is $c/D = 0.425/\beta_1$ for both circular and rectangular sections respectively. Using this value of the neutral axis depth, it is easily possible to determine the strain diagram since the compressive strain at the top fiber is known. Thus the contribution of steel and concrete to the nominal moment can be determined. By adding the contributions of concrete and steel, the maximum point on the nominal moment interaction curve can be established.

The Tension Axial Load Capacity Point: The tension axial load capacity for nominal moment of the section can be determined as

$$\frac{P_{nt}}{f_c' A_g} = -\frac{\rho_t f_y}{f_c'} \tag{4-15}$$

where all the parameters are as described before.

The two points obtained on the nominal moment capacity curve can be used to fit a second degree parabola as

$$M_n = M_{nb}\left(1-\left(\frac{P_e-P_{nb}}{P_{nt}-P_{nb}}\right)^2\right) \tag{4-16}$$

The agreement between the actual nominal moment curve and the curve fit nominal moment

curve is shown in figure 4-5.

(iii) Determination of Overstrength Factor: The ratio of the overstrength moment from equation 4-14 to the nominal moment from equation 4-16 provides the overstrength factor at the value of desired axial load level (P_e) as:

$$\lambda_{mo} = \frac{M_{po}}{M_n} = \frac{M_{bo}\left(1 - \left(\frac{P_e - P_{bo}}{P_{to} - P_{bo}}\right)^2\right)}{M_{nb}\left(1 - \left(\frac{P_e - P_{nb}}{P_{nt} - P_{nb}}\right)^2\right)} \qquad (4\text{-}17)$$

The values of overstrength obtained from the above curve fit method was determined for typical cases and plotted against those obtained from parametric studies. These are shown in figures 4-6 and 4-7 for circular and rectangular sections respectively.

4.4 Probabilistic Modeling

The moment curvature approach discussed earlier is a deterministic methodology for evaluating the overstrength corresponding to a section. The assumption built in to the method is that both the concrete and steel strengths (and constitutive relations) are known a priori without any associated uncertainty. However, in a real scenario, such an assumption can lead to gross errors because both the above quantities can have significant randomness associated with their strengths that leads to an uncertain outcome. If this is neglected, then the overstrength factor corresponding do a particular set of strengths will be the average amongst the multimode of possibilities. Alternatively, if it is assumed that both the concrete and steel strengths are probabilistically known in the form of some distribution, then the overstrength corresponding to a particular steel and concrete variety will also be known in the form of a probability distribution within certain limits of confidence. The uncertainty associated with the final answer will be as a result of the randomness in both the concrete and steel strengths. As a result it is of utmost importance that these probabilistic characteristics be known (albeit approximately) to enable the final outcome of the overstrength analysis to be represented in a fashion that gives

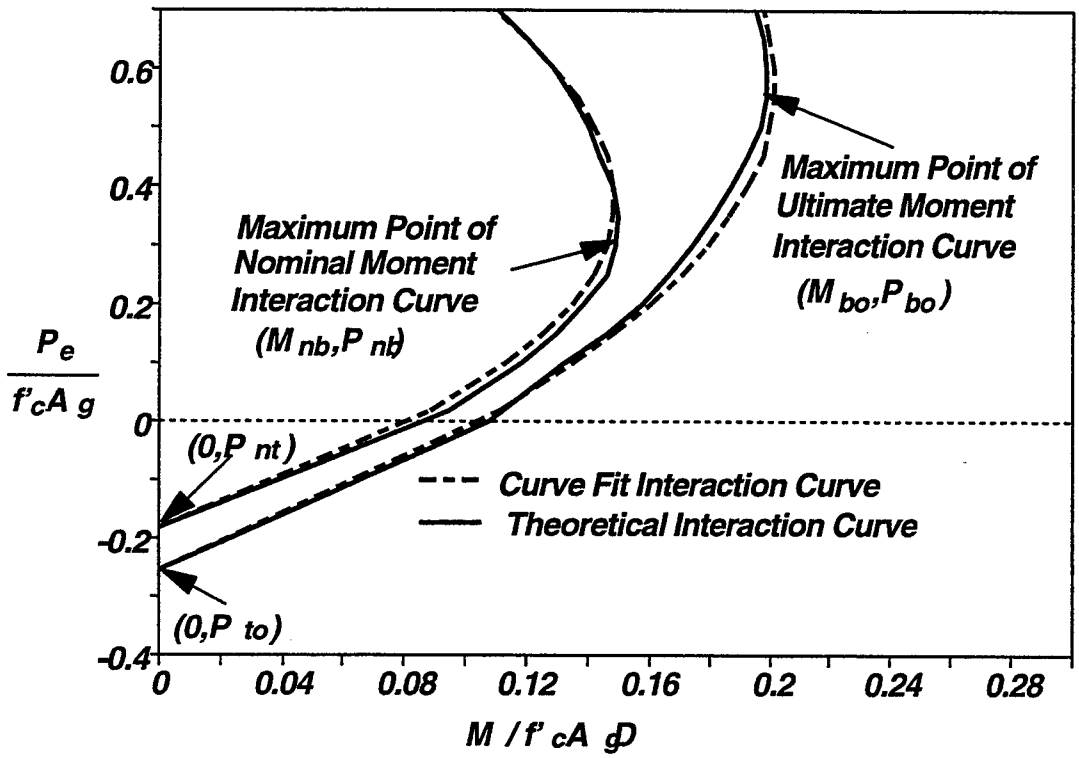

Figure 4-5 Control Parameters for the Approximate Interaction Curve.

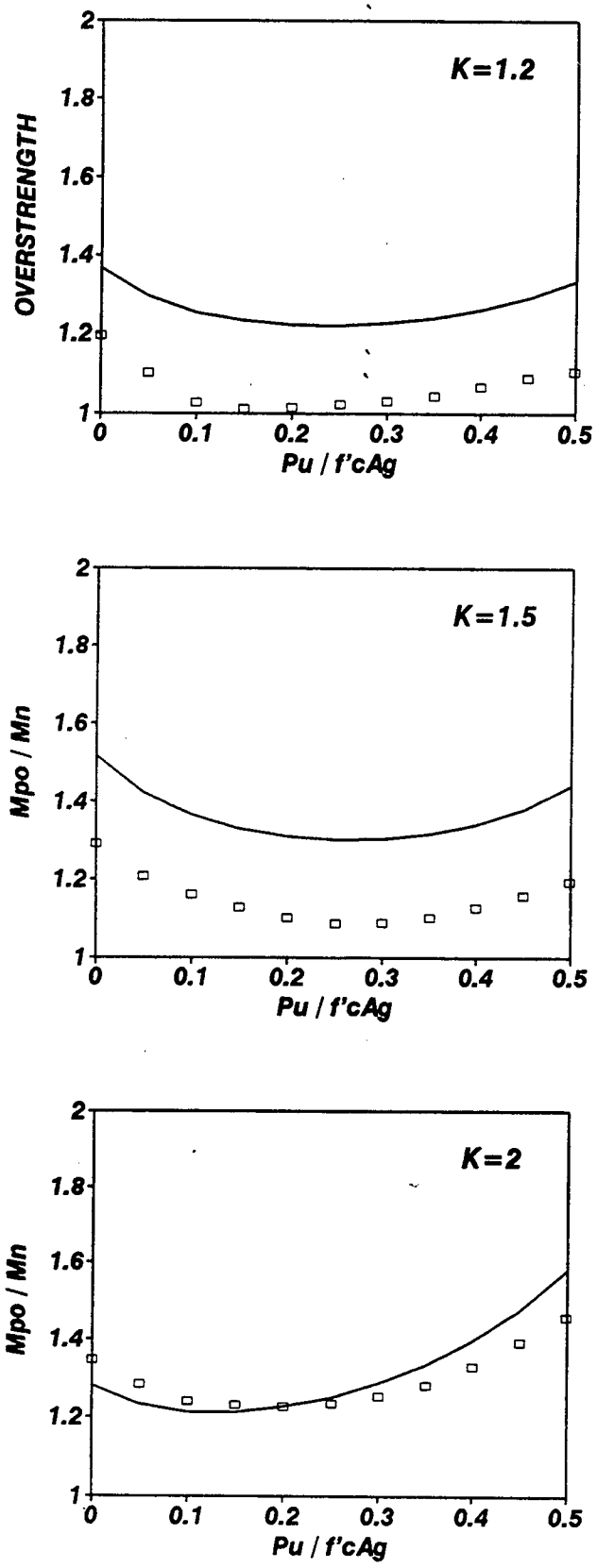

Figure 4-6 Approximate Overstrength for Circular Column Sections.

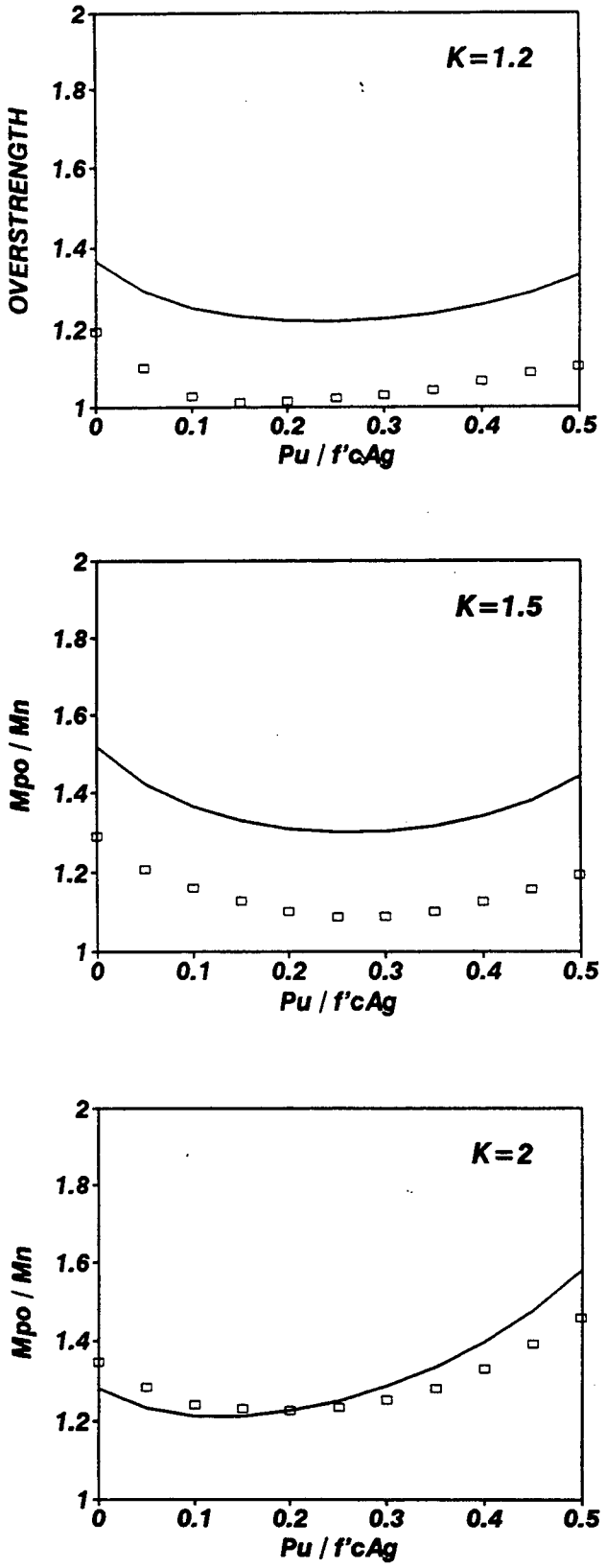

Figure 4-7 Approximate Overstrength for Rectangular Column Sections.

a dependable upper bound estimate of overstrength capacity.

4.4.1 Probability Distributions for Concrete and Steel

Concrete is a mixture of water, cement, aggregate and air. Variations in the properties or proportions of these constituents, as well as variations in transportation, placement and compaction of concrete lead to variation in the strength of the finished concrete.

The variability of concrete strength depends greatly on the quality control of the concreting operation. An unpublished analysis of concrete cylinders by Allen and Plewes from nearly 300 jobs across Canada showed that the coefficients of variation of cylinder strength were approximately 12%, 15% and 18% for pre-cast, ready-mix in-situ and site-mix in-situ respectively. A review of literature (Julian, 1955; Shalon and Reintz, 1955; Mirza et al. 1979a) indicates that the statistical variation of concrete strength can be adequately represented by a normal distribution. Since majority of the concrete used in bridge substructure is of site-mix in-situ type, a coefficient of variation of 18% can be accepted as a reasonable upper bound for average controls.

If the coefficient of variation is chosen at 18% and the variability in strength represented by a normal distribution, then using the standard normal density function the traditional bell curve (for a normalized distribution) can be obtained as shown in figure 4-8a. The cumulative distribution can be obtained by integrating the area under this curve as shown in figure 4-8b. A reasonable upper bound can be obtained from the cumulative distribution function if the confidence limit is set at 95% (5% probability of being exceeded). This corresponds to a value of 1.3 for the particular set of parameters. Hence the expected mean strength of concrete can be multiplied by the same to obtain a dependable upper bound that will account for the variabilities in strength.

A similar approach can also be adopted for reinforcing steel. Based on the test results of Mirza et al. (1979b) and Andriono and Park (1986), it is observed that the statistical variation of commonly used grades of reinforcement in the United States (Grade 40 and Grade 60) is best

represented by a lognormal distribution with a coefficient of variation of 11% representing a reasonable upper bound. The results are plotted in figure 4-9.

If the coefficient of variation is chosen at 11% and the variability in strength represented by a lognormal distribution, then the probability density and cumulative probability distributions can be obtained for normalized strengths as shown in figure 4-8a and b. Choosing a confidence limit of 95%, it can be deduced that a dependable upper bound can be obtained by multiplying the mean yield and ultimate strengths by 1.2 respectively.

4.4.2 Upper Bound Interaction Diagram

Based on test results it is observed that a dependable upper bound envelope for concrete and steel strengths are obtained by multiplying the expected man/median concrete and steel strengths by 1.3 and 1.2 respectively. Using these upper bound values, an interaction diagram of the form shown in figure 4-10 can be constructed. Note that the same expression (4-14) can be used with

$$\frac{P_{bo}}{f_c' A_g} = \frac{C_c}{f_c' A_g} = 0.65\,\alpha_{cc}\beta_{cc}^{\max} K \frac{A_{cc}}{A_g} + 0.65\,\alpha_{co}\beta_{co}\left(1 - \frac{A_{cc}}{A_g}\right) \tag{4-18}$$

$$\frac{M_{oc}}{f_c' A_g D} = 0.325\left(1 - \frac{A_{cc}}{A_g}\right)\alpha_{co}\beta_{co}(1-\kappa_o) + 0.325\,K\,\alpha_{cc}\beta_{cc}^{\max}\frac{A_{cc}}{A_g}(1-\kappa_c\,\beta_{cc})\left(\frac{D''}{D}\right) \tag{4-19}$$

$$M_{os} = 1.2\,Z_p f_{su} \tag{4-20}$$

$$\text{and} \quad \frac{P_{to}}{f_c' A_g} = -\frac{1.2\,\rho_t f_{su}}{f_c'} \tag{4-21}$$

where all the parameters are as described before. The overstrength factor obtained from such an interaction curve can adequately account for the uncertainties associated with the strengths of concrete and steel and will represent a dependable upper bound.

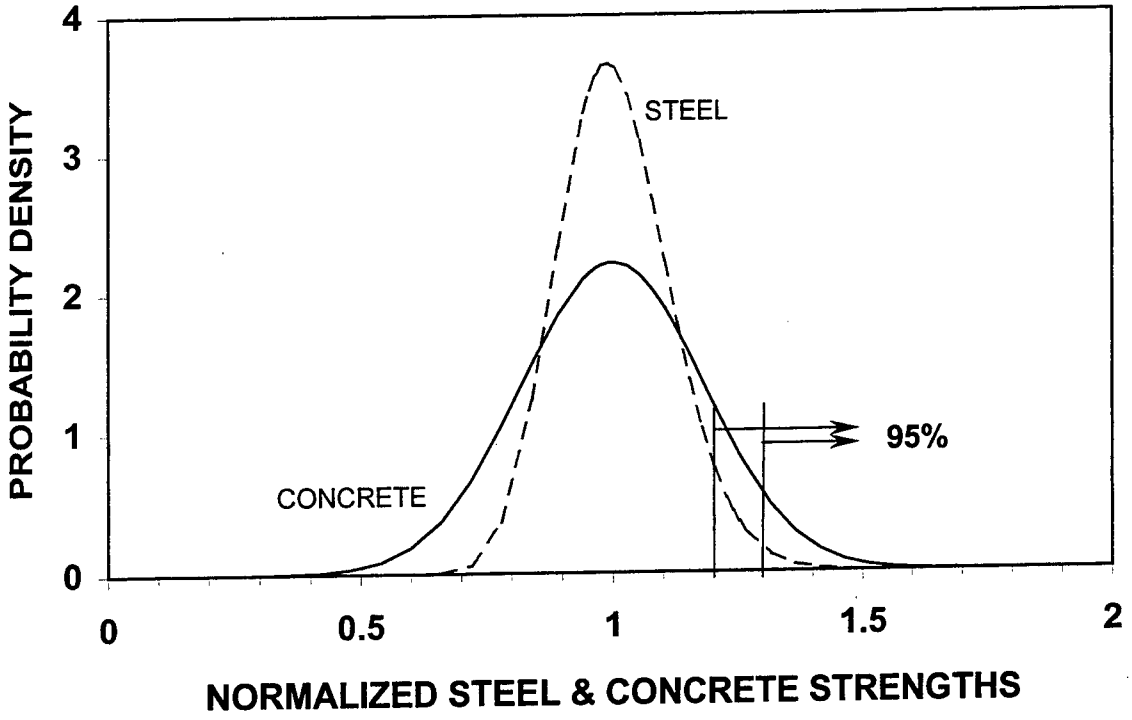

(a) Normalized Probability Density Function for Concrete and Steel

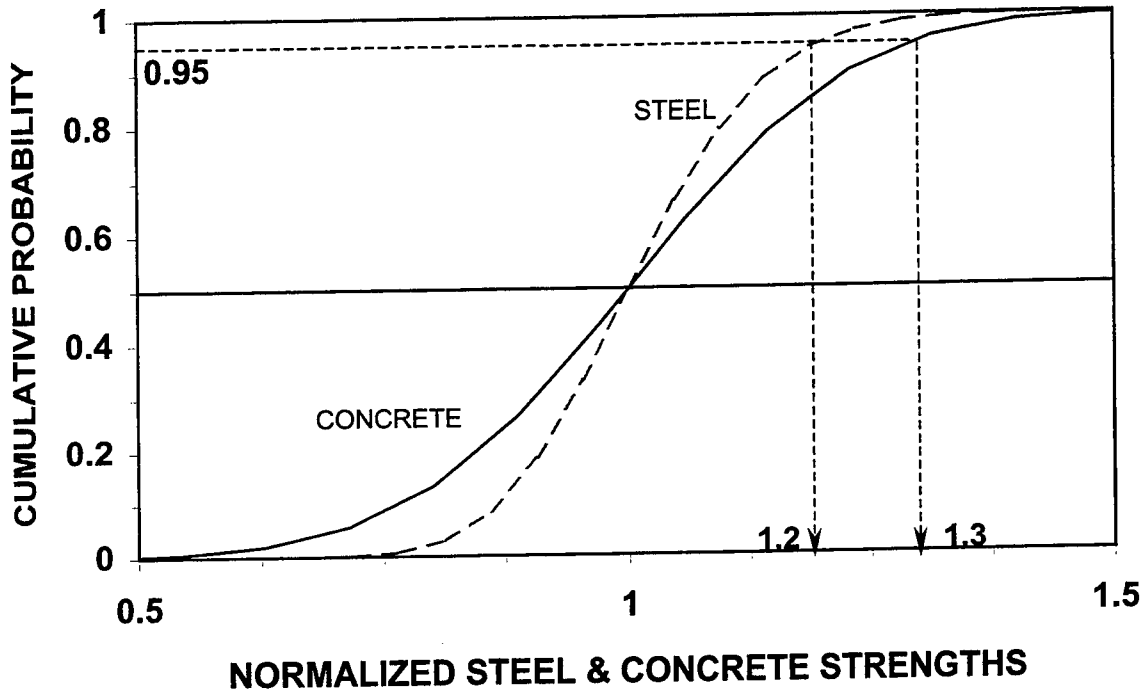

(b) Normalized Cumulative Probability Distribution Function for Concrete and Steel

Figure 4-8 Normalized Probability Distributions for Concrete and Steel.

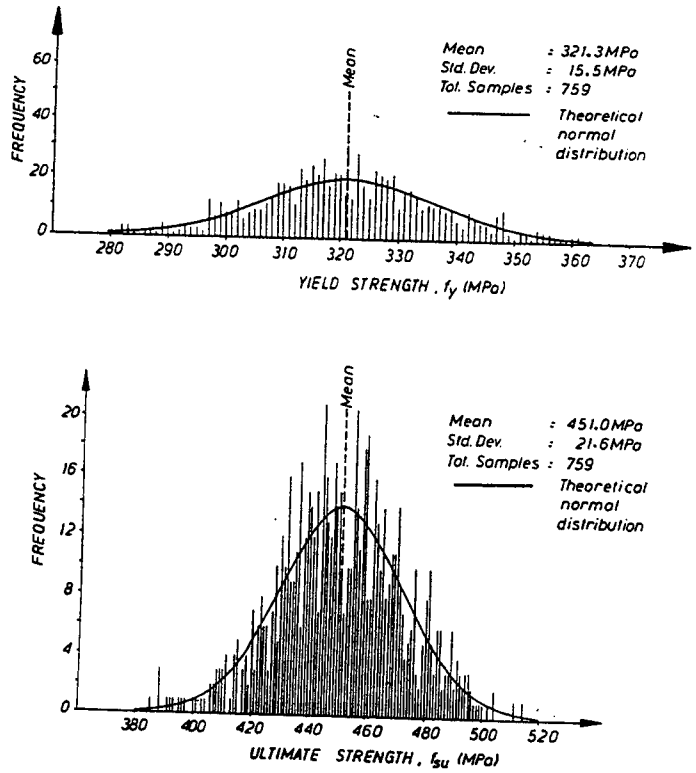

(a) Grade 40 Reinforcing Steel

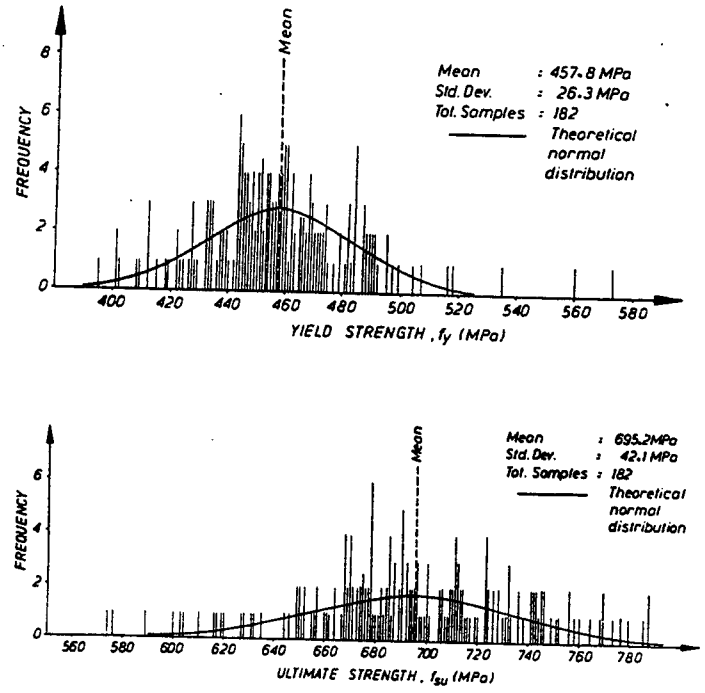

(b) Grade 60 Reinforcing Steel

Figure 4-9 Histograms of Yield and Ultimate Stress for Grade 40 and Grade 60 Reinforcing Steel after Andriono and Park (1986).

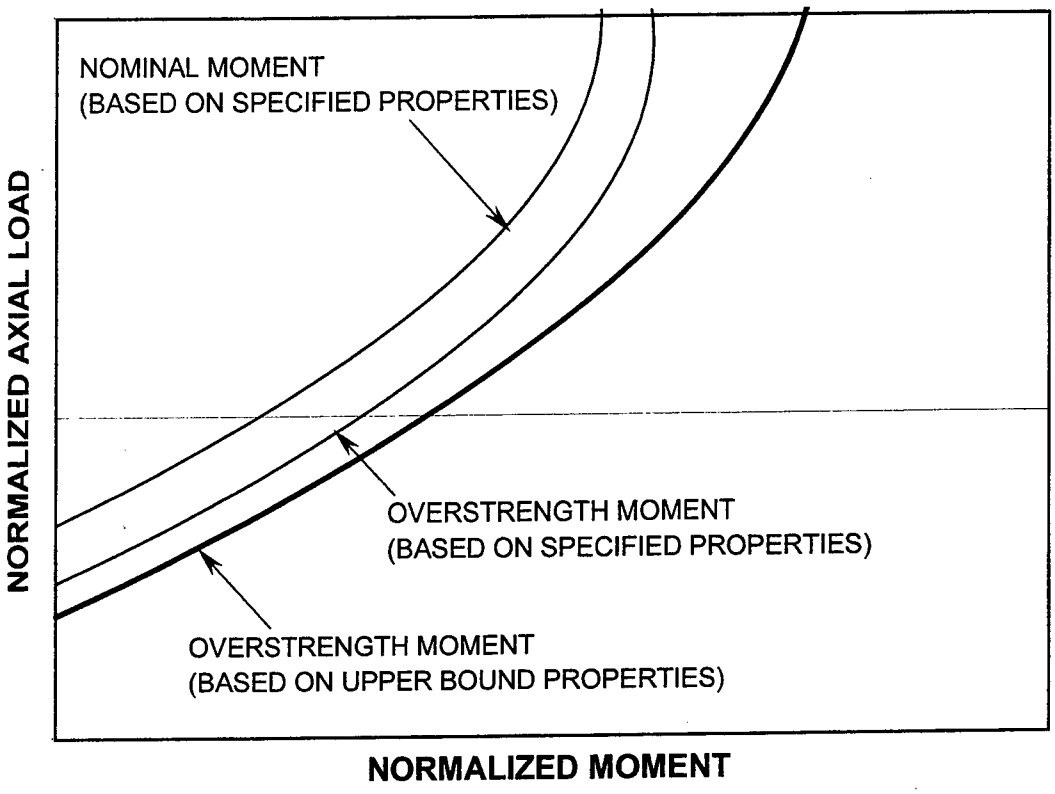

Figure 4-10 Showing Overstrength Interaction Diagram using Upper Bound Strengths of Concrete and Steel.

4.5 BIAXIAL BENDING AND OVERSTRENGTH

Oftentimes it has been observed that structural concrete columns specially in bridges are subjected to bending about both their axes. Although for circular columns this is never a problem due to symmetry, it becomes an important issue specially for non-circular sections. Traditionally the design for biaxial bending has been done assuming an elliptic interaction equation of the form

$$\left(\frac{M_x}{M_{nx}}\right)^2 + \left(\frac{M_y}{M_{ny}}\right)^2 \leq 1 \qquad \text{(4-22)}$$

where M_x, M_y = moment demands along the X and Y axes, while M_{nx}, M_{ny} = nominal moment capacities along the same axes. The same approach can be adopted for overstrength design as well. Realizing that overstrength design is required for capacity protection an expression analogous to equation (4-27) can be written as

$$\left(\frac{\lambda^x_{mo} M^x_{nw}}{M^x_{np}}\right)^2 + \left(\frac{\lambda^y_{mo} M^y_{nw}}{M^y_{np}}\right)^2 \leq 1 \qquad \text{(4-23)}$$

where $\lambda^x_{mo}, \lambda^y_{mo}$ = overstrength factors along the x and y axes for the capacity weakened element, M^x_{nw}, M^y_{nw} = nominal moments along the x and y axes for the capacity weakened element and M^x_{np}, M^y_{np} = nominal moments along the x and y axes for the capacity protected element. Use of the above interaction expression will ensure a ductile mechanism by providing the appropriate level of protection to the structural elements.

4.6 SUMMARY AND CONCLUSIONS

In this section an approximate interaction curve theory for the determination of overstrength factors was presented. This theory to determine the moment overstrength factor is a hand analysis method that enables the designer to determine the overstrength factors of a plastic hinge zone. These are used in capacity design to determine the maximum moment demands which can be imposed in the brittle regions of the structure. Comparison with the accurate method shows that the predictions from the approximate method are higher, which is desirable in capacity design. However, it should be remembered that the accurate method is a monotonic method of analysis that is unable to capture the cyclic work hardening effects on longitudinal reinforcement. Due to this, the compression reinforcement during tension excursion experiences a higher stress under the same strain amplitude. This in turn creates a higher moment contribution from the steel, thereby raising the total moment capacity and the associated overstrength factor. The predictions from the simplified interaction diagram method are therefore considered to be fairly satisfactory.

The deterministic of overstrength can be extended to account for the probabilistic variation of the concrete and steel strengths. It was shown that this can easily be handled by merely modifying the principal material properties f_c' and f_{su} to reflect the upper bound tails of their respective probability distributions. To this end uncertainty in overstrength estimates can be accounted for by enhancing the concrete and steel strengths by 1.3 and 1.2 respectively.

In the following section, this simplified method of overstrength evaluation is demonstrated with a numerical example.

SECTION 5
DESIGN RECOMMENDATIONS AND EXAMPLE

5.1 INTRODUCTION

When using the capacity design philosophy for seismic resistant structures, the designer chooses a hierarchy of failure mechanisms. Inelastic (plastic) modes of deformation which provide ductility are preferred and all undesirable potentially brittle failure mechanisms are inhibited by amplifying their dependable strength in comparison with the designer's chosen desirable mechanisms. Ductile flexure is the generally preferred inelastic mode of deformation. Brittle regions are protected by ensuring that their strength exceeds the demands originating from the maximum flexural overstrength of plastic hinge zones. Hence the determination of the flexural overstrength moment capacity of plastic hinge zones beyond their provided nominal strength is of paramount importance in capacity design. This section summarizes the methodology for determining the overstrength factor for a given reinforced concrete column using a moment-axial load interaction approach as discussed in the previous sections. A design example is then presented to illustrate the step-by-step numerical procedures necessary to determine the overstrength factor for a given longitudinal and transverse steel volume.

5.2 SUMMARY OF P-M INTERACTION THEORY FOR DETERMINING OVERSTRENGTH

Assume that the bridge column has already been designed for flexure and the longitudinal reinforcement has been selected. The concrete and steel strengths are presumed to be known without any uncertainty. Note that the flexural design is based on the design loadings; once the longitudinal steel in the primary column members has been chosen, the design forces are no longer used! Rather, column overstrength is assessed and used for all subsequent facets of design. Based on the chosen longitudinal reinforcement layout, the steps listed below are then followed to assess the provided overstrength capacity.

Step 1 : Determine the unconfined and confined concrete stress block parameters for both nominal and overstrength moment calculations.

(i) Determine the lateral confinement pressure provided by the transverse steel and from this the confinement ratio $K = f'_{cc}/f'_c$ for the column using the procedure listed in Appendix A-2

(ii) Determine the control parameters of both confined and unconfined concrete as per Appendix B

(iii) Determine the extreme compression fiber strain for maximum $\alpha\beta$ as per equation (4-3)

(iv) Determine the stress blocks for confined and unconfined concrete for the above maximum strain using equations 4-6, 4-7 and B-7

Step 2 : Determine the nominal moment capacity (M_n) for the design level of axial load.

(i) Determine the balanced failure point on the nominal interaction curve using $c/D = 0.425/\beta_1$.

(ii) Determine the tension axial load capacity of column using equation (4-15)

(iii) Calculate the nominal moment capacity for the desired axial load level using equation (4-16)

Step 3 : Determine the plastic overstrength moment (M_{po}) for the required axial load.

(i) Determine the maximum failure point on the overstrength interaction curve using equations (4-23) through (4-26)

(ii) Determine the tension axial load capacity of column using equation (4-13)

(iii) Determine the plastic overstrength moment as per equation (4-14)

Step 4 : Determine the overstrength factor

$$\lambda_{mo} = \frac{M_{po}}{M_n} \tag{5-1}$$

Step 5 : Check ductility and confinement requirements according to Dutta and Mander (1997) by which the required amount of transverse confinement reinforcement is given by:
For circular sections:

$$\rho_s = 0.008 \frac{f_c'}{U_{sf}} \left[12 \left(\frac{P_e}{f_c' A_g} + \rho_t \frac{f_y}{f_c'} \right)^2 \left(\frac{A_g}{A_{cc}} \right)^2 - 1 \right] \tag{5-2}$$

For rectangular sections:

$$\frac{A_v}{s B''} + \frac{A_v'}{s D''} = 0.008 \frac{f_c'}{U_{sf}} \left[15 \left(\frac{P_e}{f_c' A_g} + \rho_t \frac{f_y}{f_c'} \right)^2 \left(\frac{A_g}{A_{cc}} \right)^2 - 1 \right] \tag{5-3}$$

with $U_{sf} = 110\, MJ/m^3$.

Step 6 : Determine the additional seismic design moment at he centerline of the bridge deck and/or pier cap.

5.3 DESIGN EXAMPLE

A numerical example is presented to illustrate the use of the above methodology to determine the overstrength of a the plastic hinge zone of a double pier bridge bent. Although the design procedure listed immediately before illustrates the overstrength aspect of the design, the following example takes the whole issue slightly further starting the whole exercise right from the analysis stage. The example illustrates how the concept of overstrength can be used to design bridge columns that provide satisfactory energy dissipation under strong ground motion. The schematic of the bridge pier is shown in figure 5-1.

Consider a part of a "long" multispan concrete slab on steel girder bridge. Each span is 40m in length and the deck is 12.5m wide. The soffit of the superstructure is to be 8m above ground level. Design a twin column bent to be fixed to a rigid piled foundation. For simplicity assume the effective deck weight (girders + concrete + guard rails) to be 7 kPa.

The following design assumptions are made :

- Bridge is located in SPC D such that the peak ground acceleration coefficient is $A = 0.6$
- Soil type factor $S = 1.0$
- Unit weight of reinforced concrete $= 24\,kN/m^3$
- Unconfined compression strength of concrete is $f_c' = 40\,MPa$
- Longitudinal and horizontal reinforcement is Grade 60 ($f_y = 414\,MPa$)

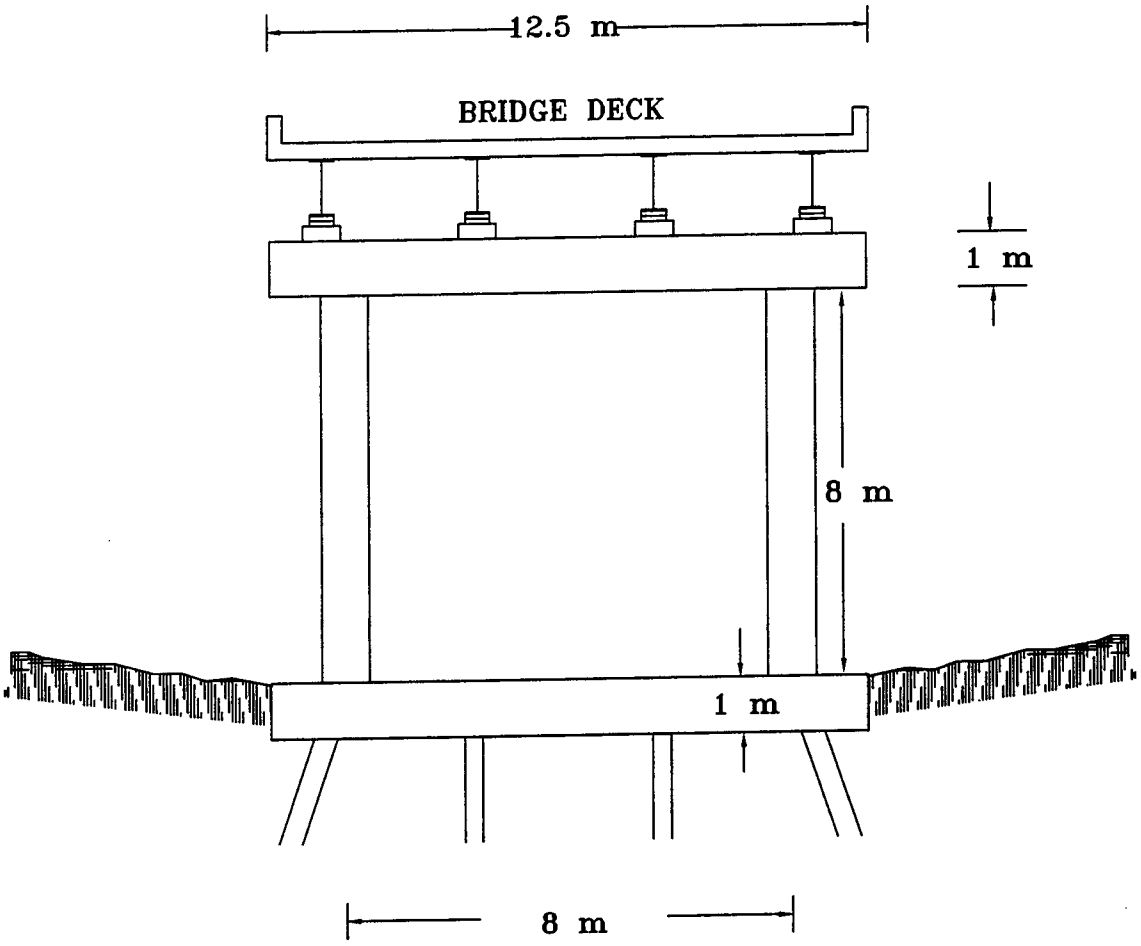

Figure 5-1 Illustrative Bridge Pier Bent used in the Design Example.

Design Solutions

Tributary gravity weight $W_T = 40 \cdot 12.5 \cdot 7;\ W_T = 3.5 \cdot 10^3$ kN

Adopting cap beam dimensions (1m high, 2m wide and 12m long), weight of the cap beam:

$W_c = 1 \cdot 2 \cdot 12 \cdot 24;\ W_c = 576$ kN

Assume concrete strength $f'_c = 40$ MPa

(1) STRUCTURAL GEOMETRY

- Assume two columns spaced 8m apart-each column with a clear height of 8m.

$L = 8$ m and $H = 8$ m

- Assuming each column carries a gravity load of $0.1f'_cA_g$, the required area for each column is:

$$A_{greqd} = \frac{W_T \cdot 1000}{2 \cdot 0.1 \cdot f'_c} \Longrightarrow A_{greqd} = 4.375 \cdot 10^5 \quad mm^2$$

Use a column with a diameter $D = 900$ mm

Gross cross sectional area of each column:

$$A_g = 0.25 \cdot \pi \cdot D^2 \Longrightarrow A_g = 6.362 \cdot 10^5 \quad mm^2$$

- Weight of columns:

$$W_{col} = H \cdot A_g \cdot 10^{-6} \cdot 24 \Longrightarrow W_{col} = 122.145 \quad kN$$

Let the normalized dead load on each column (P_D/f'_cA_g) be denoted by P_{Drat}:

$$P_{Drat} = \frac{0.5 \cdot (W_T + W_c) \cdot 1000}{f'_c \cdot A_g} \Longrightarrow P_{Drat} = 0.08$$

(2) EVALUATION OF SEISMIC DEMAND

- Participating seismic mass

$$m := \frac{W_T + W_c + W_{col}}{9.81} \quad ====> \quad m = 427.945 \quad ton$$

- Lateral stiffness of the pier

Effective moment of inertia $I_{eff} = 0.5 * I_{gross}$

$$I_{eff} := \frac{0.5 \cdot \pi \cdot D^4}{64} \quad ====> \quad I_{eff} = 1.61 \cdot 10^{10} \quad mm^4$$

Modulus of elasticity of concrete

$$E_c := 4700 \cdot \sqrt{f'_c} \quad ====> \quad E_c = 2.973 \cdot 10^4 \quad MPa$$

Assuming fixed-fixed end conditions, stiffness in the lateral direction

$$K_{lat} := \frac{2 \cdot 12 \cdot E_c \cdot I_{eff}}{(H \cdot 1000)^3} \quad ====> \quad K_{lat} = 2.244 \cdot 10^4 \quad kN/m$$

- Natural period of the structure

$$T_n := 2 \cdot \pi \cdot \sqrt{\frac{m}{K_{lat}}} \quad ==> \quad T_n = 0.868 \quad s$$

- Based on the idealized elastic design spectra, the elastic demand for Soil factor $S := 1$ and acceleration coefficient $A := 0.6$

$$C_d := \frac{1.2 \cdot S \cdot A}{T_n^{0.667}} \quad ====> \quad C_d = 0.791 \quad (<2.5A = 2.5*0.6 = 1.5 \text{ O.K.})$$

- However assuming that the column will behave inelastically under a strong ground shaking, required strength capacity for a strength reduction factor $R := 5$ is

$$C_c := \frac{C_d}{R} \quad ===> \quad C_c = 0.158$$

(3) DESIGN FORCES

- Assuming an admissible collapse mechanism as shown below, with H_c=7.5m being the distance between the centers of plastic hinges, the moment at the base of the column is given by

For $H_c := 7.5\ m$;

$$M_u := \frac{C_c \cdot m \cdot 9.81 \cdot H_c}{4} \Rightarrow M_u = 1.246 \cdot 10^3 \quad kN\text{-}m$$

- Axial reaction due to lateral load is given by

$$F_v := \frac{C_c \cdot m \cdot 9.81 \cdot H_c}{L} - \frac{2 \cdot M_u}{L} \Rightarrow F_v = 311.5 \quad kN$$

Normalized axial load ratio F_{vrat}

$$F_{vrat} := \frac{F_v \cdot 1000}{f_c \cdot A_g} \Rightarrow F_{vrat} = 0.012$$

- Assuming the pier bent is also subjected to a vertical acceleration whose magnitude is 2/3 peak horizontal ground acceleration, the maximium axial load ratio on the column is

$$P_{u1rat} := P_{Drat} \cdot \left(1 + \frac{2}{3} \cdot A\right) + F_{vrat} \Rightarrow P_{u1rat} = 0.124$$

and the minimum axial load ratio on the column

$$P_{u2rat} := P_{Drat} \cdot \left(1 - \frac{2}{3} \cdot A\right) - F_{vrat} \Rightarrow P_{u2rat} = 0.036$$

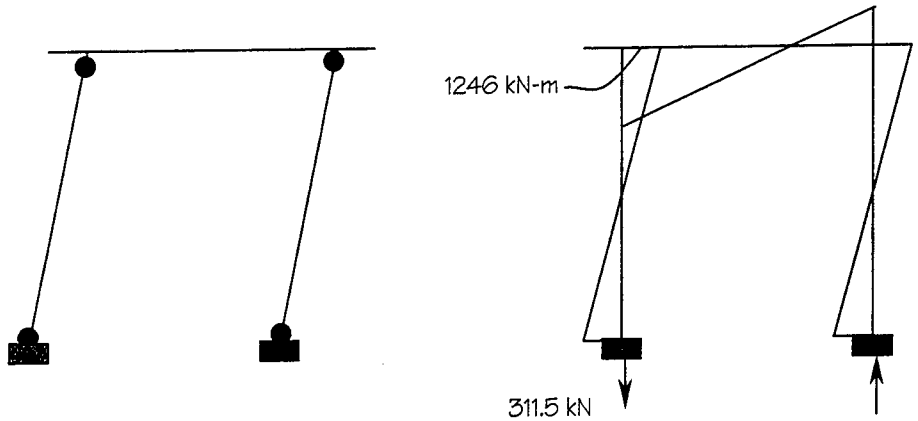

(4) COLUMN DESIGN

- Since the column axial stresses P_{u1rat} and P_{u2rat} are less than $0.2f'c$, both ϕ_1 and ϕ_2 are between 0.9 and 0.5.

$$\phi_1 := 0.9 - \frac{P_{u1rat}}{0.2 \cdot f'_c} \cdot (0.9 - 0.5) \quad =====> \quad \phi_1 = 0.894$$

$$\phi_2 := 0.9 - \frac{P_{u2rat}}{0.2 \cdot f'_c} \cdot (0.9 - 0.5) \quad =====> \quad \phi_2 = 0.898$$

- Summary of dependable ultimate strength actions required by design

$$P_{u1rat} = 0.124 \quad ; \; M_{urat} := \frac{M_u \cdot 10^6}{f'_c \cdot A_g \cdot D} \quad ====> \quad M_{urat} = 0.054$$

$$\frac{P_{u1rat}}{\phi_1} = 0.139 \quad \text{and} \quad \frac{M_{urat}}{\phi_1} = 0.061$$

$$P_{u2rat} = 0.036 \quad ; \; M_{urat} = 0.054$$

$\frac{P_{u2rat}}{\phi_2} = 0.04$ and $\frac{M_{urat}}{\phi_2} = 0.061$

- Provide 16 - #8 longitudinal bars giving a longitudinal reinforcement ratio of 1.27%.

Hence, $N = 16$ and $d_b = 25.4$ mm $f_y = 414$ MPa

Also assume a cover $cov = 51$ mm

Provided nominal capacities

$P_{n1} = 3537$ kN ====> $M_{n1} = 2113.4$ kN-m.

$P_{n2} = 1018$ kN ====> $M_{n2} = 1500$ kN-m.

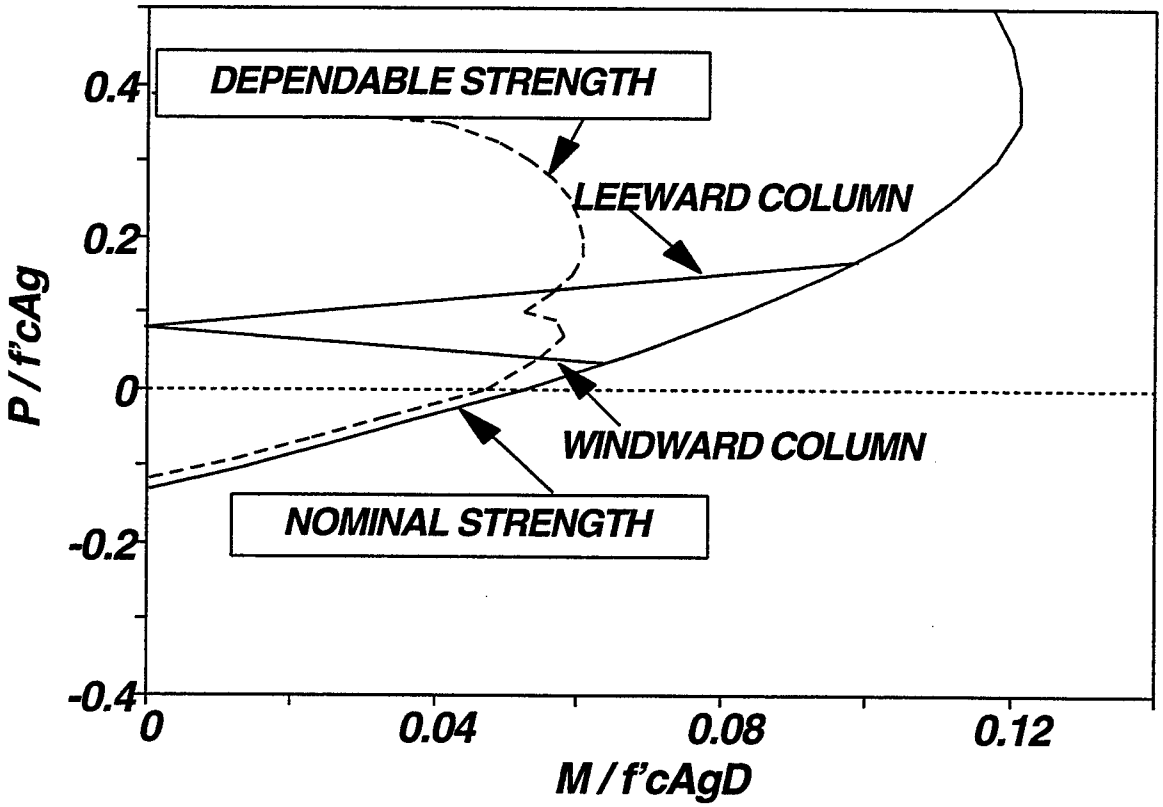

Figure 5-2 Axial Load – Moment Interaction Diagram for the Column Section.

- Design for Shear

* Inintially assume an overstrength factor of λ_{mo}=1.4. Therefore, the maximum overstrength moments and the corresponding shears to be used for design are

(a) For maximum axial load (P_{n1} = 3537 kN) with $\lambda_{mo} = 1.4$

$M_{po1} := \lambda_{mo} \cdot M_{n1}$ ====> $M_{po1} = 2.959 \cdot 10^{3}$ kN-m.

$$V_{o1} := \frac{2 \cdot M_{po1} \cdot 1000}{H_c \cdot 1000 - D} \text{ ====> } V_{o1} = 896.594 \text{ kN.}$$

(b) For minimum axial load (P_{n2} = 1018 kN)

$M_{po2} := \lambda_{mo} \cdot M_{n2}$ ====> $M_{po2} = 2.1 \cdot 10^{3}$ kN-m.

$$V_{o2} := \frac{2 \cdot M_{po2} \cdot 1000}{H_c \cdot 1000 - D} \text{ ====> } V_{o2} = 636.364 \text{ kN.}$$

* Assuming that in the plastic hinge zone concrete is fully cracked and offers no resistance, shear is entirely carried by the steel (V_s) and the diagonal compression strut (V_p). Thus according to Priestley et al. (1996)

$V_o/\phi = V_s + V_p$ where $V_p = 0.85\ P_u \tan\alpha$ and

$V_s = V_o/\phi - P_u \tan\alpha = \pi/2*(A_{sh}*f_{yh})D''/s*\cot 35$

Note that α denotes the angle from the vertical to the straight line joining the center of compression area at the top and bottom of the column and can be conservatively taken as $\alpha = \tan^{-1}(0.8*D/Hc)$ while 35 denotes the inclination of the crack.

$$V_{p1} := 0.85 \cdot \left(P_{n1} \cdot \phi_1\right) \cdot \frac{0.8 \cdot D}{H_c \cdot 1000} \text{ ====> } V_{p1} = 257.963 \text{ kN}$$

$$V_{p2} := 0.85 \cdot \left(P_{n2} \cdot \phi_2\right) \cdot \frac{0.8 \cdot D}{H_c \cdot 1000} \quad ====> \quad V_{p2} = 74.613 \quad kN$$

and assuming the undercapacity factor for shear $\phi = 0.85$

$$V_{s1} := \frac{V_{o1}}{0.85} - V_{p1} \quad ====> \quad V_{s1} = 796.854 \quad kN$$

$$V_{s2} := \frac{V_{o2}}{0.85} - V_{p2} \quad ====> \quad V_{s2} = 674.05 \quad kN$$

Hence providing #5 spirals with a specified yield stress of 414 MPa so that

$d_{bh} := 15.9 \ mm$ and $f_{yh} := 414 \ MPa$

Thus the cofined core dimension

$$D'' := D - 2 \cdot \left(cov + 0.5 \cdot d_{bh}\right)$$

$$s_1 := \frac{\frac{\pi}{2} \cdot f_{yh} \cdot \left(\pi \cdot 0.25 \cdot d_{bh}^{\ 2}\right) \cdot D'' \cdot \cot\left(35 \cdot \frac{\pi}{180}\right)}{V_{s1} \cdot 1000} \quad ===> \quad s_1 = 180.993 \quad mm$$

$$s_2 := \frac{\frac{\pi}{2} \cdot f_{yh} \cdot \left(\pi \cdot 0.25 \cdot d_{bh}^{\ 2}\right) \cdot D'' \cdot \cot\left(35 \cdot \frac{\pi}{180}\right)}{V_{s2} \cdot 1000} \quad ===> \quad s_2 = 213.967 \quad mm$$

Check for antibuckling

$$s := 6 \cdot d_b \quad ====> \quad s = 152.4 \quad mm$$

Provide #5 bars as hoop reinforcement at a pitch of 100 mm

Therefore,

$s := 100 \ mm$

(5) EVALUATION OF ADEQUACY OF HOOP REINFORCEMENT THROUGH ESTIMATION OF OVERSTRENGTH.

Step 1: Concrete stress block parameters

Probabilistic compression strength of concrete: $f'_{cm} := 1.3 \cdot f'_c$

(i) Confinement ratio K

$s' := s - d_{bh}$ ====> $s' = 84.1$ mm.

$$\rho_{cc} := \frac{N \cdot d_b^{\,2}}{D''^{\,2}} \quad \text{====>} \quad \rho_{cc} = 0.017$$

$$k_e := \frac{1 - 0.5 \cdot \frac{s'}{D''}}{\left(1 - \rho_{cc}\right)} \quad \text{====>} \quad k_e = 0.962$$

Volumetric ratio of transverse reinforcement

$$\rho_s := \frac{\pi \cdot d_{bh}^{\,2}}{s \cdot D''} \quad \text{====>} \quad \rho_s = 0.01$$

Effective lateral pressure

$f_l := 0.5 \cdot k_e \cdot \rho_s \cdot f_{yh}$ ====> $f_l = 2.023$ MPa

$$K := -1.254 + 2.254 \cdot \sqrt{1 + 7.794 \cdot \frac{f_l}{f'_{cm}}} - 2 \cdot \frac{f_l}{f'_{cm}} \quad \text{====>} \quad K = 1.241$$

(ii) Control Parameters for Concrete

- Unconfined concrete parameters are

$E_c := 8200 \cdot f'^{\,0.375}_{cm}$ ====> $E_c = 3.608 \cdot 10^4$ MPa

$$\varepsilon'_c := \frac{f'^{\,0.25}_{cm}}{1153} \quad \text{====>} \quad \varepsilon'_c = 0.002$$

$$n_u := \frac{E_c \cdot \varepsilon'_c}{f'_{cm}} \Longrightarrow n_u = 1.616$$

$$z_u := 0.3 \cdot \frac{E_c}{f'_{cm}} \Longrightarrow z_u = 208.177$$

$$x_{u20\%} := \frac{0.8}{z_u \cdot \varepsilon'_c} + 1 \Longrightarrow x_{u20\%} = 2.65$$

- Confined concrete parameters are

$$f'_{cc} := K \cdot f'_{cm} \Longrightarrow f'_{cc} = 64.55 \quad MPa$$

$$\varepsilon'_{cc} := \varepsilon'_c \cdot (1 + 5 \cdot (K - 1)) \Longrightarrow \varepsilon'_{cc} = 0.005$$

$$n_c := \frac{E_c \cdot \varepsilon'_{cc}}{f'_{cc}} \Longrightarrow n_c = 2.873$$

$$z_c := 0.3 \cdot \frac{E_c}{f'_{cm} \cdot K^7} \Longrightarrow z_c = 45.833$$

$$x_{c20\%} := \frac{0.8}{z_c \cdot \varepsilon'_{cc}} + 1 \Longrightarrow x_{c20\%} = 4.396$$

$$\varepsilon_{c20\%} := x_{c20\%} \cdot \varepsilon'_{cc} \Longrightarrow \varepsilon_{c20\%} = 0.023$$

(iv) Extreme compression fiber strain

The strain of extreme confined compression fiber is for maximum $\alpha_{cc}\,\beta_{cc}$

$$x_{\alpha\beta\,max} := \sqrt{1 + \frac{2}{(n_c + 1) \cdot z_c \cdot \varepsilon'_{cc}}} \Longrightarrow x_{\alpha\beta\,max} = 1.787$$

For unconfined cover concrete the strain is the same at the intersection of the unconfined and confined concrete and hence the corresponding value of x is

$$x_\alpha := x_{\alpha\beta\,max} \cdot \frac{\varepsilon'_{cc}}{\varepsilon'_c} \Longrightarrow x_\alpha = 3.943 \quad (>x_{u20\%})$$

(v) Confined stress block parameters for overstrength moment

$\alpha_{cc} := 0.85 + 0.12 \cdot (K - 1)^{0.4}$ ====> $\alpha_{cc} = 0.918$

$\beta_{cc} := 0.85 + 0.13 \cdot (K - 1)^{0.6}$ ====> $\beta_{cc} = 0.905$

(vi) Unconfined stress block parameters for overstrength moment

$$\alpha\beta_{co} := \frac{n_u}{(n_u + 1) \cdot x_\alpha} + \frac{0.48}{z_u \cdot \varepsilon'_c \cdot x_\alpha} + 0.2 \cdot \left(1 - \frac{x_{u20\%}}{x_\alpha}\right)$$

$\alpha\beta_{co} = 0.473$ Also, $\beta_{co} := 1.0$ (assumed)

(vii) AASHTO/ACI Stress Block Parameters for Nominal Moment

$\alpha_1 := 0.85$ and $\beta_1 := 0.76$ for $f'_c = 40$ MPa

Step 2 : Nominal Moment Capacity, M_n

(i) Balanced failure point:

Neutral axis depth at balanced failure

$$cD_{rat} := \frac{0.425}{\beta_1}$$ ====> $cD_{rat} = 0.559$

By the usual AASHTO/ACI approach, normalized balanced force and moment capacity

$P_{nbrat} := 0.5$ and $M_{nbrat} := 0.138$

Tension axial load capacity

$$\rho_t := \frac{N \cdot d_b^2}{D^2}$$ ====> $\rho_t = 0.013$

$$P_{ntrat} := -\rho_t \cdot \frac{f_y}{f'_c}$$ ====> $P_{ntrat} = -0.132$

$$M_{n1rat} := M_{nbrat} \cdot \left[1 - \left[\frac{\frac{P_{n1} \cdot 1000}{f'_c \cdot A_g} - P_{nbrat}}{\left(P_{ntrat} - P_{nbrat} \right)} \right]^2 \right] \quad ===> M_{n1rat} = 0.093$$

Step 3: Overstrength Moment Capacity M_{po}

Neutral Axis Depth Ratio = 0.5

Balanced axial load capacity is determined as

$$P_{borat} := 0.65 \cdot \left[\alpha_{cc} \cdot \beta_{cc} \cdot K \cdot \left(\frac{D''}{D} \right)^2 + \alpha\beta_{co} \cdot \left[1 - \left(\frac{D''}{D} \right)^2 \right] \right]$$

$$P_{borat} = 0.582$$

Moment contribution of concrete M_{oc} to the balanced ultimate moment is

With $\kappa_c := 0.6$; $\kappa_o := 0.4$

$$M_{ocrat} := 0.325 \cdot \left[\alpha_{cc} \cdot \beta_{cc} \cdot K \cdot \left(1 - \kappa_c \cdot \beta_{cc} \right) \cdot \left(\frac{D''}{D} \right)^3 + \alpha\beta_{co} \cdot \left[1 - \left(\frac{D''}{D} \right)^2 \right] \cdot \left(1 - \kappa_o \right) \right]$$

$$M_{ocrat} = 0.123$$

Moment contribution of steel M_{os} to the balanced ultimate moment is

With $d' := cov + d_{bh} + 0.5 \cdot d_b$ and $f_{su} := 640$ MPa

$$M_{osrat} := 0.384 \cdot \rho_t \cdot \left(1 - 2 \cdot \frac{d'}{D} \right) \cdot \left(\frac{f_{su}}{f'_c} \right) \quad ====> M_{osrat} = 0.064$$

Balance moment ratio:

$$M_{borat} := M_{ocrat} + M_{osrat} \quad ====> M_{borat} = 0.188$$

Tension axial load capacity (P_{to}) is

$$P_{torat} := -1.2 \cdot \rho_t \cdot \frac{f_{su}}{f'_c} \quad ====> P_{torat} = -0.245$$

Overstrength moment ratio is

$$M_{porat} := M_{borat} \cdot \left[1 - \left(\frac{P_{u1rat} - P_{borat}}{P_{torat} - P_{borat}}\right)^2\right] \quad ===> \quad M_{porat} = 0.13$$

Step 4: Overstrength factor

$$\lambda_{mo} := \frac{M_{porat}}{M_{n1rat}} \quad ====> \quad \lambda_{mo} = 1.4$$

This is same as the initially assumed value of 1.4. Moreover shear did not govern the design. Hence no change in the calculation is needed.

Step 5: Check Ductility and Confinement requirements

$$U_{sf} := 110 \ MJ/m^3$$

$$\rho_s := 0.008 \cdot \frac{f'_c}{U_{sf}} \cdot \left[12 \cdot \left(P_{u1rat} + \rho_t \cdot \frac{f_y}{f'_c}\right)^2 \cdot \left(\frac{D''}{D}\right)^2 - 1\right]$$

$\rho_s = -0.001$ ====> Confinement does not govern.

Step 6: Additional seismic design moment at the centerline of the cap beam

Assuming the maximum overstrength moment in the column occurs at a depth D/2 from the face of the cap beam and the point of contraflexure is eaxctly at half the clear length of the column, seismic design moment for the cap beam is

For $D_{cap} := 1000$ mm

$$M_{cap} := M_{porat} \cdot f'_c \cdot \frac{\pi}{4} \cdot D^3 \cdot \frac{H_c \cdot 1000 + 0.5 \cdot D_{cap}}{H_c \cdot 1000 - 0.5 \cdot D} \cdot 10^{-6}$$

$M_{cap} = 3.381 \cdot 10^3$ kN-m

and the nominal flexural cap beam requirements

$$M_{ncap} := \frac{M_{cap}}{0.9} \quad ====> \quad M_{ncap} = 3.757 \cdot 10^{3} \quad \text{kN-m}$$

This will ensure an admissible failure mechanism with hinging in the column.

SECTION 6
SUMMARY, CONCLUSIONS AND RECOMMENDATIONS FOR CODE DEVELOPMENT

6.1 Executive Summary

When using the capacity design philosophy for designing earthquake resistant structures, the designer chooses a hierarchy of failure mechanisms. Inelastic (plastic) modes of deformation which provide ductility are preferred; this generally means flexural plastic hinging through ductile detailing. All other undesirable brittle failure mechanisms such as shear, bond and anchorage, compression failure (of both bars and concrete) are inhibited. Brittle regions are protected by ensuring their strength exceeds the demands originating from the maximum overstrength that can be generated at potential plastic hinge zones.

This study had been concerned with determination of maximum moment capacity and overstrength factors of reinforced concrete bridge columns by using a Gaussian Quadrature method of numerical integration—an analysis procedure which is easily suited to spreadsheet type computer programming. The proposed analysis procedure was then used to conduct parametric studies on overstrength factors in the plastic hinge zones of concrete columns and to develop design curves of overstrength factors. It was observed that the values of overstrength factors from the analytical studies developed compared well with the experimental results.

In view of the apparent complexity involved in the Gaussian Quadrature approach, an alternative technique based on stress block analysis was also introduced as part of this research report. Explicit expressions for stress block factors obtained by integration of concrete stress-strain relations were derived with due consideration to confining action of the transverse reinforcement. Using these stress block factors, a parabolic interaction curve was traced that represented the overstrength actions due to the strain hardening of the longitudinal reinforcement and the confining action of the transverse reinforcement. A similar approach was also adopted

for the AASHTO/ACI nominal interaction curve. Overstrength factors were thus obtained as ratios of the overstrength and nominal interaction expressions corresponding to a particular axial load level. It was also observed that the overstrength interaction curve can be suitably adjusted by altering the concrete and steel strengths to account for the uncertainties in their respective strengths. A further contrast of the overstrength factors with those obtained from rigorous analysis revealed satisfactory results. The presented parabolic axial load-moment interaction curve procedure for the determination of overstrength factors is a straight-forward design method for the engineer to determine the overstrength factors of plastic hinge regions of concrete columns.

6.2 Specific Conclusions

Specific conclusions derived from this study are as follows:

(i) At low levels of axial load overstrength is mainly contributed by strain hardening of the longitudinal reinforcement. Hence reinforcement varieties that have a significantly long strain hardening plateau can result in enhancement of overall ductility of the structural concrete section by prolonging the ultimate curvature at which the overstrength moment occurs.

(ii) At high levels of axial load, concrete is the main contributor to overstrength. Hence concrete sections with high confining reinforcement display a higher value of the overstrength moment.

(iii) A simplified stress block analysis can be used to obtain overstrength factors using principles of plastic analysis. The concrete and steel properties can also be adjusted by multiplying their mean and median values by 1.3 and 1.2 respectively to account for randomness in their strengths.

6.3 Recommendations for Code Development

It is recommended that the following language be adopted by code writers for assessing the overstrength factors for flexural hinge zones.

6.3.1 Notation

A_{bh} = area of cross section of a single transverse reinforcement

A_{cc} = area of core concrete measured to the centerline of transverse reinforcement

A_g = gross area of the concrete section

A_{st} = total area of longitudinal reinforcement

A_{sx} = total area of cross section of transverse reinforcement in the X direction

A_{sy} = total area of cross section of transverse reinforcement in the Y direction

D = overall depth of the section

D' = depth of the section measured from centers of extreme tension and compression steel

D'' = depth of the section measured from the centers of transverse reinforcement

K = confinement ratio of concrete

M_{bo} = maximum overstrength moment in an overstrength moment interaction curve

M_n = provided nominal moment capacity of the plastic hinge zone

M_{nb} = maximum nominal moment in a nominal moment interaction curve

M_{oc} = maximum overstrength concrete moment

M_{os} = maximum overstrength steel moment

M_{po} = overstrength moment capacity at the center of the hinge

P_{bo} = axial load corresponding to M_{bo} in overstrength moment interaction curve

P_e = applied axial load on a section

P_{nb} = axial load corresponding to M_{nb} nominal moment interaction curve

P_{nt} = nominal tensile axial load capacity

P_{to} = overstrength tensile axial load capacity

b' = lateral dimension of a rectangular section measured from centerline of outermost steel

b'' = breadth of the confined core concrete

f_c' = unconfined compression strength of concrete

f_{cc}' = peak value of confined concrete stress

f_{ce}' = expected mean unconfined compression strength of concrete

f_{co}' = upper bound unconfined compression strength of concrete

f_l = confining stress exerted by the transverse reinforcement in circular and square sections

f_{l_x} = confining stress exerted by the transverse reinforcement in the X direction

f_{l_y} = confining stress exerted by the transverse reinforcement in the Y direction

f_{su} = ultimate stress of the longitudinal reinforcement

f_y = yield strength of the longitudinal reinforcement

f_{ye} = expected mean yield strength of the longitudinal reinforcement

f_{yo} = upper bound yield strength of the longitudinal reinforcement

k_e = confinement effectiveness coefficient

s = center to center spacing of transverse reinforcement

s' = clear spacing of transverse reinforcement

w_i = width of the parabola forming between two adjacent longitudinal reinforcement

α_{co}, β_{co} = unconfined concrete stress block factors

α_{cc}, β_{cc}^{max} = maximum product of confined concrete stress block parameters

χ = a parameter = 0.5 for spirals and = 1.0 for circular hoops

κ_c = factor that locates the position of the plastic centroid of core cover concrete

κ_0 = factor that locates the position of the plastic centroid of core cover concrete

λ_{mo} = moment overstrength factor

ρ_{cc} = longitudinal steel ratio with respect to the core concrete

ρ_s = volumetric ratio of transverse reinforcement

ρ_t = longitudinal steel ratio

ρ_x = volumetric ratio of transverse reinforcement in the X direction

ρ_y = volumetric ratio of transverse reinforcement in the Y direction

The flexural overstrength factor for plastic hinge zones shall be determined by one of the following three methods. The methods are given in order of complexity. Higher order methods will give more precise results with less conservatism.

6.3.2 Method 1: Empirical Equation Method

The overstrength factor shall be taken as

$$\lambda_{mo} = 1 + \frac{P_u}{f_c' A_g} \tag{6-1}$$

but not less than $\lambda_{mo} = 1.4$.

6.3.2 Method 2: Interaction Diagram Approach

The overstrength factor shall be calculated as the ratio of strengths given by the flexural overstrength capacity to the nominal flexural strength. The following equation may be used to interpolate at various axial loads:

$$\lambda_{mo} = \frac{M_{po}}{M_n} = \frac{\dfrac{M_{bo}}{f_c' A_g D}\left(1 - \left(\dfrac{P_e/f_c' A_g - P_{bo}/f_c' A_g}{P_{to}/f_c' A_g - P_{bo}/f_c' A_g}\right)^2\right)}{\dfrac{M_{nb}}{f_c' A_g D}\left(1 - \left(\dfrac{P_e/f_c' A_g - P_{nb}/f_c' A_g}{P_{to}/f_c' A_g - P_{nb}/f_c' A_g}\right)^2\right)} \tag{6-2}$$

where the following expressions shall be adopted for the parameters given in equation (6-2).

$$\frac{M_{bo}}{f_c' A_g D} = \frac{M_{oc}}{f_c' A_g D} + \frac{M_{os}}{f_c' A_g D} \tag{6-3}$$

$$\frac{M_{oc}}{f_c' A_g D} = 0.325\left(1 - \frac{A_{cc}}{A_g}\right)\alpha_{co}\beta_{co}(1-\kappa_o) + 0.325\,K\,\alpha_{cc}\beta_{cc}^{\max}\frac{A_{cc}}{A_g}(1-\kappa_c\beta_{cc})\left(\frac{D''}{D}\right) \tag{6-4}$$

$$\frac{M_{os}}{f_c' A_g D} = \text{II}\frac{1.2\,\rho_t f_{su}}{f_c'}\frac{D'}{D} \tag{6-5}$$

where II shall be taken as 0.32 and 0.375 for circular and square columns, and for rectangular columns

$$\text{II} = \frac{1}{4}\left(1 + \frac{2b'}{D'}\right)\left(\frac{D'}{b' + D'}\right) \tag{6-6}$$

Also,

$$\frac{P_{bo}}{f_c' A_g} = 0.65\,\alpha_{cc}\beta_{cc}^{\max} K\frac{A_{cc}}{A_g} + 0.65\,\alpha_{co}\beta_{co}\left(1 - \frac{A_{cc}}{A_g}\right) \tag{6-7}$$

$$\frac{P_{to}}{f_c' A_g} = -1.2\,\rho_t\frac{f_{su}}{f_c'} \tag{6-8}$$

$$\frac{P_{nt}}{f_c' A_g} = -\rho_t\frac{f_y}{f_c'} \tag{6-9}$$

where for circular sections $\kappa_o = 0.4\,;\kappa_c = 0.6$. For rectangular sections $\kappa_c = 0.5$ and κ_o shall be determined by using principles of strength of materials. The nominal interaction parameters (M_{nb}, P_{nb}) shall be determined by the usual AASHTO/ACI procedure.

The stress block parameters for confined and unconfined concrete shall be taken as

$$\alpha_{cc} = 0.85 + 0.12\,(K - 1)^{0.4} \tag{6-10}$$

$$\text{and}\quad \beta_{cc}^{\max} = 0.85 + 0.13\,(K - 1)^{0.6} \tag{6-11}$$

For unconfined concrete

$$\alpha_{co} = 0.45 \quad \text{and} \quad \beta_{co} = 1.0 \tag{6-12}$$

The enhancement in concrete strength due to confinement ($K = f'_{cc}/f'_c$) shall be obtained for circular and square sections by

$$K = \frac{f'_{cc}}{f'_c} = -1.254 + 2.254\sqrt{1 + 7.94\frac{f_l}{f'_c}} - 2\frac{f_l}{f'_c} \tag{6-13}$$

Following parameters shall be used for circular sections:

$$f_l = \frac{1}{2} k_e \rho_s f_y \tag{6-14}$$

$$\rho_s = \frac{4A_{bh}}{s D''} \tag{6-15}$$

$$k_e = \frac{(1 - \chi s'/D'')}{(1 - \rho_{cc})} \tag{6-16}$$

$$\rho_{cc} = \frac{4A_{st}}{\pi D''^2} \tag{6-17}$$

χ = coefficient having values 0.5 and 1.0 for spirals and hoops respectively. For rectangular sections:

$$f_{l_y} = k_e \rho_y f_{yh} \tag{6-18}$$

$$f_{l_x} = k_e \rho_x f_{yh} \tag{6-19}$$

in which

$$\rho_x = \frac{A_{sx}}{s D''}$$
$$\rho_y = \frac{A_{sy}}{s b''} \qquad (6\text{-}20)$$

$$k_e = \frac{\left(1 - \frac{1}{6}\sum_{i=1}^{n} w_i'^2\right)\left(1 - 0.5\frac{s'}{b''}\right)\left(1 - 0.5\frac{s'}{D''}\right)}{(1 - \rho_{cc})} \qquad (6\text{-}21)$$

$$\rho_{cc} = \frac{A_{st}}{b'' D''} \qquad (6\text{-}22)$$

The confined strength ratio shall be calculated using the minimum of f_{l_x} and f_{l_y} in conjunction with figure 6-1.

6.3.4 Method 3: Moment Curvature Analysis

The overstrength factor shall be calculated as the ratio of the maximum moment achieved in a moment-curvature analysis over the range of curvatures expected in a maximum credible earthquake with respect to the nominal flexural strength. When calculating overstrength capacities, expected upper bound material properties shall be assumed as follows:

$$f'_{co} = 1.3\, f'_{ce} \qquad (6\text{-}23)$$

$$\text{and } f_{yo} = 1.2\, f_{ye} \qquad (6\text{-}24)$$

where f'_{ce} and f_{ye} are expected mean strengths of concrete and steel respectively.

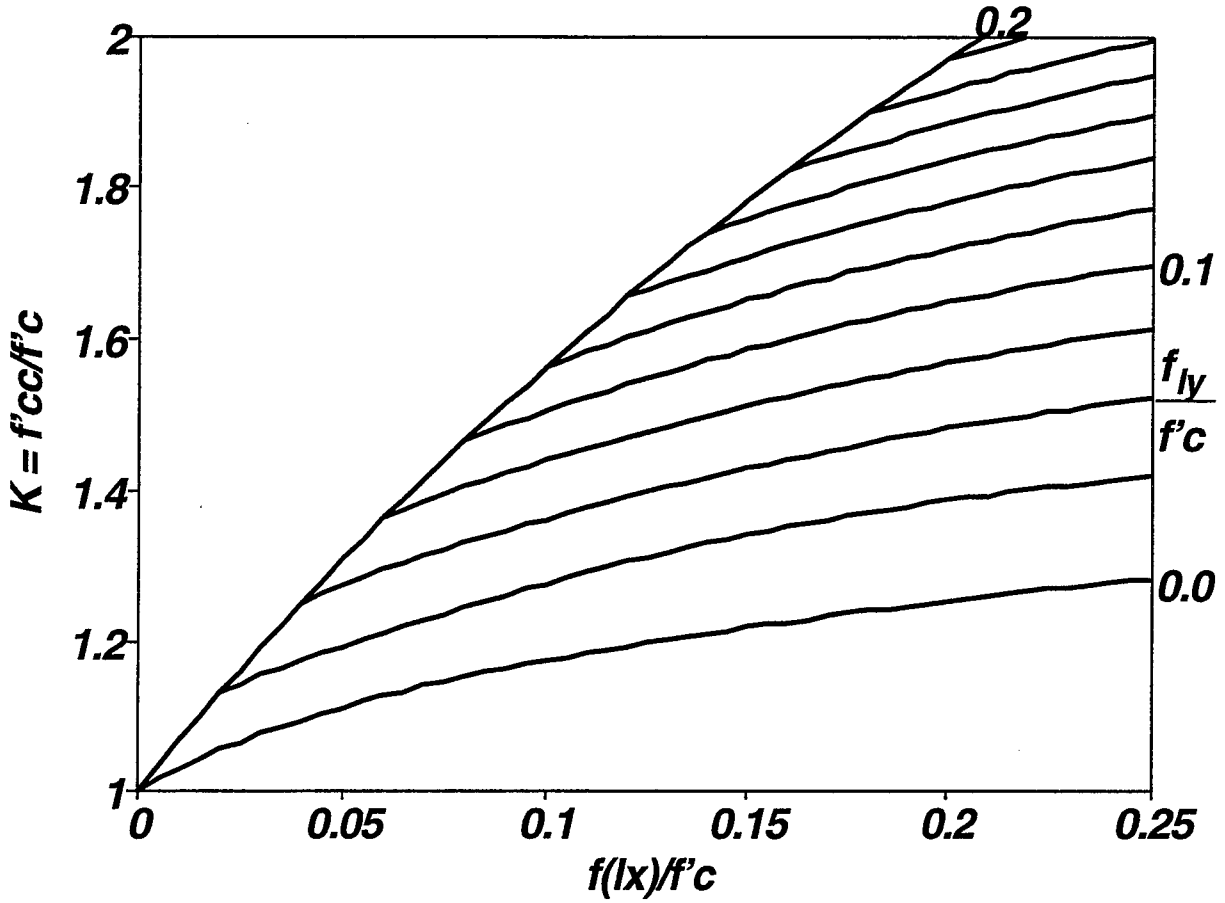

Figure 6-1 Confined Strength Ratio based on Multiaxial Confinement Model.

SECTION 7
REFERENCES

AASHTO (1996), *AASHTO Standard Specification for Highway Bridges*, 16th. ed.,American Association of State Highway and Transportation Officials, Washington, D.C.

American Concrete Institute, (1995), *Building Code Requirements for Reinforced Concrete*, ACI-318-95, Detroit, Michigan.

Andriono, T. and Park, R.(1986), *Seismic Design Considerations of the Properties of New Zealand Manufactured Steel Reinforcing Bars*, Bulletin of the New Zealand National Society for Earthquake Engineering, Vol. 19, No.3, Sep. 1986, pp. 213-246.

Andriono, T. and Park, R.(1987), Seismic Design Considerations of the Properties of New Zealand Manufactured Steel Reinforcing Bars, *Proceedings* of the Pacific Conference of Earthquake Engineering, Vol 1. pp 13-24, New Zealand.

Chang, G.A. and Mander, J.B.(1994a) "Seismic Energy Based Fatigue Damage Analysis of Bridge Columns: Part I - Evaluation of Seismic Capacity," Technical Report NCEER-94-0006, National Center for Earthquake Engineering Research, State University of New York at Buffalo.

Chang, G.A. and Mander, J.B.(1994b) "Seismic Energy Based Fatigue Damage Analysis of Bridge Columns: Part II - Evaluation of Seismic Demand," Technical Report NCEER-94-0013, National Center for Earthquake Engineering Research, State

University of New York at Buffalo.

Chapra, S.C. and Canale, R.P.(1995) Numerical Methods for Engineers, McGraw Hill Publishing Co., New York.

Dutta, A. and Mander, J.B.(1998) "Fatigue analysis and Design of Confined Concrete Sections" Technical Report NCEER-98-00xx (in review), National Center for Earthquake Engineering Research, State University of New York at Buffalo.

Julian, O.G. (1955), discussion of Strength Variations in Ready-Mixed Concrete, by A.E. Cummings, *Proceedings*, American Concrete Institute, Vol. 51, No. 12, Dec. 1955., pp. 772-4-772-8.

Mirza, S.A. and MacGregor, J.G. (1979a), *Variability of Mechanical Properties of Reinforcing Bars*, Journal of the Structural Division, ASCE, Vol. 105, No. ST5, May 1979, pp. 921-937.

Mirza, S.A., Hatzinikolas, M. and MacGregor, J.G. (1979b), *Statistical Descriptions of Strength of Concrete*, Journal of the Structural Division, ASCE, Vol. 105, No. ST6, June 1979, pp. 1021-1037.

Kent, D.C. and Park, R.,(1971), *Flexural Members with Confined Concrete,* Journal of the Structural Division, ASCE, Vol.97, No. ST7, Jul-71,pp.1969-1990.

Mander, J.B. and Dutta, A. (1996). "A Practical Energy-Based Design Methodology for Performance Based Seismic Engineering," Proceedings, SEAOC Annual Convention, 1996, Maui, Hawaii.

Mander, J.B., Priestley, M.J.N. and Park, R.,(1988a), *Theoretical Stress-Strain Model for Confined Concrete,* Journal of Structural Engineering, Vol. 114, No. 8, Aug-88, pp. 1804-1826.

Mander, J.B., Priestley, M.J.N. and Park, R.,(1988b), *Observed Stress-Strain Behavior of Confined Concrete,* Journal of Structural Engineering, Vol. 114, No. 8, Aug-88, pp. 1827-1849.

Mander, J.B., Priestley, M.J.N. and Park, R.,(1984), *Seismic Design of Bridge Piers,* Department of Civil Engineering, University of Canterbury, Report 84-2, Feb-84, 483 pp.

Mander, J.B., Priestley, M.J.N. and Park, R.,(1983), *Behavior of Ductile Hollow Reinforced Concrete Columns,* Bulletin of the New Zealand national Society for Earthquake Engineering, Vol.16, No.4, Dec-83, pp.273-290.

Park, R. and Paulay, T.,(1975),Reinforced Concrete Structures, John Wiley, New York, 1975.

Paulay, T. and Priestley, M.J.N.(1992) Seismic Design of Reinforced Concrete and Masonry Structures, John Wiley and Sons, Inc., New York.

Popovics, S.,(1970), *A Review of Stress-Strain Relationship for Concrete,* Journal of the American Concrete Institute, Vol. 67, No. 3, Mar-70, pp. 243-248.

Shalon, R. and Reintz. R.C., (1955), Interpretation of Strengths Distribution as a factor in Quality Control of Concrete, *Proceedings*, Reunion Internationale des Laboratories d'Essais et de Recherches sur les Materiaux et les Constructions, Symposium on the Observation of Substructures, Vol. 2, Laboratorio Naciano de

Engenharia Civil, Lisbon, Potugal, pp. 100-116.

Tsai, W.T.,(1988),*Uniaxial Compressional Stress-Strain Relations of Concrete,* Journal of Structural Engineering, Vol. 114, No. 8, Sep-88, pp. 2133-2136.

APPENDIX A
STRESS-STRAIN EQUATIONS AND STRESS BLOCK PARAMETERS FOR UNCONFINED AND CONFINED CONCRETE

A-1 Equation for Unconfined Concrete

The equation to describe the monotonic compressive stress-strain curve for unconfined concrete is based on Tsai's equation:

$$y = \frac{nx}{1 + \left(n - \frac{r}{r-1}\right)x + \frac{x^r}{r-1}} \qquad \text{(A-1)}$$

where $x = \varepsilon_{co}/\varepsilon_c'$, $y = f_{co}/f_c'$ with f_c' and ε_c' being the peak ordinate and the corresponding abscissae, and n, r are parameters to control the shape of the curve.

The equation parameter n is defined by the initial modulus of elasticity, the concrete strength and the corresponding strain. In S.I. units, the initial modulus of elasticity and strain at peak stress are given by

$$E_c = 8200 f_c'^{3/8}$$
$$\varepsilon_c' = \frac{f_c'^{1/4}}{1153} \qquad \text{(A-2)}$$

Thus the parameter n is defined as:

$$n = \frac{E_c \varepsilon_c'}{f_c'} = \frac{E_c}{E_{sec}} = \frac{7.2}{f_c'^{3/8}} \quad MPa \qquad \text{(A-3)}$$

and the parameter r as:

$$r = \frac{f_c'}{5.2} - 1.9 \quad MPa \qquad \text{(A-4)}$$

However, to adequately reflect the behavior of unconfined cover concrete, a modification as

suggested by Mander et al. (1988a) was adopted. It was decided that the cover concrete beyond a strain of $2\varepsilon_c'$ would be made to decay to zero linearly up to a strain ratio of x_{max} according to

$$y = y_{2\varepsilon_c'} - \frac{x-2}{\tan\alpha} \tag{A-5}$$

where $y_{2\varepsilon_c'}$ = normalized stress at $x=2$ and $\tan\alpha = 1/|dy/dx|_{2\varepsilon_c'}$, with

$$\left(\frac{dy}{dx}\right)_{2\varepsilon_c'} = \frac{n(1-2^r-2)}{\left[1+2\left(n-\frac{r}{r-1}\right)+\frac{2^r}{r-1}\right]^2} \tag{A-6}$$

and

$$x_{max} = 2 + y_{2\varepsilon_c'}\tan\alpha \tag{A-7}$$

A-2 Equation for Confined Concrete

The same equation A-1 can be used to describe the behavior of confined concrete. The peak strength enhancement due to ductility can be obtained using the procedure suggested by Mander et al. (1984, 1988a) and described in detail in subsections A-2.1 and A-2.2. Thus in equation A-1, the parameters can be redefined for confined concrete as $x=\varepsilon_{cc}/\varepsilon_{cc}'$ and $y=f_{cc}/f_{cc}'$ where f_{cc}' and ε_{cc}' are the confined concrete peak ordinate ($=Kf_c'$) and the corresponding abscissae given by Richart et al.(1929) as

$$\varepsilon_{cc}' = \varepsilon_c'(1+5(K-1)) \tag{A-8}$$

However, in order to have better control on the falling branch of the confined concrete, Mander et al. (1988b) based on experimental observations added a point on the falling branch. The following empirical relationship was proposed

$$\begin{aligned} \varepsilon_f &= 3\,\varepsilon_{cc}' \\ f_f &= f_{cc}' - \Delta f_{cc} \\ \Delta f_{cc} &= K\,\Delta f_c\left(\frac{0.8}{K^5}+0.2\right) \end{aligned} \tag{A-9}$$

where Δf_{cc} = stress drop of the confined concrete at a strain of $3\,\varepsilon_{cc}'$, and Δf_c = stress drop of

the unconfined concrete at a strain of $3\varepsilon_c'$. Thus using $n = E_c/E_{sec}$ for confined concrete, the parameter r can be solved algebraically which will give a more realistic stress decay in the falling branch. Thus a complete stress-strain history of confined concrete can be obtained.

A-2.1 Confinement Coefficient for Circular Sections

Using the model proposed by Mander et al. (1988a), the effective lateral pressure for circular sections is given by

$$f_l = \frac{1}{2} k_e \rho_s f_s \tag{A-10}$$

with k_e as the confinement effectiveness coefficient given by

$$k_e = \frac{A_e}{A_{cc}} \tag{A-11}$$

The confining bars are assumed to yield by the time the maximum stress in the concrete is reached in which case $f_s = f_y$.

The effectively confined area shown in figure A-1a is calculated as

$$A_e = \frac{\pi D''^2}{4}\left(1 - \chi \frac{s'}{D''}\right)^2 \tag{A-12}$$

where D'' = diameter of the core concrete, s' = clear longitudinal spacing between spirals/hoops in which arching action of concrete develops, and χ = coefficient having values 0.25 and 0.5 for spirals and hoops respectively.

The concrete core area is calculated as

$$A_{cc} = (1 - \rho_{cc}) \frac{\pi D''^2}{4} \tag{A-13}$$

where ρ_s is the volumetric ratio of the transverse reinforcement to the confining core given by: with A_{sh} = cross sectional area of the lateral steel and ρ_{cc} = volumetric ratio of the longitudinal

$$\rho_s = \frac{4A_{sh}}{sD''} \tag{A-14}$$

steel in the confined core given by:

$$\rho_{cc} = \frac{4A_{st}}{\pi D''^2} \tag{A-15}$$

where A_{st} = total area of the longitudinal reinforcement. With the maximum lateral pressure thus obtained, the peak confinement strength ratio can be obtained from

$$K = \frac{f'_{cc}}{f'_c} = -1.254 + 2.254\sqrt{1 + 7.94\frac{f_l}{f'_c}} - 2\frac{f_l}{f'_c} \tag{A-16}$$

A-2.2 Confinement Coefficient for Rectangular Sections

The effectively confined area for rectangular sections shown in figure A-1b is given by

$$A_e = \left(b''D'' - \sum_{i=1}^{n}\frac{w_i'^2}{6}\right)\left(1 - 0.5\frac{s'}{b''}\right)\left(1 - 0.5\frac{s'}{D''}\right) \tag{A-17}$$

The concrete core area is given by

$$A_{cc} = b''D'' - A_{st} \tag{A-18}$$

The lateral confinement pressure for rectangular sections can have different values in each direction. In this case a general three dimensional state of stress is obtained. The lateral pressure for each direction (x and y) is calculated as:

$$f_{l_y} = k_e \rho_y f_{yh} \tag{A-19}$$

$$f_{l_x} = k_e \rho_x f_{yh} \tag{A-20}$$

in which

$$\rho_x = \frac{A_{sx}}{s D''} \qquad \rho_y = \frac{A_{sy}}{s b''} \tag{A-21}$$

with A_{sx}, A_{sy} = total area of transverse reinforcement parallel to the x and y axis respectively. With the minimum value of f_l / f_c' (i.e. either f_{l_x} / f_c' or f_{l_y} / f_c'), the confined strength ratio can be obtained from figure A-2.

A-3 Stress Block Analysis for Confined Concrete

Stress block analysis is a very efficient hand method of analysis by which the distribution of concrete stress over the compressed part of the section can be replaced by a constant stress block having the same magnitude and location as the original variable stress distribution. As was observed from the preceding discussion, the effect of confinement is to increase the ductility level of the concrete by increasing the level of maximum attainable stress and the corresponding strain. Stress block parameters which can capture the effect of confinement is thus necessary to accurately model the behavior of confined concrete. Such stress block parameters can be obtained from first principles as illustrated below.

A-3.1 General Stress Block Theory

Stress block parameters that are stress-strain curve dependent can be obtained from stress block theory. The distribution of concrete stress over the compressed part of the section may be found from the strain diagram and the stress-strain curve for concrete. This complex stress distribution can be replaced by an equivalent one of simpler rectangular outline such that it results in the same total compression force C_c applied at the same location as in the actual member. The average concrete stress ratio α and the stress block depth factor β of this equivalent rectangular stress block distribution can be determined as:

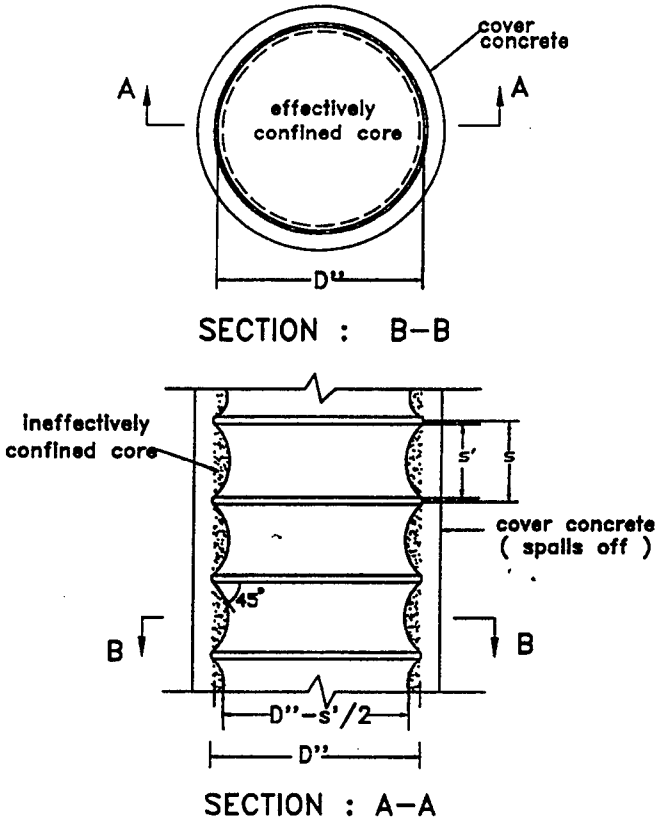

(a) Circular Section

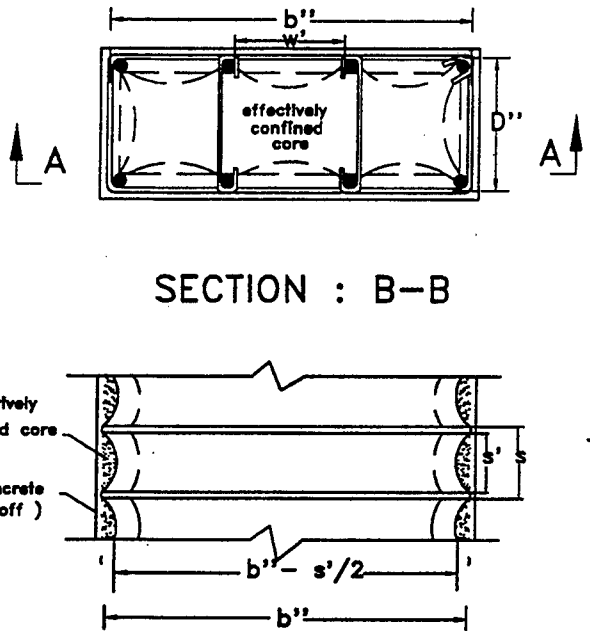

(b) Rectangular Section

Figure A-1 Showing effectively Confined Core Areas for Circular and Rectangular Sections.

(i) Effective Average Concrete Stress Ratio, α: The area (A_c) under the stress-strain curve is

$$A_c = \int_0^{\varepsilon_{cm}} f_c \, d\varepsilon = \alpha \beta f_c' \varepsilon_{cm} \tag{A-22}$$

Thus,

$$\alpha\beta = \frac{\int_0^{\varepsilon_{cm}} f_c \, d\varepsilon}{f_c' \varepsilon_{cm}} \tag{A-23}$$

(ii) Effective Stress Block Depth Factor, β: The first moment of area (M_c) about the origin of area under the stress-strain curve is

$$M_c = \int_0^{\varepsilon_{cm}} f_c \varepsilon_c \, d\varepsilon = \left(1 - \frac{\beta}{2}\right) \varepsilon_{cm} \int_0^{\varepsilon_{cm}} f_c \, d\varepsilon \tag{A-24}$$

Rearranging,

$$\beta = 2 - 2 \frac{\int_0^{\varepsilon_{cm}} f_c \varepsilon_c \, d\varepsilon}{\varepsilon_{cm} \int_0^{\varepsilon_{cm}} f_c \, d\varepsilon} \tag{A-25}$$

For circular sections, studies conducted have shown that the compressive force C_c can be approximated to act at a distance of $0.6\beta c$ from the extreme compression fiber. Hence, the expression of $\alpha\beta$ will remain same as in rectangular sections. For stress block depth factor β, first moment of area under stress-strain can be expressed as:

$$M_c = \int_0^{\varepsilon_{cm}} f_c \varepsilon_c \, d\varepsilon = (1 - 0.6\,\beta)\, \varepsilon_{cm} \int_0^{\varepsilon_{cm}} f_c \, d\varepsilon \tag{A-26}$$

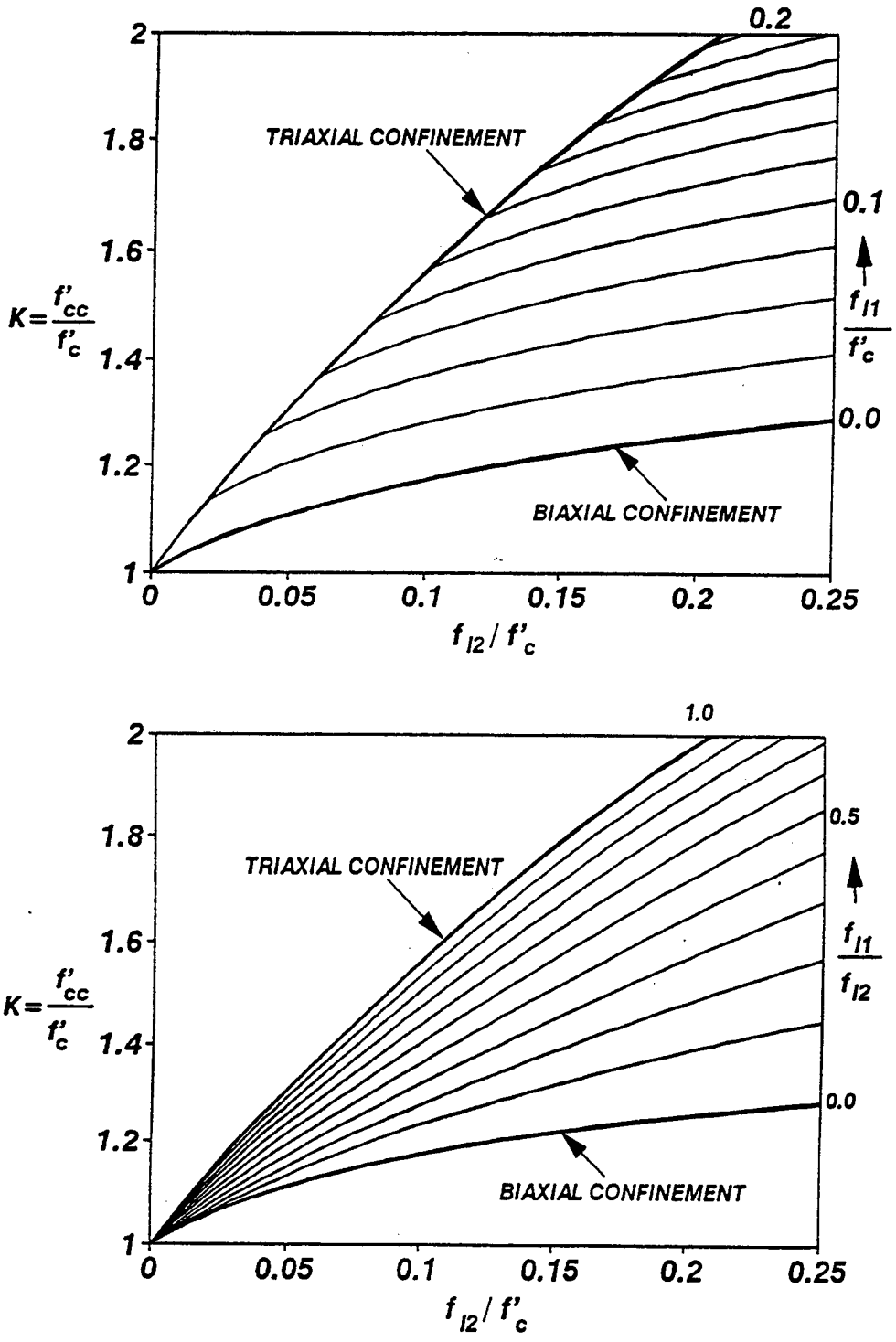

Figure A-2 **Confined Concrete Strength Ratio based on the Multiaxial confinement Model of Mander et al. (1988a).**

Rearranging,

$$\beta = \frac{1}{0.6}\left(1 - \frac{\int_0^{\varepsilon_{cm}} f_c \varepsilon_c d\varepsilon}{\varepsilon_{cm} \int_0^{\varepsilon_{cm}} f_c d\varepsilon}\right) \quad (4\text{-}8)$$

A-3.2 Mander's Stress Block Parameters

Mander et al. (1984) used the stress-strain equation suggested by Popovics (1973) to obtain the equivalent stress block parameters for confined concrete by numerically integrating Popovics equation to give values of α and β. These are shown in figure A-3 which provide stress block parameters for confined concrete when K varies from 1.0 for unconfined concrete, to 2.0, an upper limit for members with transverse reinforcing steel. However they cannot be used in computational moment-curvature analysis because of their graphical form.

A-3.3 Stress Block Parameters suggested by Chang and Mander

Using the modified version of the Tsai equation, Chang and Mander (1994a), obtained the stress block parameters for confined and unconfined concrete by a numerical integration procedure. These are illustrated in figure A-3. Similar to the stress block parameters of Mander et al. (1984), these also suffer from the shortcoming of being graphical in nature, thus unsuitable for automation. Hence, a stress strain equation for describing the behavior of both confined and unconfined concrete is proposed (Appendix B) which can be easily integrated to obtain explicit stress block parameters.

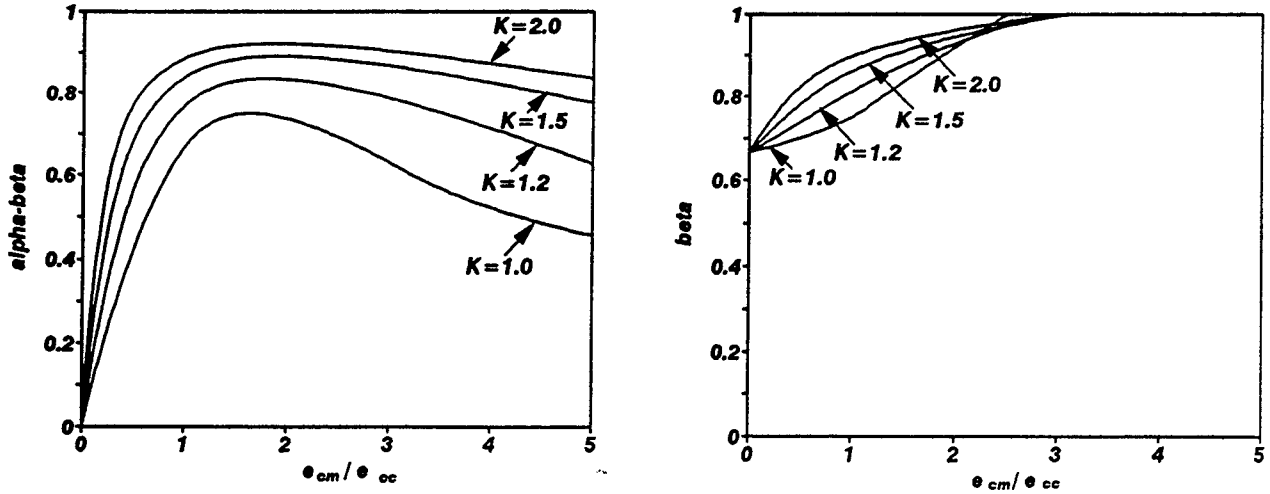

(a) Stress Block Parameters by Mander et al. (1984)

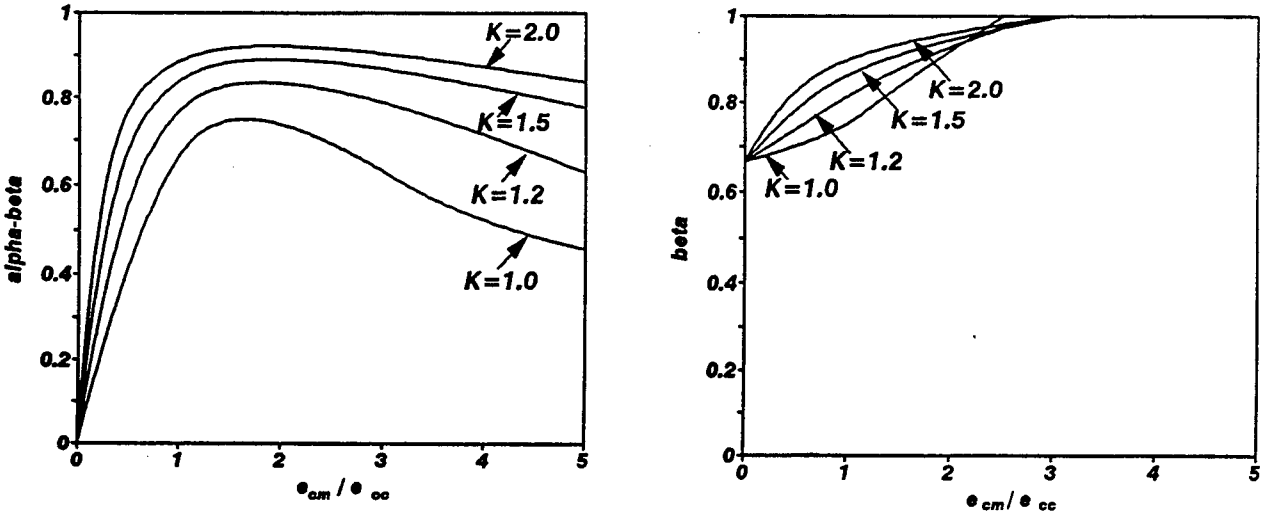

(b) Streess Block Parameters by Chang & Mander (1994a)

Figure A-3 Stress Block Parameters for $f_c' = 30\,MPa$.

APPENDIX B
EXPLICIT STRESS BLOCK PARAMETERS USING A PROPOSED STRESS-STRAIN EQUATION

B-1 PROPOSED EQUATION

In the present study attributes from the original models of Chang and Mander (1994), Mander et al. (1988a) and Kent and Park (1971) have been combined to propose a series of piece-wise stress-strain relationships applicable to both confined and unconfined concrete that can be easily integrated to give explicit closed form solutions for the stress block parameters. Equations for the proposed stress-strain model are as follows:

(i) Ascending Branch: A power curve (figure B-1) is assumed to describe the ascending branch of the stress-strain relation:

$$f_c = f_c' \left[1 - \left(\frac{\varepsilon_c}{\varepsilon_c'} - 1 \right)^n \right] \tag{B-1}$$

in which

$$n = \frac{E_c \varepsilon_c'}{f_c'} \tag{B-2}$$

where ε_c = the strain at any stress of concrete f_c, and E_c = modulus of elasticity of concrete = $8200 f_c'^{3/8}$.

(ii) Descending Branch: The curve for the descending branch is assumed as a straight line:

$$f_c = f_c' \left(1 - E_f (\varepsilon_c - \varepsilon_c') \right) \tag{B-3}$$

where E_f = modulus of the falling branch. Based on series of experiments performed by Mander

et al. (1988b), the following empirical relationship for the modulus of the falling branch is proposed:

$$E_f = 0.3\,E_c\,K^{-6} \qquad \text{(B-4)}$$

where K = confinement ratio of confined concrete. For equation B-3 f_c should not be less than $0.2f_c'$ as shown in figure B-1.

B-2 Explicit Stress Block Parameters

The proposed piece-wise equations were integrated as in equations A-23 and A-25 to obtain explicit closed form analytical expressions for the stress block parameters that are function of the concrete strength, level of confinement and maximum strain. Since piecewise stress-strain model consists of three parts (figure B-1), three expressions were derived for the concrete stress ratio, $\alpha\beta$ and for stress block depth factor, β corresponding to the maximum strain of concrete and are presented below. In the following equations the normalized slope of the stress-strain curve is given by $z = E_f / Kf_c'$ and $x_{20\%} = 0.8/z\varepsilon_{cc}' + 1$.

(i) Equations for concrete stress ratio, $\alpha\beta$: The following equations were obtained for concrete stress ratio, $\alpha\beta$:

(a) For $\varepsilon_c < \varepsilon_c'$, *i.e.* $x<1$

$$\alpha\beta = \left[1 - \frac{(1-x)^{n+1}}{(n+1)x} - \frac{1}{(n+1)x}\right] \qquad \text{(B-5)}$$

(b) For $\varepsilon_c' \le \varepsilon_c \le \left(\varepsilon_c' + \frac{0.8}{z}\right)$, *i.e.* $1 \le x \le \left(1 + \frac{0.8}{z\varepsilon_c'}\right)$

$$\alpha\beta = \left(\frac{n}{(n+1)x}\right) + \left(1 - \frac{1}{x}\right)\left(1 - 0.5z\varepsilon_{cc}(x-1)\right) \qquad \text{(B-6)}$$

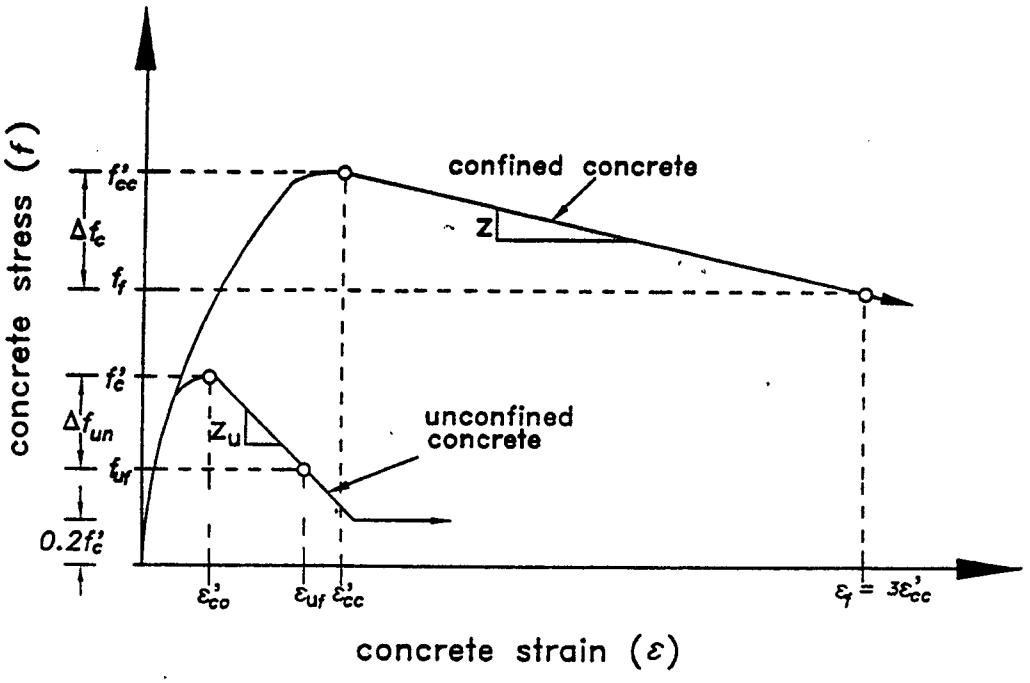

Figure B-1 Proposed Stress Strain Equation for Unconfined and Confined Concrete.

(c) For $\varepsilon \geq \left(\frac{0.8}{z} + \varepsilon_c'\right)$, *i.e* $x \geq x_{20\%}$

$$\alpha\beta = \left(\frac{n}{(n+1)x}\right) + \frac{0.48}{z\varepsilon_{cc}x} + 0.2\left(1 - \frac{x_{20\%}}{x}\right) \tag{B-7}$$

(ii) Equations for stress block depth factor, β : The following equations were obtained for stress block depth factor, β :

(a) For $\varepsilon_c < \varepsilon_c'$, *i.e.* $x<1$

$$\beta = 2\left\{1 - \frac{\left(\frac{x^2}{2} - \frac{(1-x)^{n+2}}{n+2} + \frac{(1-x)^{n+1}}{n+1} - \frac{1}{(n+1)(n+2)}\right)}{x^2\alpha\beta}\right\} \tag{B-8}$$

(b) For $\varepsilon_c' \leq \varepsilon_c \leq \left(\varepsilon_c' + \frac{0.8}{z}\right)$ *i.e.* $1 \leq x \leq \left(1 + \frac{0.8}{z\varepsilon_c'}\right)$

$$\beta = 2 - \frac{\left[(x^2-1) - \frac{z\varepsilon_{cc}}{3}(2x^3 - 3x^2 + 1) + \frac{n(n+3)}{(n+1)(n+2)}\right]}{x^2\alpha\beta} \tag{B-9}$$

(c) For $\varepsilon \geq \left(\frac{0.8}{z} + \varepsilon_{cc}'\right)$ *i.e* $x \geq x_{20\%}$

$$\beta = 2 - \left[\frac{((x_{20\%}^2 - 1) - \frac{z\varepsilon_{cc}}{3}\left(2x_{20\%}^3 - 3x_{20\%}^2 + 1\right) + \frac{n(n+3)}{(n+1)(n+2)} + 0.2\left(x^2 - x_{20\%}^2\right)}{x^2\alpha\beta}\right] \tag{B-10}$$

The stress block parameters for confined concrete can easily be derived using equivalent notations. Figure B-2 shows the plot of equivalent rectangular stress-block parameters calculated using the proposed closed form analytical expressions of stress block parameters. It may be observed that at nominal ultimate strain of 0.003 the value of the stress block parameters

proposed by ACI and those obtained from the analytical expressions have approximately the same value. In the same figure the explicit stress block parameters are also compared with the stress block parameters of Mander et al.(1984) and Chang and Mander (1994a). These exact rectangular stress block parameters may be derived by numerical integration of their expressions using the various models of stress-strain curve studied before. It can be seen that the stress block parameters from the closed form equations compare well with those from other stress-strain relations.

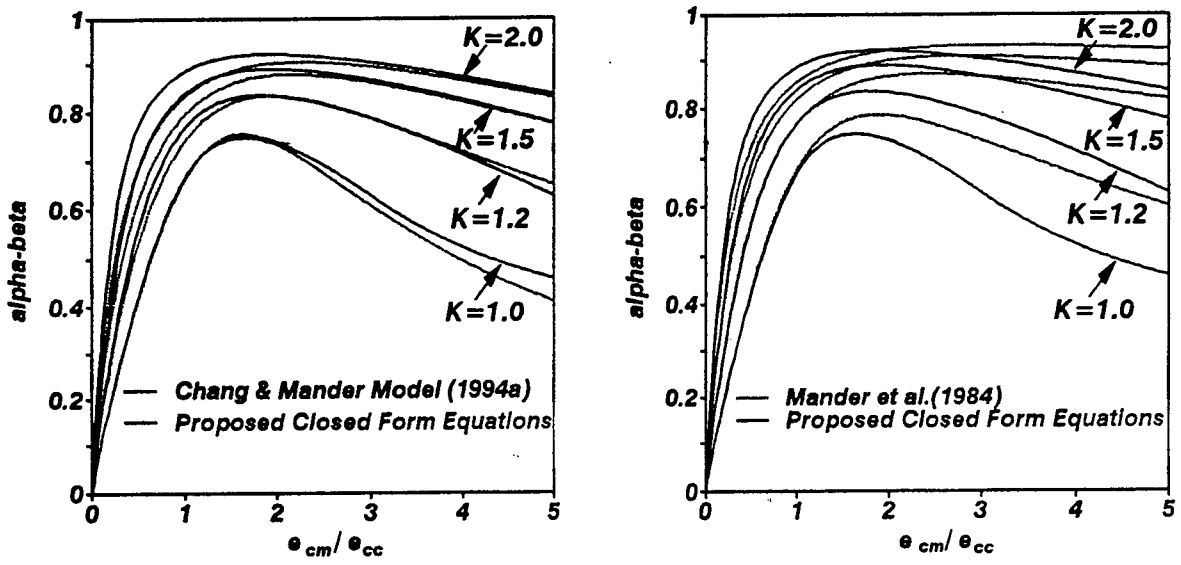

(a) alpha-beta parameter

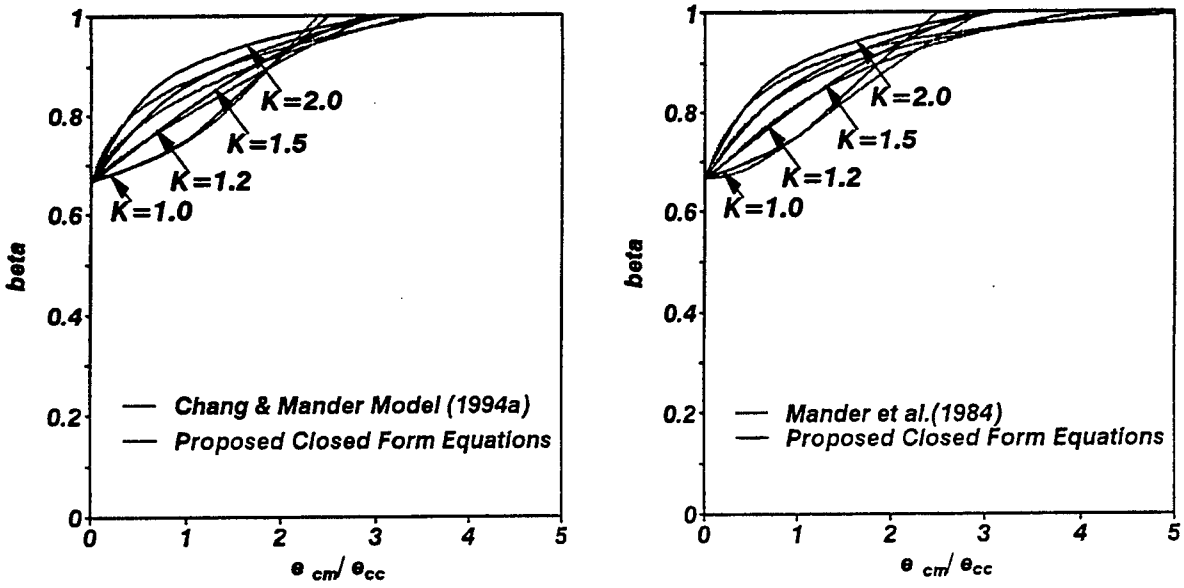

(b) beta parameter

Figure B-2 Proposed Stress Block Parameters for f'c=30MPa.

Multidisciplinary Center for Earthquake Engineering Research
List of Technical Reports

The Multidisciplinary Center for Earthquake Engineering Research (MCEER) publishes technical reports on a variety of subjects related to earthquake engineering written by authors funded through MCEER. These reports are available from both MCEER Publications and the National Technical Information Service (NTIS). Requests for reports should be directed to MCEER Publications, Multidisciplinary Center for Earthquake Engineering Research, State University of New York at Buffalo, Red Jacket Quadrangle, Buffalo, New York 14261. Reports can also be requested through NTIS, 5285 Port Royal Road, Springfield, Virginia 22161. NTIS accession numbers are shown in parenthesis, if available.

NCEER-87-0001 "First-Year Program in Research, Education and Technology Transfer," 3/5/87, (PB88-134275, A04, MF-A01).

NCEER-87-0002 "Experimental Evaluation of Instantaneous Optimal Algorithms for Structural Control," by R.C. Lin, T.T. Soong and A.M. Reinhorn, 4/20/87, (PB88-134341, A04, MF-A01).

NCEER-87-0003 "Experimentation Using the Earthquake Simulation Facilities at University at Buffalo," by A.M. Reinhorn and R.L. Ketter, to be published.

NCEER-87-0004 "The System Characteristics and Performance of a Shaking Table," by J.S. Hwang, K.C. Chang and G.C. Lee, 6/1/87, (PB88-134259, A03, MF-A01). This report is available only through NTIS (see address given above).

NCEER-87-0005 "A Finite Element Formulation for Nonlinear Viscoplastic Material Using a Q Model," by O. Gyebi and G. Dasgupta, 11/2/87, (PB88-213764, A08, MF-A01).

NCEER-87-0006 "Symbolic Manipulation Program (SMP) - Algebraic Codes for Two and Three Dimensional Finite Element Formulations," by X. Lee and G. Dasgupta, 11/9/87, (PB88-218522, A05, MF-A01).

NCEER-87-0007 "Instantaneous Optimal Control Laws for Tall Buildings Under Seismic Excitations," by J.N. Yang, A. Akbarpour and P. Ghaemmaghami, 6/10/87, (PB88-134333, A06, MF-A01). This report is only available through NTIS (see address given above).

NCEER-87-0008 "IDARC: Inelastic Damage Analysis of Reinforced Concrete Frame - Shear-Wall Structures," by Y.J. Park, A.M. Reinhorn and S.K. Kunnath, 7/20/87, (PB88-134325, A09, MF-A01). This report is only available through NTIS (see address given above).

NCEER-87-0009 "Liquefaction Potential for New York State: A Preliminary Report on Sites in Manhattan and Buffalo," by M. Budhu, V. Vijayakumar, R.F. Giese and L. Baumgras, 8/31/87, (PB88-163704, A03, MF-A01). This report is available only through NTIS (see address given above).

NCEER-87-0010 "Vertical and Torsional Vibration of Foundations in Inhomogeneous Media," by A.S. Veletsos and K.W. Dotson, 6/1/87, (PB88-134291, A03, MF-A01). This report is only available through NTIS (see address given above).

NCEER-87-0011 "Seismic Probabilistic Risk Assessment and Seismic Margins Studies for Nuclear Power Plants," by Howard H.M. Hwang, 6/15/87, (PB88-134267, A03, MF-A01). This report is only available through NTIS (see address given above).

NCEER-87-0012 "Parametric Studies of Frequency Response of Secondary Systems Under Ground-Acceleration Excitations," by Y. Yong and Y.K. Lin, 6/10/87, (PB88-134309, A03, MF-A01). This report is only available through NTIS (see address given above).

NCEER-87-0013 "Frequency Response of Secondary Systems Under Seismic Excitation," by J.A. HoLung, J. Cai and Y.K. Lin, 7/31/87, (PB88-134317, A05, MF-A01). This report is only available through NTIS (see address given above).

NCEER-87-0014 "Modelling Earthquake Ground Motions in Seismically Active Regions Using Parametric Time Series Methods," by G.W. Ellis and A.S. Cakmak, 8/25/87, (PB88-134283, A08, MF-A01). This report is only available through NTIS (see address given above).

NCEER-87-0015 "Detection and Assessment of Seismic Structural Damage," by E. DiPasquale and A.S. Cakmak, 8/25/87, (PB88-163712, A05, MF-A01). This report is only available through NTIS (see address given above).

NCEER-87-0016 "Pipeline Experiment at Parkfield, California," by J. Isenberg and E. Richardson, 9/15/87, (PB88-163720, A03, MF-A01). This report is available only through NTIS (see address given above).

NCEER-87-0017 "Digital Simulation of Seismic Ground Motion," by M. Shinozuka, G. Deodatis and T. Harada, 8/31/87, (PB88-155197, A04, MF-A01). This report is available only through NTIS (see address given above).

NCEER-87-0018 "Practical Considerations for Structural Control: System Uncertainty, System Time Delay and Truncation of Small Control Forces," J.N. Yang and A. Akbarpour, 8/10/87, (PB88-163738, A08, MF-A01). This report is only available through NTIS (see address given above).

NCEER-87-0019 "Modal Analysis of Nonclassically Damped Structural Systems Using Canonical Transformation," by J.N. Yang, S. Sarkani and F.X. Long, 9/27/87, (PB88-187851, A04, MF-A01).

NCEER-87-0020 "A Nonstationary Solution in Random Vibration Theory," by J.R. Red-Horse and P.D. Spanos, 11/3/87, (PB88-163746, A03, MF-A01).

NCEER-87-0021 "Horizontal Impedances for Radially Inhomogeneous Viscoelastic Soil Layers," by A.S. Veletsos and K.W. Dotson, 10/15/87, (PB88-150859, A04, MF-A01).

NCEER-87-0022 "Seismic Damage Assessment of Reinforced Concrete Members," by Y.S. Chung, C. Meyer and M. Shinozuka, 10/9/87, (PB88-150867, A05, MF-A01). This report is available only through NTIS (see address given above).

NCEER-87-0023 "Active Structural Control in Civil Engineering," by T.T. Soong, 11/11/87, (PB88-187778, A03, MF-A01).

NCEER-87-0024 "Vertical and Torsional Impedances for Radially Inhomogeneous Viscoelastic Soil Layers," by K.W. Dotson and A.S. Veletsos, 12/87, (PB88-187786, A03, MF-A01).

NCEER-87-0025 "Proceedings from the Symposium on Seismic Hazards, Ground Motions, Soil-Liquefaction and Engineering Practice in Eastern North America," October 20-22, 1987, edited by K.H. Jacob, 12/87, (PB88-188115, A23, MF-A01).

NCEER-87-0026 "Report on the Whittier-Narrows, California, Earthquake of October 1, 1987," by J. Pantelic and A. Reinhorn, 11/87, (PB88-187752, A03, MF-A01). This report is available only through NTIS (see address given above).

NCEER-87-0027 "Design of a Modular Program for Transient Nonlinear Analysis of Large 3-D Building Structures," by S. Srivastav and J.F. Abel, 12/30/87, (PB88-187950, A05, MF-A01). This report is only available through NTIS (see address given above).

NCEER-87-0028 "Second-Year Program in Research, Education and Technology Transfer," 3/8/88, (PB88-219480, A04, MF-A01).

NCEER-88-0001 "Workshop on Seismic Computer Analysis and Design of Buildings With Interactive Graphics," by W. McGuire, J.F. Abel and C.H. Conley, 1/18/88, (PB88-187760, A03, MF-A01). This report is only available through NTIS (see address given above).

NCEER-88-0002 "Optimal Control of Nonlinear Flexible Structures," by J.N. Yang, F.X. Long and D. Wong, 1/22/88, (PB88-213772, A06, MF-A01).

NCEER-88-0003 "Substructuring Techniques in the Time Domain for Primary-Secondary Structural Systems," by G.D. Manolis and G. Juhn, 2/10/88, (PB88-213780, A04, MF-A01).

NCEER-88-0004 "Iterative Seismic Analysis of Primary-Secondary Systems," by A. Singhal, L.D. Lutes and P.D. Spanos, 2/23/88, (PB88-213798, A04, MF-A01).

NCEER-88-0005 "Stochastic Finite Element Expansion for Random Media," by P.D. Spanos and R. Ghanem, 3/14/88, (PB88-213806, A03, MF-A01).

NCEER-88-0006 "Combining Structural Optimization and Structural Control," by F.Y. Cheng and C.P. Pantelides, 1/10/88, (PB88-213814, A05, MF-A01).

NCEER-88-0007 "Seismic Performance Assessment of Code-Designed Structures," by H.H-M. Hwang, J-W. Jaw and H-J. Shau, 3/20/88, (PB88-219423, A04, MF-A01). This report is only available through NTIS (see address given above).

NCEER-88-0008 "Reliability Analysis of Code-Designed Structures Under Natural Hazards," by H.H-M. Hwang, H. Ushiba and M. Shinozuka, 2/29/88, (PB88-229471, A07, MF-A01). This report is only available through NTIS (see address given above).

NCEER-88-0009 "Seismic Fragility Analysis of Shear Wall Structures," by J-W Jaw and H.H-M. Hwang, 4/30/88, (PB89-102867, A04, MF-A01).

NCEER-88-0010 "Base Isolation of a Multi-Story Building Under a Harmonic Ground Motion - A Comparison of Performances of Various Systems," by F-G Fan, G. Ahmadi and I.G. Tadjbakhsh, 5/18/88, (PB89-122238, A06, MF-A01). This report is only available through NTIS (see address given above).

NCEER-88-0011 "Seismic Floor Response Spectra for a Combined System by Green's Functions," by F.M. Lavelle, L.A. Bergman and P.D. Spanos, 5/1/88, (PB89-102875, A03, MF-A01).

NCEER-88-0012 "A New Solution Technique for Randomly Excited Hysteretic Structures," by G.Q. Cai and Y.K. Lin, 5/16/88, (PB89-102883, A03, MF-A01).

NCEER-88-0013 "A Study of Radiation Damping and Soil-Structure Interaction Effects in the Centrifuge," by K. Weissman, supervised by J.H. Prevost, 5/24/88, (PB89-144703, A06, MF-A01).

NCEER-88-0014 "Parameter Identification and Implementation of a Kinematic Plasticity Model for Frictional Soils," by J.H. Prevost and D.V. Griffiths, to be published.

NCEER-88-0015 "Two- and Three- Dimensional Dynamic Finite Element Analyses of the Long Valley Dam," by D.V. Griffiths and J.H. Prevost, 6/17/88, (PB89-144711, A04, MF-A01).

NCEER-88-0016 "Damage Assessment of Reinforced Concrete Structures in Eastern United States," by A.M. Reinhorn, M.J. Seidel, S.K. Kunnath and Y.J. Park, 6/15/88, (PB89-122220, A04, MF-A01). This report is only available through NTIS (see address given above).

NCEER-88-0017 "Dynamic Compliance of Vertically Loaded Strip Foundations in Multilayered Viscoelastic Soils," by S. Ahmad and A.S.M. Israil, 6/17/88, (PB89-102891, A04, MF-A01).

NCEER-88-0018 "An Experimental Study of Seismic Structural Response With Added Viscoelastic Dampers," by R.C. Lin, Z. Liang, T.T. Soong and R.H. Zhang, 6/30/88, (PB89-122212, A05, MF-A01). This report is available only through NTIS (see address given above).

NCEER-88-0019 "Experimental Investigation of Primary - Secondary System Interaction," by G.D. Manolis, G. Juhn and A.M. Reinhorn, 5/27/88, (PB89-122204, A04, MF-A01).

NCEER-88-0020 "A Response Spectrum Approach For Analysis of Nonclassically Damped Structures," by J.N. Yang, S. Sarkani and F.X. Long, 4/22/88, (PB89-102909, A04, MF-A01).

NCEER-88-0021 "Seismic Interaction of Structures and Soils: Stochastic Approach," by A.S. Veletsos and A.M. Prasad, 7/21/88, (PB89-122196, A04, MF-A01). This report is only available through NTIS (see address given above).

NCEER-88-0022 "Identification of the Serviceability Limit State and Detection of Seismic Structural Damage," by E. DiPasquale and A.S. Cakmak, 6/15/88, (PB89-122188, A05, MF-A01). This report is available only through NTIS (see address given above).

NCEER-88-0023 "Multi-Hazard Risk Analysis: Case of a Simple Offshore Structure," by B.K. Bhartia and E.H. Vanmarcke, 7/21/88, (PB89-145213, A05, MF-A01).

NCEER-88-0024 "Automated Seismic Design of Reinforced Concrete Buildings," by Y.S. Chung, C. Meyer and M. Shinozuka, 7/5/88, (PB89-122170, A06, MF-A01). This report is available only through NTIS (see address given above).

NCEER-88-0025 "Experimental Study of Active Control of MDOF Structures Under Seismic Excitations," by L.L. Chung, R.C. Lin, T.T. Soong and A.M. Reinhorn, 7/10/88, (PB89-122600, A04, MF-A01).

NCEER-88-0026 "Earthquake Simulation Tests of a Low-Rise Metal Structure," by J.S. Hwang, K.C. Chang, G.C. Lee and R.L. Ketter, 8/1/88, (PB89-102917, A04, MF-A01).

NCEER-88-0027 "Systems Study of Urban Response and Reconstruction Due to Catastrophic Earthquakes," by F. Kozin and H.K. Zhou, 9/22/88, (PB90-162348, A04, MF-A01).

NCEER-88-0028 "Seismic Fragility Analysis of Plane Frame Structures," by H.H-M. Hwang and Y.K. Low, 7/31/88, (PB89-131445, A06, MF-A01).

NCEER-88-0029 "Response Analysis of Stochastic Structures," by A. Kardara, C. Bucher and M. Shinozuka, 9/22/88, (PB89-174429, A04, MF-A01).

NCEER-88-0030 "Nonnormal Accelerations Due to Yielding in a Primary Structure," by D.C.K. Chen and L.D. Lutes, 9/19/88, (PB89-131437, A04, MF-A01).

NCEER-88-0031 "Design Approaches for Soil-Structure Interaction," by A.S. Veletsos, A.M. Prasad and Y. Tang, 12/30/88, (PB89-174437, A03, MF-A01). This report is available only through NTIS (see address given above).

NCEER-88-0032 "A Re-evaluation of Design Spectra for Seismic Damage Control," by C.J. Turkstra and A.G. Tallin, 11/7/88, (PB89-145221, A05, MF-A01).

NCEER-88-0033 "The Behavior and Design of Noncontact Lap Splices Subjected to Repeated Inelastic Tensile Loading," by V.E. Sagan, P. Gergely and R.N. White, 12/8/88, (PB89-163737, A08, MF-A01).

NCEER-88-0034 "Seismic Response of Pile Foundations," by S.M. Mamoon, P.K. Banerjee and S. Ahmad, 11/1/88, (PB89-145239, A04, MF-A01).

NCEER-88-0035 "Modeling of R/C Building Structures With Flexible Floor Diaphragms (IDARC2)," by A.M. Reinhorn, S.K. Kunnath and N. Panahshahi, 9/7/88, (PB89-207153, A07, MF-A01).

NCEER-88-0036 "Solution of the Dam-Reservoir Interaction Problem Using a Combination of FEM, BEM with Particular Integrals, Modal Analysis, and Substructuring," by C-S. Tsai, G.C. Lee and R.L. Ketter, 12/31/88, (PB89-207146, A04, MF-A01).

NCEER-88-0037 "Optimal Placement of Actuators for Structural Control," by F.Y. Cheng and C.P. Pantelides, 8/15/88, (PB89-162846, A05, MF-A01).

NCEER-88-0038 "Teflon Bearings in Aseismic Base Isolation: Experimental Studies and Mathematical Modeling," by A. Mokha, M.C. Constantinou and A.M. Reinhorn, 12/5/88, (PB89-218457, A10, MF-A01). This report is available only through NTIS (see address given above).

NCEER-88-0039 "Seismic Behavior of Flat Slab High-Rise Buildings in the New York City Area," by P. Weidlinger and M. Ettouney, 10/15/88, (PB90-145681, A04, MF-A01).

NCEER-88-0040 "Evaluation of the Earthquake Resistance of Existing Buildings in New York City," by P. Weidlinger and M. Ettouney, 10/15/88, to be published.

NCEER-88-0041 "Small-Scale Modeling Techniques for Reinforced Concrete Structures Subjected to Seismic Loads," by W. Kim, A. El-Attar and R.N. White, 11/22/88, (PB89-189625, A05, MF-A01).

NCEER-88-0042 "Modeling Strong Ground Motion from Multiple Event Earthquakes," by G.W. Ellis and A.S. Cakmak, 10/15/88, (PB89-174445, A03, MF-A01).

NCEER-88-0043 "Nonstationary Models of Seismic Ground Acceleration," by M. Grigoriu, S.E. Ruiz and E. Rosenblueth, 7/15/88, (PB89-189617, A04, MF-A01).

NCEER-88-0044 "SARCF User's Guide: Seismic Analysis of Reinforced Concrete Frames," by Y.S. Chung, C. Meyer and M. Shinozuka, 11/9/88, (PB89-174452, A08, MF-A01).

NCEER-88-0045 "First Expert Panel Meeting on Disaster Research and Planning," edited by J. Pantelic and J. Stoyle, 9/15/88, (PB89-174460, A05, MF-A01). This report is only available through NTIS (see address given above).

NCEER-88-0046 "Preliminary Studies of the Effect of Degrading Infill Walls on the Nonlinear Seismic Response of Steel Frames," by C.Z. Chrysostomou, P. Gergely and J.F. Abel, 12/19/88, (PB89-208383, A05, MF-A01).

NCEER-88-0047 "Reinforced Concrete Frame Component Testing Facility - Design, Construction, Instrumentation and Operation," by S.P. Pessiki, C. Conley, T. Bond, P. Gergely and R.N. White, 12/16/88, (PB89-174478, A04, MF-A01).

NCEER-89-0001 "Effects of Protective Cushion and Soil Compliancy on the Response of Equipment Within a Seismically Excited Building," by J.A. HoLung, 2/16/89, (PB89-207179, A04, MF-A01).

NCEER-89-0002 "Statistical Evaluation of Response Modification Factors for Reinforced Concrete Structures," by H.H-M. Hwang and J-W. Jaw, 2/17/89, (PB89-207187, A05, MF-A01).

NCEER-89-0003 "Hysteretic Columns Under Random Excitation," by G-Q. Cai and Y.K. Lin, 1/9/89, (PB89-196513, A03, MF-A01).

NCEER-89-0004 "Experimental Study of `Elephant Foot Bulge' Instability of Thin-Walled Metal Tanks," by Z-H. Jia and R.L. Ketter, 2/22/89, (PB89-207195, A03, MF-A01).

NCEER-89-0005 "Experiment on Performance of Buried Pipelines Across San Andreas Fault," by J. Isenberg, E. Richardson and T.D. O'Rourke, 3/10/89, (PB89-218440, A04, MF-A01). This report is available only through NTIS (see address given above).

NCEER-89-0006 "A Knowledge-Based Approach to Structural Design of Earthquake-Resistant Buildings," by M. Subramani, P. Gergely, C.H. Conley, J.F. Abel and A.H. Zaghw, 1/15/89, (PB89-218465, A06, MF-A01).

NCEER-89-0007 "Liquefaction Hazards and Their Effects on Buried Pipelines," by T.D. O'Rourke and P.A. Lane, 2/1/89, (PB89-218481, A09, MF-A01).

NCEER-89-0008 "Fundamentals of System Identification in Structural Dynamics," by H. Imai, C-B. Yun, O. Maruyama and M. Shinozuka, 1/26/89, (PB89-207211, A04, MF-A01).

NCEER-89-0009 "Effects of the 1985 Michoacan Earthquake on Water Systems and Other Buried Lifelines in Mexico," by A.G. Ayala and M.J. O'Rourke, 3/8/89, (PB89-207229, A06, MF-A01).

NCEER-89-R010 "NCEER Bibliography of Earthquake Education Materials," by K.E.K. Ross, Second Revision, 9/1/89, (PB90-125352, A05, MF-A01). This report is replaced by NCEER-92-0018.

NCEER-89-0011 "Inelastic Three-Dimensional Response Analysis of Reinforced Concrete Building Structures (IDARC-3D), Part I - Modeling," by S.K. Kunnath and A.M. Reinhorn, 4/17/89, (PB90-114612, A07, MF-A01).

NCEER-89-0012 "Recommended Modifications to ATC-14," by C.D. Poland and J.O. Malley, 4/12/89, (PB90-108648, A15, MF-A01).

NCEER-89-0013 "Repair and Strengthening of Beam-to-Column Connections Subjected to Earthquake Loading," by M. Corazao and A.J. Durrani, 2/28/89, (PB90-109885, A06, MF-A01).

NCEER-89-0014 "Program EXKAL2 for Identification of Structural Dynamic Systems," by O. Maruyama, C-B. Yun, M. Hoshiya and M. Shinozuka, 5/19/89, (PB90-109877, A09, MF-A01).

NCEER-89-0015 "Response of Frames With Bolted Semi-Rigid Connections, Part I - Experimental Study and Analytical Predictions," by P.J. DiCorso, A.M. Reinhorn, J.R. Dickerson, J.B. Radziminski and W.L. Harper, 6/1/89, to be published.

NCEER-89-0016 "ARMA Monte Carlo Simulation in Probabilistic Structural Analysis," by P.D. Spanos and M.P. Mignolet, 7/10/89, (PB90-109893, A03, MF-A01).

NCEER-89-P017 "Preliminary Proceedings from the Conference on Disaster Preparedness - The Place of Earthquake Education in Our Schools," Edited by K.E.K. Ross, 6/23/89, (PB90-108606, A03, MF-A01).

NCEER-89-0017 "Proceedings from the Conference on Disaster Preparedness - The Place of Earthquake Education in Our Schools," Edited by K.E.K. Ross, 12/31/89, (PB90-207895, A012, MF-A02). This report is available only through NTIS (see address given above).

NCEER-89-0018 "Multidimensional Models of Hysteretic Material Behavior for Vibration Analysis of Shape Memory Energy Absorbing Devices, by E.J. Graesser and F.A. Cozzarelli, 6/7/89, (PB90-164146, A04, MF-A01).

NCEER-89-0019 "Nonlinear Dynamic Analysis of Three-Dimensional Base Isolated Structures (3D-BASIS)," by S. Nagarajaiah, A.M. Reinhorn and M.C. Constantinou, 8/3/89, (PB90-161936, A06, MF-A01). This report has been replaced by NCEER-93-0011.

NCEER-89-0020 "Structural Control Considering Time-Rate of Control Forces and Control Rate Constraints," by F.Y. Cheng and C.P. Pantelides, 8/3/89, (PB90-120445, A04, MF-A01).

NCEER-89-0021 "Subsurface Conditions of Memphis and Shelby County," by K.W. Ng, T-S. Chang and H-H.M. Hwang, 7/26/89, (PB90-120437, A03, MF-A01).

NCEER-89-0022 "Seismic Wave Propagation Effects on Straight Jointed Buried Pipelines," by K. Elhmadi and M.J. O'Rourke, 8/24/89, (PB90-162322, A10, MF-A02).

NCEER-89-0023 "Workshop on Serviceability Analysis of Water Delivery Systems," edited by M. Grigoriu, 3/6/89, (PB90-127424, A03, MF-A01).

NCEER-89-0024 "Shaking Table Study of a 1/5 Scale Steel Frame Composed of Tapered Members," by K.C. Chang, J.S. Hwang and G.C. Lee, 9/18/89, (PB90-160169, A04, MF-A01).

NCEER-89-0025 "DYNA1D: A Computer Program for Nonlinear Seismic Site Response Analysis - Technical Documentation," by Jean H. Prevost, 9/14/89, (PB90-161944, A07, MF-A01). This report is available only through NTIS (see address given above).

NCEER-89-0026 "1:4 Scale Model Studies of Active Tendon Systems and Active Mass Dampers for Aseismic Protection," by A.M. Reinhorn, T.T. Soong, R.C. Lin, Y.P. Yang, Y. Fukao, H. Abe and M. Nakai, 9/15/89, (PB90-173246, A10, MF-A02).

NCEER-89-0027 "Scattering of Waves by Inclusions in a Nonhomogeneous Elastic Half Space Solved by Boundary Element Methods," by P.K. Hadley, A. Askar and A.S. Cakmak, 6/15/89, (PB90-145699, A07, MF-A01).

NCEER-89-0028 "Statistical Evaluation of Deflection Amplification Factors for Reinforced Concrete Structures," by H.H.M. Hwang, J-W. Jaw and A.L. Ch'ng, 8/31/89, (PB90-164633, A05, MF-A01).

NCEER-89-0029 "Bedrock Accelerations in Memphis Area Due to Large New Madrid Earthquakes," by H.H.M. Hwang, C.H.S. Chen and G. Yu, 11/7/89, (PB90-162330, A04, MF-A01).

NCEER-89-0030 "Seismic Behavior and Response Sensitivity of Secondary Structural Systems," by Y.Q. Chen and T.T. Soong, 10/23/89, (PB90-164658, A08, MF-A01).

NCEER-89-0031 "Random Vibration and Reliability Analysis of Primary-Secondary Structural Systems," by Y. Ibrahim, M. Grigoriu and T.T. Soong, 11/10/89, (PB90-161951, A04, MF-A01).

NCEER-89-0032 "Proceedings from the Second U.S. - Japan Workshop on Liquefaction, Large Ground Deformation and Their Effects on Lifelines, September 26-29, 1989," Edited by T.D. O'Rourke and M. Hamada, 12/1/89, (PB90-209388, A22, MF-A03).

NCEER-89-0033 "Deterministic Model for Seismic Damage Evaluation of Reinforced Concrete Structures," by J.M. Bracci, A.M. Reinhorn, J.B. Mander and S.K. Kunnath, 9/27/89, (PB91-108803, A06, MF-A01).

NCEER-89-0034 "On the Relation Between Local and Global Damage Indices," by E. DiPasquale and A.S. Cakmak, 8/15/89, (PB90-173865, A05, MF-A01).

NCEER-89-0035 "Cyclic Undrained Behavior of Nonplastic and Low Plasticity Silts," by A.J. Walker and H.E. Stewart, 7/26/89, (PB90-183518, A10, MF-A01).

NCEER-89-0036 "Liquefaction Potential of Surficial Deposits in the City of Buffalo, New York," by M. Budhu, R. Giese and L. Baumgrass, 1/17/89, (PB90-208455, A04, MF-A01).

NCEER-89-0037 "A Deterministic Assessment of Effects of Ground Motion Incoherence," by A.S. Veletsos and Y. Tang, 7/15/89, (PB90-164294, A03, MF-A01).

NCEER-89-0038 "Workshop on Ground Motion Parameters for Seismic Hazard Mapping," July 17-18, 1989, edited by R.V. Whitman, 12/1/89, (PB90-173923, A04, MF-A01).

NCEER-89-0039 "Seismic Effects on Elevated Transit Lines of the New York City Transit Authority," by C.J. Costantino, C.A. Miller and E. Heymsfield, 12/26/89, (PB90-207887, A06, MF-A01).

NCEER-89-0040 "Centrifugal Modeling of Dynamic Soil-Structure Interaction," by K. Weissman, Supervised by J.H. Prevost, 5/10/89, (PB90-207879, A07, MF-A01).

NCEER-89-0041 "Linearized Identification of Buildings With Cores for Seismic Vulnerability Assessment," by I-K. Ho and A.E. Aktan, 11/1/89, (PB90-251943, A07, MF-A01).

NCEER-90-0001 "Geotechnical and Lifeline Aspects of the October 17, 1989 Loma Prieta Earthquake in San Francisco," by T.D. O'Rourke, H.E. Stewart, F.T. Blackburn and T.S. Dickerman, 1/90, (PB90-208596, A05, MF-A01).

NCEER-90-0002 "Nonnormal Secondary Response Due to Yielding in a Primary Structure," by D.C.K. Chen and L.D. Lutes, 2/28/90, (PB90-251976, A07, MF-A01).

NCEER-90-0003 "Earthquake Education Materials for Grades K-12," by K.E.K. Ross, 4/16/90, (PB91-251984, A05, MF-A05). This report has been replaced by NCEER-92-0018.

NCEER-90-0004 "Catalog of Strong Motion Stations in Eastern North America," by R.W. Busby, 4/3/90, (PB90-251984, A05, MF-A01).

NCEER-90-0005 "NCEER Strong-Motion Data Base: A User Manual for the GeoBase Release (Version 1.0 for the Sun3)," by P. Friberg and K. Jacob, 3/31/90 (PB90-258062, A04, MF-A01).

NCEER-90-0006 "Seismic Hazard Along a Crude Oil Pipeline in the Event of an 1811-1812 Type New Madrid Earthquake," by H.H.M. Hwang and C-H.S. Chen, 4/16/90, (PB90-258054, A04, MF-A01).

NCEER-90-0007 "Site-Specific Response Spectra for Memphis Sheahan Pumping Station," by H.H.M. Hwang and C.S. Lee, 5/15/90, (PB91-108811, A05, MF-A01).

NCEER-90-0008 "Pilot Study on Seismic Vulnerability of Crude Oil Transmission Systems," by T. Ariman, R. Dobry, M. Grigoriu, F. Kozin, M. O'Rourke, T. O'Rourke and M. Shinozuka, 5/25/90, (PB91-108837, A06, MF-A01).

NCEER-90-0009 "A Program to Generate Site Dependent Time Histories: EQGEN," by G.W. Ellis, M. Srinivasan and A.S. Cakmak, 1/30/90, (PB91-108829, A04, MF-A01).

NCEER-90-0010 "Active Isolation for Seismic Protection of Operating Rooms," by M.E. Talbott, Supervised by M. Shinozuka, 6/8/9, (PB91-110205, A05, MF-A01).

NCEER-90-0011 "Program LINEARID for Identification of Linear Structural Dynamic Systems," by C-B. Yun and M. Shinozuka, 6/25/90, (PB91-110312, A08, MF-A01).

NCEER-90-0012 "Two-Dimensional Two-Phase Elasto-Plastic Seismic Response of Earth Dams," by A.N. Yiagos, Supervised by J.H. Prevost, 6/20/90, (PB91-110197, A13, MF-A02).

NCEER-90-0013 "Secondary Systems in Base-Isolated Structures: Experimental Investigation, Stochastic Response and Stochastic Sensitivity," by G.D. Manolis, G. Juhn, M.C. Constantinou and A.M. Reinhorn, 7/1/90, (PB91-110320, A08, MF-A01).

NCEER-90-0014 "Seismic Behavior of Lightly-Reinforced Concrete Column and Beam-Column Joint Details," by S.P. Pessiki, C.H. Conley, P. Gergely and R.N. White, 8/22/90, (PB91-108795, A11, MF-A02).

NCEER-90-0015 "Two Hybrid Control Systems for Building Structures Under Strong Earthquakes," by J.N. Yang and A. Danielians, 6/29/90, (PB91-125393, A04, MF-A01).

NCEER-90-0016 "Instantaneous Optimal Control with Acceleration and Velocity Feedback," by J.N. Yang and Z. Li, 6/29/90, (PB91-125401, A03, MF-A01).

NCEER-90-0017 "Reconnaissance Report on the Northern Iran Earthquake of June 21, 1990," by M. Mehrain, 10/4/90, (PB91-125377, A03, MF-A01).

NCEER-90-0018 "Evaluation of Liquefaction Potential in Memphis and Shelby County," by T.S. Chang, P.S. Tang, C.S. Lee and H. Hwang, 8/10/90, (PB91-125427, A09, MF-A01).

NCEER-90-0019 "Experimental and Analytical Study of a Combined Sliding Disc Bearing and Helical Steel Spring Isolation System," by M.C. Constantinou, A.S. Mokha and A.M. Reinhorn, 10/4/90, (PB91-125385, A06, MF-A01). This report is available only through NTIS (see address given above).

NCEER-90-0020 "Experimental Study and Analytical Prediction of Earthquake Response of a Sliding Isolation System with a Spherical Surface," by A.S. Mokha, M.C. Constantinou and A.M. Reinhorn, 10/11/90, (PB91-125419, A05, MF-A01).

NCEER-90-0021 "Dynamic Interaction Factors for Floating Pile Groups," by G. Gazetas, K. Fan, A. Kaynia and E. Kausel, 9/10/90, (PB91-170381, A05, MF-A01).

NCEER-90-0022 "Evaluation of Seismic Damage Indices for Reinforced Concrete Structures," by S. Rodriguez-Gomez and A.S. Cakmak, 9/30/90, PB91-171322, A06, MF-A01).

NCEER-90-0023 "Study of Site Response at a Selected Memphis Site," by H. Desai, S. Ahmad, E.S. Gazetas and M.R. Oh, 10/11/90, (PB91-196857, A03, MF-A01).

NCEER-90-0024 "A User's Guide to Strongmo: Version 1.0 of NCEER's Strong-Motion Data Access Tool for PCs and Terminals," by P.A. Friberg and C.A.T. Susch, 11/15/90, (PB91-171272, A03, MF-A01).

NCEER-90-0025 "A Three-Dimensional Analytical Study of Spatial Variability of Seismic Ground Motions," by L-L. Hong and A.H.-S. Ang, 10/30/90, (PB91-170399, A09, MF-A01).

NCEER-90-0026 "MUMOID User's Guide - A Program for the Identification of Modal Parameters," by S. Rodriguez-Gomez and E. DiPasquale, 9/30/90, (PB91-171298, A04, MF-A01).

NCEER-90-0027 "SARCF-II User's Guide - Seismic Analysis of Reinforced Concrete Frames," by S. Rodriguez-Gomez, Y.S. Chung and C. Meyer, 9/30/90, (PB91-171280, A05, MF-A01).

NCEER-90-0028 "Viscous Dampers: Testing, Modeling and Application in Vibration and Seismic Isolation," by N. Makris and M.C. Constantinou, 12/20/90 (PB91-190561, A06, MF-A01).

NCEER-90-0029 "Soil Effects on Earthquake Ground Motions in the Memphis Area," by H. Hwang, C.S. Lee, K.W. Ng and T.S. Chang, 8/2/90, (PB91-190751, A05, MF-A01).

NCEER-91-0001 "Proceedings from the Third Japan-U.S. Workshop on Earthquake Resistant Design of Lifeline Facilities and Countermeasures for Soil Liquefaction, December 17-19, 1990," edited by T.D. O'Rourke and M. Hamada, 2/1/91, (PB91-179259, A99, MF-A04).

NCEER-91-0002 "Physical Space Solutions of Non-Proportionally Damped Systems," by M. Tong, Z. Liang and G.C. Lee, 1/15/91, (PB91-179242, A04, MF-A01).

NCEER-91-0003 "Seismic Response of Single Piles and Pile Groups," by K. Fan and G. Gazetas, 1/10/91, (PB92-174994, A04, MF-A01).

NCEER-91-0004 "Damping of Structures: Part 1 - Theory of Complex Damping," by Z. Liang and G. Lee, 10/10/91, (PB92-197235, A12, MF-A03).

NCEER-91-0005 "3D-BASIS - Nonlinear Dynamic Analysis of Three Dimensional Base Isolated Structures: Part II," by S. Nagarajaiah, A.M. Reinhorn and M.C. Constantinou, 2/28/91, (PB91-190553, A07, MF-A01). This report has been replaced by NCEER-93-0011.

NCEER-91-0006 "A Multidimensional Hysteretic Model for Plasticity Deforming Metals in Energy Absorbing Devices," by E.J. Graesser and F.A. Cozzarelli, 4/9/91, (PB92-108364, A04, MF-A01).

NCEER-91-0007 "A Framework for Customizable Knowledge-Based Expert Systems with an Application to a KBES for Evaluating the Seismic Resistance of Existing Buildings," by E.G. Ibarra-Anaya and S.J. Fenves, 4/9/91, (PB91-210930, A08, MF-A01).

NCEER-91-0008 "Nonlinear Analysis of Steel Frames with Semi-Rigid Connections Using the Capacity Spectrum Method," by G.G. Deierlein, S-H. Hsieh, Y-J. Shen and J.F. Abel, 7/2/91, (PB92-113828, A05, MF-A01).

NCEER-91-0009 "Earthquake Education Materials for Grades K-12," by K.E.K. Ross, 4/30/91, (PB91-212142, A06, MF-A01). This report has been replaced by NCEER-92-0018.

NCEER-91-0010 "Phase Wave Velocities and Displacement Phase Differences in a Harmonically Oscillating Pile," by N. Makris and G. Gazetas, 7/8/91, (PB92-108356, A04, MF-A01).

NCEER-91-0011 "Dynamic Characteristics of a Full-Size Five-Story Steel Structure and a 2/5 Scale Model," by K.C. Chang, G.C. Yao, G.C. Lee, D.S. Hao and Y.C. Yeh," 7/2/91, (PB93-116648, A06, MF-A02).

NCEER-91-0012 "Seismic Response of a 2/5 Scale Steel Structure with Added Viscoelastic Dampers," by K.C. Chang, T.T. Soong, S-T. Oh and M.L. Lai, 5/17/91, (PB92-110816, A05, MF-A01).

NCEER-91-0013 "Earthquake Response of Retaining Walls; Full-Scale Testing and Computational Modeling," by S. Alampalli and A-W.M. Elgamal, 6/20/91, to be published.

NCEER-91-0014 "3D-BASIS-M: Nonlinear Dynamic Analysis of Multiple Building Base Isolated Structures," by P.C. Tsopelas, S. Nagarajaiah, M.C. Constantinou and A.M. Reinhorn, 5/28/91, (PB92-113885, A09, MF-A02).

NCEER-91-0015 "Evaluation of SEAOC Design Requirements for Sliding Isolated Structures," by D. Theodossiou and M.C. Constantinou, 6/10/91, (PB92-114602, A11, MF-A03).

NCEER-91-0016 "Closed-Loop Modal Testing of a 27-Story Reinforced Concrete Flat Plate-Core Building," by H.R. Somaprasad, T. Toksoy, H. Yoshiyuki and A.E. Aktan, 7/15/91, (PB92-129980, A07, MF-A02).

NCEER-91-0017 "Shake Table Test of a 1/6 Scale Two-Story Lightly Reinforced Concrete Building," by A.G. El-Attar, R.N. White and P. Gergely, 2/28/91, (PB92-222447, A06, MF-A02).

NCEER-91-0018 "Shake Table Test of a 1/8 Scale Three-Story Lightly Reinforced Concrete Building," by A.G. El-Attar, R.N. White and P. Gergely, 2/28/91, (PB93-116630, A08, MF-A02).

NCEER-91-0019 "Transfer Functions for Rigid Rectangular Foundations," by A.S. Veletsos, A.M. Prasad and W.H. Wu, 7/31/91, to be published.

NCEER-91-0020 "Hybrid Control of Seismic-Excited Nonlinear and Inelastic Structural Systems," by J.N. Yang, Z. Li and A. Danielians, 8/1/91, (PB92-143171, A06, MF-A02).

NCEER-91-0021 "The NCEER-91 Earthquake Catalog: Improved Intensity-Based Magnitudes and Recurrence Relations for U.S. Earthquakes East of New Madrid," by L. Seeber and J.G. Armbruster, 8/28/91, (PB92-176742, A06, MF-A02).

NCEER-91-0022 "Proceedings from the Implementation of Earthquake Planning and Education in Schools: The Need for Change - The Roles of the Changemakers," by K.E.K. Ross and F. Winslow, 7/23/91, (PB92-129998, A12, MF-A03).

NCEER-91-0023 "A Study of Reliability-Based Criteria for Seismic Design of Reinforced Concrete Frame Buildings," by H.H.M. Hwang and H-M. Hsu, 8/10/91, (PB92-140235, A09, MF-A02).

NCEER-91-0024 "Experimental Verification of a Number of Structural System Identification Algorithms," by R.G. Ghanem, H. Gavin and M. Shinozuka, 9/18/91, (PB92-176577, A18, MF-A04).

NCEER-91-0025 "Probabilistic Evaluation of Liquefaction Potential," by H.H.M. Hwang and C.S. Lee," 11/25/91, (PB92-143429, A05, MF-A01).

NCEER-91-0026 "Instantaneous Optimal Control for Linear, Nonlinear and Hysteretic Structures - Stable Controllers," by J.N. Yang and Z. Li, 11/15/91, (PB92-163807, A04, MF-A01).

NCEER-91-0027 "Experimental and Theoretical Study of a Sliding Isolation System for Bridges," by M.C. Constantinou, A. Kartoum, A.M. Reinhorn and P. Bradford, 11/15/91, (PB92-176973, A10, MF-A03).

NCEER-92-0001 "Case Studies of Liquefaction and Lifeline Performance During Past Earthquakes, Volume 1: Japanese Case Studies," Edited by M. Hamada and T. O'Rourke, 2/17/92, (PB92-197243, A18, MF-A04).

NCEER-92-0002 "Case Studies of Liquefaction and Lifeline Performance During Past Earthquakes, Volume 2: United States Case Studies," Edited by T. O'Rourke and M. Hamada, 2/17/92, (PB92-197250, A20, MF-A04).

NCEER-92-0003 "Issues in Earthquake Education," Edited by K. Ross, 2/3/92, (PB92-222389, A07, MF-A02).

NCEER-92-0004 "Proceedings from the First U.S. - Japan Workshop on Earthquake Protective Systems for Bridges," Edited by I.G. Buckle, 2/4/92, (PB94-142239, A99, MF-A06).

NCEER-92-0005 "Seismic Ground Motion from a Haskell-Type Source in a Multiple-Layered Half-Space," A.P. Theoharis, G. Deodatis and M. Shinozuka, 1/2/92, to be published.

NCEER-92-0006 "Proceedings from the Site Effects Workshop," Edited by R. Whitman, 2/29/92, (PB92-197201, A04, MF-A01).

NCEER-92-0007 "Engineering Evaluation of Permanent Ground Deformations Due to Seismically-Induced Liquefaction," by M.H. Baziar, R. Dobry and A-W.M. Elgamal, 3/24/92, (PB92-222421, A13, MF-A03).

NCEER-92-0008 "A Procedure for the Seismic Evaluation of Buildings in the Central and Eastern United States," by C.D. Poland and J.O. Malley, 4/2/92, (PB92-222439, A20, MF-A04).

NCEER-92-0009 "Experimental and Analytical Study of a Hybrid Isolation System Using Friction Controllable Sliding Bearings," by M.Q. Feng, S. Fujii and M. Shinozuka, 5/15/92, (PB93-150282, A06, MF-A02).

NCEER-92-0010 "Seismic Resistance of Slab-Column Connections in Existing Non-Ductile Flat-Plate Buildings," by A.J. Durrani and Y. Du, 5/18/92, (PB93-116812, A06, MF-A02).

NCEER-92-0011 "The Hysteretic and Dynamic Behavior of Brick Masonry Walls Upgraded by Ferrocement Coatings Under Cyclic Loading and Strong Simulated Ground Motion," by H. Lee and S.P. Prawel, 5/11/92, to be published.

NCEER-92-0012 "Study of Wire Rope Systems for Seismic Protection of Equipment in Buildings," by G.F. Demetriades, M.C. Constantinou and A.M. Reinhorn, 5/20/92, (PB93-116655, A08, MF-A02).

NCEER-92-0013 "Shape Memory Structural Dampers: Material Properties, Design and Seismic Testing," by P.R. Witting and F.A. Cozzarelli, 5/26/92, (PB93-116663, A05, MF-A01).

NCEER-92-0014 "Longitudinal Permanent Ground Deformation Effects on Buried Continuous Pipelines," by M.J. O'Rourke, and C. Nordberg, 6/15/92, (PB93-116671, A08, MF-A02).

NCEER-92-0015 "A Simulation Method for Stationary Gaussian Random Functions Based on the Sampling Theorem," by M. Grigoriu and S. Balopoulou, 6/11/92, (PB93-127496, A05, MF-A01).

NCEER-92-0016 "Gravity-Load-Designed Reinforced Concrete Buildings: Seismic Evaluation of Existing Construction and Detailing Strategies for Improved Seismic Resistance," by G.W. Hoffmann, S.K. Kunnath, A.M. Reinhorn and J.B. Mander, 7/15/92, (PB94-142007, A08, MF-A02).

NCEER-92-0017 "Observations on Water System and Pipeline Performance in the Limón Area of Costa Rica Due to the April 22, 1991 Earthquake," by M. O'Rourke and D. Ballantyne, 6/30/92, (PB93-126811, A06, MF-A02).

NCEER-92-0018 "Fourth Edition of Earthquake Education Materials for Grades K-12," Edited by K.E.K. Ross, 8/10/92, (PB93-114023, A07, MF-A02).

NCEER-92-0019 "Proceedings from the Fourth Japan-U.S. Workshop on Earthquake Resistant Design of Lifeline Facilities and Countermeasures for Soil Liquefaction," Edited by M. Hamada and T.D. O'Rourke, 8/12/92, (PB93-163939, A99, MF-E11).

NCEER-92-0020 "Active Bracing System: A Full Scale Implementation of Active Control," by A.M. Reinhorn, T.T. Soong, R.C. Lin, M.A. Riley, Y.P. Wang, S. Aizawa and M. Higashino, 8/14/92, (PB93-127512, A06, MF-A02).

NCEER-92-0021 "Empirical Analysis of Horizontal Ground Displacement Generated by Liquefaction-Induced Lateral Spreads," by S.F. Bartlett and T.L. Youd, 8/17/92, (PB93-188241, A06, MF-A02).

NCEER-92-0022 "IDARC Version 3.0: Inelastic Damage Analysis of Reinforced Concrete Structures," by S.K. Kunnath, A.M. Reinhorn and R.F. Lobo, 8/31/92, (PB93-227502, A07, MF-A02).

NCEER-92-0023 "A Semi-Empirical Analysis of Strong-Motion Peaks in Terms of Seismic Source, Propagation Path and Local Site Conditions, by M. Kamiyama, M.J. O'Rourke and R. Flores-Berrones, 9/9/92, (PB93-150266, A08, MF-A02).

NCEER-92-0024 "Seismic Behavior of Reinforced Concrete Frame Structures with Nonductile Details, Part I: Summary of Experimental Findings of Full Scale Beam-Column Joint Tests," by A. Beres, R.N. White and P. Gergely, 9/30/92, (PB93-227783, A05, MF-A01).

NCEER-92-0025 "Experimental Results of Repaired and Retrofitted Beam-Column Joint Tests in Lightly Reinforced Concrete Frame Buildings," by A. Beres, S. El-Borgi, R.N. White and P. Gergely, 10/29/92, (PB93-227791, A05, MF-A01).

NCEER-92-0026 "A Generalization of Optimal Control Theory: Linear and Nonlinear Structures," by J.N. Yang, Z. Li and S. Vongchavalitkul, 11/2/92, (PB93-188621, A05, MF-A01).

NCEER-92-0027 "Seismic Resistance of Reinforced Concrete Frame Structures Designed Only for Gravity Loads: Part I - Design and Properties of a One-Third Scale Model Structure," by J.M. Bracci, A.M. Reinhorn and J.B. Mander, 12/1/92, (PB94-104502, A08, MF-A02).

NCEER-92-0028 "Seismic Resistance of Reinforced Concrete Frame Structures Designed Only for Gravity Loads: Part II - Experimental Performance of Subassemblages," by L.E. Aycardi, J.B. Mander and A.M. Reinhorn, 12/1/92, (PB94-104510, A08, MF-A02).

NCEER-92-0029 "Seismic Resistance of Reinforced Concrete Frame Structures Designed Only for Gravity Loads: Part III - Experimental Performance and Analytical Study of a Structural Model," by J.M. Bracci, A.M. Reinhorn and J.B. Mander, 12/1/92, (PB93-227528, A09, MF-A01).

NCEER-92-0030 "Evaluation of Seismic Retrofit of Reinforced Concrete Frame Structures: Part I - Experimental Performance of Retrofitted Subassemblages," by D. Choudhuri, J.B. Mander and A.M. Reinhorn, 12/8/92, (PB93-198307, A07, MF-A02).

NCEER-92-0031 "Evaluation of Seismic Retrofit of Reinforced Concrete Frame Structures: Part II - Experimental Performance and Analytical Study of a Retrofitted Structural Model," by J.M. Bracci, A.M. Reinhorn and J.B. Mander, 12/8/92, (PB93-198315, A09, MF-A03).

NCEER-92-0032 "Experimental and Analytical Investigation of Seismic Response of Structures with Supplemental Fluid Viscous Dampers," by M.C. Constantinou and M.D. Symans, 12/21/92, (PB93-191435, A10, MF-A03).

NCEER-92-0033 "Reconnaissance Report on the Cairo, Egypt Earthquake of October 12, 1992," by M. Khater, 12/23/92, (PB93-188621, A03, MF-A01).

NCEER-92-0034 "Low-Level Dynamic Characteristics of Four Tall Flat-Plate Buildings in New York City," by H. Gavin, S. Yuan, J. Grossman, E. Pekelis and K. Jacob, 12/28/92, (PB93-188217, A07, MF-A02).

NCEER-93-0001 "An Experimental Study on the Seismic Performance of Brick-Infilled Steel Frames With and Without Retrofit," by J.B. Mander, B. Nair, K. Wojtkowski and J. Ma, 1/29/93, (PB93-227510, A07, MF-A02).

NCEER-93-0002 "Social Accounting for Disaster Preparedness and Recovery Planning," by S. Cole, E. Pantoja and V. Razak, 2/22/93, (PB94-142114, A12, MF-A03).

NCEER-93-0003 "Assessment of 1991 NEHRP Provisions for Nonstructural Components and Recommended Revisions," by T.T. Soong, G. Chen, Z. Wu, R-H. Zhang and M. Grigoriu, 3/1/93, (PB93-188639, A06, MF-A02).

NCEER-93-0004 "Evaluation of Static and Response Spectrum Analysis Procedures of SEAOC/UBC for Seismic Isolated Structures," by C.W. Winters and M.C. Constantinou, 3/23/93, (PB93-198299, A10, MF-A03).

NCEER-93-0005 "Earthquakes in the Northeast - Are We Ignoring the Hazard? A Workshop on Earthquake Science and Safety for Educators," edited by K.E.K. Ross, 4/2/93, (PB94-103066, A09, MF-A02).

NCEER-93-0006 "Inelastic Response of Reinforced Concrete Structures with Viscoelastic Braces," by R.F. Lobo, J.M. Bracci, K.L. Shen, A.M. Reinhorn and T.T. Soong, 4/5/93, (PB93-227486, A05, MF-A02).

NCEER-93-0007 "Seismic Testing of Installation Methods for Computers and Data Processing Equipment," by K. Kosar, T.T. Soong, K.L. Shen, J.A. HoLung and Y.K. Lin, 4/12/93, (PB93-198299, A07, MF-A02).

NCEER-93-0008 "Retrofit of Reinforced Concrete Frames Using Added Dampers," by A. Reinhorn, M. Constantinou and C. Li, to be published.

NCEER-93-0009 "Seismic Behavior and Design Guidelines for Steel Frame Structures with Added Viscoelastic Dampers," by K.C. Chang, M.L. Lai, T.T. Soong, D.S. Hao and Y.C. Yeh, 5/1/93, (PB94-141959, A07, MF-A02).

NCEER-93-0010 "Seismic Performance of Shear-Critical Reinforced Concrete Bridge Piers," by J.B. Mander, S.M. Waheed, M.T.A. Chaudhary and S.S. Chen, 5/12/93, (PB93-227494, A08, MF-A02).

NCEER-93-0011 "3D-BASIS-TABS: Computer Program for Nonlinear Dynamic Analysis of Three Dimensional Base Isolated Structures," by S. Nagarajaiah, C. Li, A.M. Reinhorn and M.C. Constantinou, 8/2/93, (PB94-141819, A09, MF-A02).

NCEER-93-0012 "Effects of Hydrocarbon Spills from an Oil Pipeline Break on Ground Water," by O.J. Helweg and H.H.M. Hwang, 8/3/93, (PB94-141942, A06, MF-A02).

NCEER-93-0013 "Simplified Procedures for Seismic Design of Nonstructural Components and Assessment of Current Code Provisions," by M.P. Singh, L.E. Suarez, E.E. Matheu and G.O. Maldonado, 8/4/93, (PB94-141827, A09, MF-A02).

NCEER-93-0014 "An Energy Approach to Seismic Analysis and Design of Secondary Systems," by G. Chen and T.T. Soong, 8/6/93, (PB94-142767, A11, MF-A03).

NCEER-93-0015 "Proceedings from School Sites: Becoming Prepared for Earthquakes - Commemorating the Third Anniversary of the Loma Prieta Earthquake," Edited by F.E. Winslow and K.E.K. Ross, 8/16/93, (PB94-154275, A16, MF-A02).

NCEER-93-0016 "Reconnaissance Report of Damage to Historic Monuments in Cairo, Egypt Following the October 12, 1992 Dahshur Earthquake," by D. Sykora, D. Look, G. Croci, E. Karaesmen and E. Karaesmen, 8/19/93, (PB94-142221, A08, MF-A02).

NCEER-93-0017 "The Island of Guam Earthquake of August 8, 1993," by S.W. Swan and S.K. Harris, 9/30/93, (PB94-141843, A04, MF-A01).

NCEER-93-0018 "Engineering Aspects of the October 12, 1992 Egyptian Earthquake," by A.W. Elgamal, M. Amer, K. Adalier and A. Abul-Fadl, 10/7/93, (PB94-141983, A05, MF-A01).

NCEER-93-0019 "Development of an Earthquake Motion Simulator and its Application in Dynamic Centrifuge Testing," by I. Krstelj, Supervised by J.H. Prevost, 10/23/93, (PB94-181773, A-10, MF-A03).

NCEER-93-0020 "NCEER-Taisei Corporation Research Program on Sliding Seismic Isolation Systems for Bridges: Experimental and Analytical Study of a Friction Pendulum System (FPS)," by M.C. Constantinou, P. Tsopelas, Y-S. Kim and S. Okamoto, 11/1/93, (PB94-142775, A08, MF-A02).

NCEER-93-0021 "Finite Element Modeling of Elastomeric Seismic Isolation Bearings," by L.J. Billings, Supervised by R. Shepherd, 11/8/93, to be published.

NCEER-93-0022 "Seismic Vulnerability of Equipment in Critical Facilities: Life-Safety and Operational Consequences," by K. Porter, G.S. Johnson, M.M. Zadeh, C. Scawthorn and S. Eder, 11/24/93, (PB94-181765, A16, MF-A03).

NCEER-93-0023 "Hokkaido Nansei-oki, Japan Earthquake of July 12, 1993, by P.I. Yanev and C.R. Scawthorn, 12/23/93, (PB94-181500, A07, MF-A01).

NCEER-94-0001 "An Evaluation of Seismic Serviceability of Water Supply Networks with Application to the San Francisco Auxiliary Water Supply System," by I. Markov, Supervised by M. Grigoriu and T. O'Rourke, 1/21/94, (PB94-204013, A07, MF-A02).

NCEER-94-0002 "NCEER-Taisei Corporation Research Program on Sliding Seismic Isolation Systems for Bridges: Experimental and Analytical Study of Systems Consisting of Sliding Bearings, Rubber Restoring Force Devices and Fluid Dampers," Volumes I and II, by P. Tsopelas, S. Okamoto, M.C. Constantinou, D. Ozaki and S. Fujii, 2/4/94, (PB94-181740, A09, MF-A02 and PB94-181757, A12, MF-A03).

NCEER-94-0003 "A Markov Model for Local and Global Damage Indices in Seismic Analysis," by S. Rahman and M. Grigoriu, 2/18/94, (PB94-206000, A12, MF-A03).

NCEER-94-0004 "Proceedings from the NCEER Workshop on Seismic Response of Masonry Infills," edited by D.P. Abrams, 3/1/94, (PB94-180783, A07, MF-A02).

NCEER-94-0005 "The Northridge, California Earthquake of January 17, 1994: General Reconnaissance Report," edited by J.D. Goltz, 3/11/94, (PB193943, A10, MF-A03).

NCEER-94-0006 "Seismic Energy Based Fatigue Damage Analysis of Bridge Columns: Part I - Evaluation of Seismic Capacity," by G.A. Chang and J.B. Mander, 3/14/94, (PB94-219185, A11, MF-A03).

NCEER-94-0007 "Seismic Isolation of Multi-Story Frame Structures Using Spherical Sliding Isolation Systems," by T.M. Al-Hussaini, V.A. Zayas and M.C. Constantinou, 3/17/94, (PB193745, A09, MF-A02).

NCEER-94-0008 "The Northridge, California Earthquake of January 17, 1994: Performance of Highway Bridges," edited by I.G. Buckle, 3/24/94, (PB94-193851, A06, MF-A02).

NCEER-94-0009 "Proceedings of the Third U.S.-Japan Workshop on Earthquake Protective Systems for Bridges," edited by I.G. Buckle and I. Friedland, 3/31/94, (PB94-195815, A99, MF-A06).

NCEER-94-0010 "3D-BASIS-ME: Computer Program for Nonlinear Dynamic Analysis of Seismically Isolated Single and Multiple Structures and Liquid Storage Tanks," by P.C. Tsopelas, M.C. Constantinou and A.M. Reinhorn, 4/12/94, (PB94-204922, A09, MF-A02).

NCEER-94-0011 "The Northridge, California Earthquake of January 17, 1994: Performance of Gas Transmission Pipelines," by T.D. O'Rourke and M.C. Palmer, 5/16/94, (PB94-204989, A05, MF-A01).

NCEER-94-0012 "Feasibility Study of Replacement Procedures and Earthquake Performance Related to Gas Transmission Pipelines," by T.D. O'Rourke and M.C. Palmer, 5/25/94, (PB94-206638, A09, MF-A02).

NCEER-94-0013 "Seismic Energy Based Fatigue Damage Analysis of Bridge Columns: Part II - Evaluation of Seismic Demand," by G.A. Chang and J.B. Mander, 6/1/94, (PB95-18106, A08, MF-A02).

NCEER-94-0014 "NCEER-Taisei Corporation Research Program on Sliding Seismic Isolation Systems for Bridges: Experimental and Analytical Study of a System Consisting of Sliding Bearings and Fluid Restoring Force/Damping Devices," by P. Tsopelas and M.C. Constantinou, 6/13/94, (PB94-219144, A10, MF-A03).

NCEER-94-0015 "Generation of Hazard-Consistent Fragility Curves for Seismic Loss Estimation Studies," by H. Hwang and J-R. Huo, 6/14/94, (PB95-181996, A09, MF-A02).

NCEER-94-0016 "Seismic Study of Building Frames with Added Energy-Absorbing Devices," by W.S. Pong, C.S. Tsai and G.C. Lee, 6/20/94, (PB94-219136, A10, A03).

NCEER-94-0017 "Sliding Mode Control for Seismic-Excited Linear and Nonlinear Civil Engineering Structures," by J. Yang, J. Wu, A. Agrawal and Z. Li, 6/21/94, (PB95-138483, A06, MF-A02).

NCEER-94-0018 "3D-BASIS-TABS Version 2.0: Computer Program for Nonlinear Dynamic Analysis of Three Dimensional Base Isolated Structures," by A.M. Reinhorn, S. Nagarajaiah, M.C. Constantinou, P. Tsopelas and R. Li, 6/22/94, (PB95-182176, A08, MF-A02).

NCEER-94-0019 "Proceedings of the International Workshop on Civil Infrastructure Systems: Application of Intelligent Systems and Advanced Materials on Bridge Systems," Edited by G.C. Lee and K.C. Chang, 7/18/94, (PB95-252474, A20, MF-A04).

NCEER-94-0020 "Study of Seismic Isolation Systems for Computer Floors," by V. Lambrou and M.C. Constantinou, 7/19/94, (PB95-138533, A10, MF-A03).

NCEER-94-0021 "Proceedings of the U.S.-Italian Workshop on Guidelines for Seismic Evaluation and Rehabilitation of Unreinforced Masonry Buildings," Edited by D.P. Abrams and G.M. Calvi, 7/20/94, (PB95-138749, A13, MF-A03).

NCEER-94-0022 "NCEER-Taisei Corporation Research Program on Sliding Seismic Isolation Systems for Bridges: Experimental and Analytical Study of a System Consisting of Lubricated PTFE Sliding Bearings and Mild Steel Dampers," by P. Tsopelas and M.C. Constantinou, 7/22/94, (PB95-182184, A08, MF-A02).

NCEER-94-0023 "Development of Reliability-Based Design Criteria for Buildings Under Seismic Load," by Y.K. Wen, H. Hwang and M. Shinozuka, 8/1/94, (PB95-211934, A08, MF-A02).

NCEER-94-0024 "Experimental Verification of Acceleration Feedback Control Strategies for an Active Tendon System," by S.J. Dyke, B.F. Spencer, Jr., P. Quast, M.K. Sain, D.C. Kaspari, Jr. and T.T. Soong, 8/29/94, (PB95-212320, A05, MF-A01).

NCEER-94-0025 "Seismic Retrofitting Manual for Highway Bridges," Edited by I.G. Buckle and I.F. Friedland, published by the Federal Highway Administration (PB95-212676, A15, MF-A03).

NCEER-94-0026 "Proceedings from the Fifth U.S.-Japan Workshop on Earthquake Resistant Design of Lifeline Facilities and Countermeasures Against Soil Liquefaction," Edited by T.D. O'Rourke and M. Hamada, 11/7/94, (PB95-220802, A99, MF-E08).

NCEER-95-0001 "Experimental and Analytical Investigation of Seismic Retrofit of Structures with Supplemental Damping: Part 1 - Fluid Viscous Damping Devices," by A.M. Reinhorn, C. Li and M.C. Constantinou, 1/3/95, (PB95-266599, A09, MF-A02).

NCEER-95-0002 "Experimental and Analytical Study of Low-Cycle Fatigue Behavior of Semi-Rigid Top-And-Seat Angle Connections," by G. Pekcan, J.B. Mander and S.S. Chen, 1/5/95, (PB95-220042, A07, MF-A02).

NCEER-95-0003 "NCEER-ATC Joint Study on Fragility of Buildings," by T. Anagnos, C. Rojahn and A.S. Kiremidjian, 1/20/95, (PB95-220026, A06, MF-A02).

NCEER-95-0004 "Nonlinear Control Algorithms for Peak Response Reduction," by Z. Wu, T.T. Soong, V. Gattulli and R.C. Lin, 2/16/95, (PB95-220349, A05, MF-A01).

NCEER-95-0005 "Pipeline Replacement Feasibility Study: A Methodology for Minimizing Seismic and Corrosion Risks to Underground Natural Gas Pipelines," by R.T. Eguchi, H.A. Seligson and D.G. Honegger, 3/2/95, (PB95-252326, A06, MF-A02).

NCEER-95-0006 "Evaluation of Seismic Performance of an 11-Story Frame Building During the 1994 Northridge Earthquake," by F. Naeim, R. DiSulio, K. Benuska, A. Reinhorn and C. Li, to be published.

NCEER-95-0007 "Prioritization of Bridges for Seismic Retrofitting," by N. Basöz and A.S. Kiremidjian, 4/24/95, (PB95-252300, A08, MF-A02).

NCEER-95-0008 "Method for Developing Motion Damage Relationships for Reinforced Concrete Frames," by A. Singhal and A.S. Kiremidjian, 5/11/95, (PB95-266607, A06, MF-A02).

NCEER-95-0009 "Experimental and Analytical Investigation of Seismic Retrofit of Structures with Supplemental Damping: Part II - Friction Devices," by C. Li and A.M. Reinhorn, 7/6/95, (PB96-128087, A11, MF-A03).

NCEER-95-0010 "Experimental Performance and Analytical Study of a Non-Ductile Reinforced Concrete Frame Structure Retrofitted with Elastomeric Spring Dampers," by G. Pekcan, J.B. Mander and S.S. Chen, 7/14/95, (PB96-137161, A08, MF-A02).

NCEER-95-0011 "Development and Experimental Study of Semi-Active Fluid Damping Devices for Seismic Protection of Structures," by M.D. Symans and M.C. Constantinou, 8/3/95, (PB96-136940, A23, MF-A04).

NCEER-95-0012 "Real-Time Structural Parameter Modification (RSPM): Development of Innervated Structures," by Z. Liang, M. Tong and G.C. Lee, 4/11/95, (PB96-137153, A06, MF-A01).

NCEER-95-0013 "Experimental and Analytical Investigation of Seismic Retrofit of Structures with Supplemental Damping: Part III - Viscous Damping Walls," by A.M. Reinhorn and C. Li, 10/1/95, (PB96-176409, A11, MF-A03).

NCEER-95-0014 "Seismic Fragility Analysis of Equipment and Structures in a Memphis Electric Substation," by J-R. Huo and H.H.M. Hwang, (PB96-128087, A09, MF-A02), 8/10/95.

NCEER-95-0015 "The Hanshin-Awaji Earthquake of January 17, 1995: Performance of Lifelines," Edited by M. Shinozuka, 11/3/95, (PB96-176383, A15, MF-A03).

NCEER-95-0016 "Highway Culvert Performance During Earthquakes," by T.L. Youd and C.J. Beckman, available as NCEER-96-0015.

NCEER-95-0017 "The Hanshin-Awaji Earthquake of January 17, 1995: Performance of Highway Bridges," Edited by I.G. Buckle, 12/1/95, to be published.

NCEER-95-0018 "Modeling of Masonry Infill Panels for Structural Analysis," by A.M. Reinhorn, A. Madan, R.E. Valles, Y. Reichmann and J.B. Mander, 12/8/95.

NCEER-95-0019 "Optimal Polynomial Control for Linear and Nonlinear Structures," by A.K. Agrawal and J.N. Yang, 12/11/95, (PB96-168737, A07, MF-A02).

NCEER-95-0020 "Retrofit of Non-Ductile Reinforced Concrete Frames Using Friction Dampers," by R.S. Rao, P. Gergely and R.N. White, 12/22/95, (PB97-133508, A10, MF-A02).

NCEER-95-0021 "Parametric Results for Seismic Response of Pile-Supported Bridge Bents," by G. Mylonakis, A. Nikolaou and G. Gazetas, 12/22/95, (PB97-100242, A12, MF-A03).

NCEER-95-0022 "Kinematic Bending Moments in Seismically Stressed Piles," by A. Nikolaou, G. Mylonakis and G. Gazetas, 12/23/95.

NCEER-96-0001 "Dynamic Response of Unreinforced Masonry Buildings with Flexible Diaphragms," by A.C. Costley and D.P. Abrams," 10/10/96.

NCEER-96-0002 "State of the Art Review: Foundations and Retaining Structures," by I. Po Lam, to be published.

NCEER-96-0003 "Ductility of Rectangular Reinforced Concrete Bridge Columns with Moderate Confinement," by N. Wehbe, M. Saiidi, D. Sanders and B. Douglas, 11/7/96, (PB97-133557, A06, MF-A02).

NCEER-96-0004 "Proceedings of the Long-Span Bridge Seismic Research Workshop," edited by I.G. Buckle and I.M. Friedland, to be published.

NCEER-96-0005 "Establish Representative Pier Types for Comprehensive Study: Eastern United States," by J. Kulicki and Z. Prucz, 5/28/96, (PB98-119217, A07, MF-A02).

NCEER-96-0006 "Establish Representative Pier Types for Comprehensive Study: Western United States," by R. Imbsen, R.A. Schamber and T.A. Osterkamp, 5/28/96, (PB98-118607, A07, MF-A02).

NCEER-96-0007 "Nonlinear Control Techniques for Dynamical Systems with Uncertain Parameters," by R.G. Ghanem and M.I. Bujakov, 5/27/96, (PB97-100259, A17, MF-A03).

NCEER-96-0008 "Seismic Evaluation of a 30-Year Old Non-Ductile Highway Bridge Pier and Its Retrofit," by J.B. Mander, B. Mahmoodzadegan, S. Bhadra and S.S. Chen, 5/31/96.

NCEER-96-0009 "Seismic Performance of a Model Reinforced Concrete Bridge Pier Before and After Retrofit," by J.B. Mander, J.H. Kim and C.A. Ligozio, 5/31/96.

NCEER-96-0010 "IDARC2D Version 4.0: A Computer Program for the Inelastic Damage Analysis of Buildings," by R.E. Valles, A.M. Reinhorn, S.K. Kunnath, C. Li and A. Madan, 6/3/96, (PB97-100234, A17, MF-A03).

NCEER-96-0011 "Estimation of the Economic Impact of Multiple Lifeline Disruption: Memphis Light, Gas and Water Division Case Study," by S.E. Chang, H.A. Seligson and R.T. Eguchi, 8/16/96, (PB97-133490, A11, MF-A03).

NCEER-96-0012 "Proceedings from the Sixth Japan-U.S. Workshop on Earthquake Resistant Design of Lifeline Facilities and Countermeasures Against Soil Liquefaction, Edited by M. Hamada and T. O'Rourke, 9/11/96, (PB97-133581, A99, MF-A06).

NCEER-96-0013 "Chemical Hazards, Mitigation and Preparedness in Areas of High Seismic Risk: A Methodology for Estimating the Risk of Post-Earthquake Hazardous Materials Release," by H.A. Seligson, R.T. Eguchi, K.J. Tierney and K. Richmond, 11/7/96.

NCEER-96-0014 "Response of Steel Bridge Bearings to Reversed Cyclic Loading," by J.B. Mander, D-K. Kim, S.S. Chen and G.J. Premus, 11/13/96, (PB97-140735, A12, MF-A03).

NCEER-96-0015 "Highway Culvert Performance During Past Earthquakes," by T.L. Youd and C.J. Beckman, 11/25/96, (PB97-133532, A06, MF-A01).

NCEER-97-0001 "Evaluation, Prevention and Mitigation of Pounding Effects in Building Structures," by R.E. Valles and A.M. Reinhorn, 2/20/97, (PB97-159552, A14, MF-A03).

NCEER-97-0002 "Seismic Design Criteria for Bridges and Other Highway Structures," by C. Rojahn, R. Mayes, D.G. Anderson, J. Clark, J.H. Hom, R.V. Nutt and M.J. O'Rourke, 4/30/97, (PB97-194658, A06, MF-A03).

NCEER-97-0003 "Proceedings of the U.S.-Italian Workshop on Seismic Evaluation and Retrofit," Edited by D.P. Abrams and G.M. Calvi, 3/19/97, (PB97-194666, A13, MF-A03).

NCEER-97-0004 "Investigation of Seismic Response of Buildings with Linear and Nonlinear Fluid Viscous Dampers," by A.A. Seleemah and M.C. Constantinou, 5/21/97, (PB98-109002, A15, MF-A03).

NCEER-97-0005 "Proceedings of the Workshop on Earthquake Engineering Frontiers in Transportation Facilities," edited by G.C. Lee and I.M. Friedland, 8/29/97, (PB98-128911, A25, MR-A04).

NCEER-97-0006 "Cumulative Seismic Damage of Reinforced Concrete Bridge Piers," by S.K. Kunnath, A. El-Bahy, A. Taylor and W. Stone, 9/2/97, (PB98-108814, A11, MF-A03).

NCEER-97-0007 "Structural Details to Accommodate Seismic Movements of Highway Bridges and Retaining Walls," by R.A. Imbsen, R.A. Schamber, E. Thorkildsen, A. Kartoum, B.T. Martin, T.N. Rosser and J.M. Kulicki, 9/3/97.

NCEER-97-0008 "A Method for Earthquake Motion-Damage Relationships with Application to Reinforced Concrete Frames," by A. Singhal and A.S. Kiremidjian, 9/10/97, (PB98-108988, A13, MF-A03).

NCEER-97-0009 "Seismic Analysis and Design of Bridge Abutments Considering Sliding and Rotation," by K. Fishman and R. Richards, Jr., 9/15/97, (PB98-108897, A06, MF-A02).

NCEER-97-0010 "Proceedings of the FHWA/NCEER Workshop on the National Representation of Seismic Ground Motion for New and Existing Highway Facilities," edited by I.M. Friedland, M.S. Power and R.L. Mayes, 9/22/97.

NCEER-97-0011 "Seismic Analysis for Design or Retrofit of Gravity Bridge Abutments," by K.L. Fishman, R. Richards, Jr. and R.C. Divito, 10/2/97, (PB98-128937, A08, MF-A02).

NCEER-97-0012 "Evaluation of Simplified Methods of Analysis for Yielding Structures," by P. Tsopelas, M.C. Constantinou, C.A. Kircher and A.S. Whittaker, 10/31/97, (PB98-128929, A10, MF-A03).

NCEER-97-0013 "Seismic Design of Bridge Columns Based on Control and Repairability of Damage," by C-T. Cheng and J.B. Mander, 12/8/97.

NCEER-97-0014 "Seismic Resistance of Bridge Piers Based on Damage Avoidance Design," by J.B. Mander and C-T. Cheng, 12/10/97.

NCEER-97-0015 "Seismic Response of Nominally Symmetric Systems with Strength Uncertainty," by S. Balopoulou and M. Grigoriu, 12/23/97.

NCEER-97-0016 "Evaluation of Seismic Retrofit Methods for Reinforced Concrete Bridge Columns," by T.J. Wipf, F.W. Klaiber and F.M. Russo, 12/28/97.

NCEER-97-0017 "Seismic Fragility of Existing Conventional Reinforced Concrete Highway Bridges," by C.L. Mullen and A.S. Cakmak, 12/30/97.

NCEER-97-0018 "Loss Asssessment of Memphis Buildings," edited by D.P. Abrams and M. Shinozuka, 12/31/97.

NCEER-97-0019 "Seismic Evaluation of Frames with Infill Walls Using Quasi-static Experiments," by K.M. Mosalam, R.N. White and P. Gergely, 12/31/97.

NCEER-97-0020 "Seismic Evaluation of Frames with Infill Walls Using Pseudo-dynamic Experiments," by K.M. Mosalam, R.N. White and P. Gergely, 12/31/97.

NCEER-97-0021 "Computational Strategies for Frames with Infill Walls: Discrete and Smeared Crack Analyses and Seismic Fragility," by K.M. Mosalam, R.N. White and P. Gergely, 12/31/97.

NCEER-97-0022 "Proceedings of the NCEER Workshop on Evaluation of Liquefaction Resistance of Soils," edited by T.L. Youd and I.M. Idriss, 12/31/97.

MCEER-98-0001 "Extraction of Nonlinear Hysteretic Properties of Seismically Isolated Bridges from Quick-Release Field Tests," by Q. Chen, B.M. Douglas, E.M. Maragakis and I.G. Buckle, 5/26/98.

MCEER-98-0002 "Evaluation of Structure Importance," by A. Thomas, S. Eshenaur and J. Kulicki, 5/29/98.

MCEER-98-0003 "Capacity Design of Bridge Piers and the Analysis of Overstrength," by J.B. Mander, A. Dutta and P. Goel, 6/1/98.